IDENTIFICATION OF A PHOSPHOPANTETHEINYL TRANSFERASE INHIBITOR THAT KILLS *MYCOBACTERIUM TUBERCULOSIS* AND A NOVEL MECHANISM OF RESISTANCE INVOLVING AN ENZYME OF PREVIOUSLY UNKNOWN FUNCTION: PHOSPHOPANTETHEINYL HYDROLASE

A Dissertation

Presented to the Faculty of Weill Cornell Graduate School

of Medical Sciences

In Partial Fulfillment of the Requirements for the Degree of

Doctor of Philosophy

By

Elaine Ballinger

January 2018

IDENTIFICATION OF A PHOSPHOPANTETHEINYL TRANSFERASE INHIBITOR THAT KILLS *MYCOBACTERIUM TUBERCULOSIS* AND A NOVEL MECHANISM OF RESISTANCE INVOLVING AN ENZYME OF PREVIOUSLY UNKNOWN FUNCTION: PHOSPHOPANTETHEINYL HYDROLASE

Elaine Ballinger, Ph.D.

Cornell University 2018

Tuberculosis (TB) is the leading cause of death from infectious disease, and new drugs are needed to treat emerging resistant TB infections. Using genetic, metabolomic, crystallographic, and recombinant enzyme assays we discovered a compound that kills *Mycobacterium tuberculosis* (Mtb) upon binding the active site of phosphopantetheinyl transferase (PptT). PptT is an essential enzyme for Mtb, and has been a desired drug target for many years. PptT uses coenzyme A (CoA) as a substrate to activate acyl carrier proteins (ACPs) by transferring phosphopantheine (Ppt) from CoA onto the ACP. ACPs then use the Ppt group for synthesis of lipids critical for Mtb's cell wall and virulence. The compound did not fully abolish PptT activity, and we found that killing of Mtb by the inhibitor depended on the activity of a newly identified enzyme, a Ppt hydrolase (PptH) that can remove Ppt from ACPs. While PptH is highly conserved among mycobacteria, it's opposing function to an essential process has no obvious utility to the cell. This activity was revealed by a new mechanism of antimicrobial resistance: loss of function in an enzyme (PptH) that opposes the action of the enzyme (PptT) targeted by the inhibitor. The opposing PptT/PptH reactions invite exploration of a regulatory pathway in CoA physiology, as the two enzymes oppose each other and may be involved in stress-response signaling.

BIOGRAPHICAL SKETCH

Elaine Ballinger grew up in California and graduated from Stanford University in 2012 with a Bachelor of Science in Chemistry with an emphasis on biological chemistry, and a minor in Classic literature. Her undergraduate research under the mentorship of Dr. Justin Sonnenburg focused on the differences between humanized or gnotobiotic mice fed a standard or high fat diet. She moved to New York City in 2012 to pursue a doctorate in Pharmacology at Weill Cornell Medicine. At Weill she joined the lab of Dr. Carl Nathan in late 2013, and studied the target and mechanism of resistance of a new anti-*Mycobacteria* compound.

ACKNOWLEDGEMENTS

I am deeply grateful for the opportunity to have learned from Dr. Carl Nathan. The depth of your knowledge is awe-inspiring and I have learned so much from your creative approaches to problem solving. You have always been patient with me while also pushing me to become a more competent and professional scientist, and I would not have been able to get where I am today without you. It has been an honor being in your lab and I really can't emphasize enough how much I have learned.

I am also incredibly thankful for the additional mentorship I have received from Drs. Kristin Burns-Huang and Ben Gold. Our meetings have been so helpful especially with breaking down experimental variables when things weren't working, which was often. Being able to troubleshoot and get feedback on my ideas no doubt saved me many headaches. I am also very appreciative for the personal support Kristin was always willing to give when I was having problems outside of lab. Your door was always open (even if I sort of barged in) and your assurances always made me feel more confident that I could handle things.

My thesis committee including Dr. Dirk Schnappinger and Dr. Lonny Levin has been invaluable in my training. Your scientific and logistical guidance has been invaluable to navigating the complexity of managing experiments and analyzing results on a reasonable timeline. I would also like to thank Drs. Kirk Deitsch, and Daniel Heller for being on my day-of defense committee.

The mentorship I have received was incredible, and no small part of that was from members of the Nathan lab. I am constantly reminded how lucky I am to work with such interesting, smart, and knowledgeable people. I would particularly like to thank Dr. Tania Lupoli for all your guidance- I was constantly blown away by how much you know, and your willingness to show me a new technique or discuss issues I

was having. It might have been annoying to be so knowledgeable about so many topics because I would always come bother you first if I had a question. Dr. Landys Lopez-Quezada, you have always been a great friend and partner through our many meetings, and your suggestions have helped me immeasurably. Drs. Thulasi Warrier and Travis Hartman you have also been invaluable for guidance and help figuring out the complexities of Mtb experiments, and Dr. Kyu Rhee for his oversight on metabolomics. I am grateful to Julia Roberts, Madeline Woods, Dr. Kohta Saito, Roxanne Morris and Elaina Weber for your friendship and support, we have had shared a lot of priceless moments and laughter which made coming to work so much better.

I am also grateful for the collaborations I was able to be a part of with scientists outside WMC. Our collaborators at Sanofi have been instrumental to the progression of our progress, in particular I would like to thank Christine Roubert for her excellent feedback and kindness. I am also grateful to Laurent Goullieux, Isabelle Blanc, Sophie Lagrange, Laurent Fraisse, Cedric Couturier, and Eric Bacque at Sanofi for their help with this project. John Mosior and Jim Sacchettini at Texas A & M were critical for this project and I am very grateful for the enzymatic expertise they brought to this largely microbiological project. Guangbin Yang and Ouathek Ouerfelli synthesized a standard that proved essential for supporting our hypothesis, and Tom Ioerger and Jamie Bean performed genomic sequencing of mutant DNA. Additionally Jeff Aube and Sarah Marie Scarry at UNC were extremely generous and helpful with providing us with compounds and creative with new structures to test.

I am completely certain that I would not have been able to survive living in New York without the friends that I have made in school here; Ali Ochoa-Cohen, Cynthia Quintero, Susannah Calhoun, Corey Anderson, Michael Levine, Raphael Bendriem, Hadar Koren-Roth, and Catie Profaci. When I moved to New York I knew

absolutely no one living here and I was terrified that in addition to the stresses of school I would have no friends to share the ups and downs of school and life. I am so glad those fears were completely unfounded. We have had so many incredible, hilarious, and weird times together, and you have all been there in times of need. I will miss our brunches together as we all move on. I may not be the biggest fan of New York, but you guys are the best group of friends and I am incredibly grateful to have you all in my life.

I would also like to thank my parents, who have been instrumental to getting me where I am today. I think sometimes you guys are… bemused? by my choices but you have always supported me wholeheartedly, encouraged my independence, and done whatever you can to help me achieve my goals.

I have always felt that people are stronger together but nothing has strengthened that belief for me more than my experience during my PhD. I have been supported by such a wide net of people, all of whom were selflessly helping me learn and grow. I feel so lucky that so many people have taken time and shared their knowledge and advice with me, and I will always do my best to follow the amazing example of support and kindness that has been set for me.

TABLE OF CONTENTS

LIST OF FIGURES

Chapter 1

Chapter 2

Chapter 3

Chapter 4

Chapter 5

Chapter 6

LIST OF TABLES

Chapter 1

Chapter 2

Chapter 5

LIST OF ABBREVIATIONS

CFU: Colony forming unit

Mtb: *Mycobacterium tuberculosis*

Msm: *Mycobacterium smegmatis*

WT: Wild-type

MT: Mutant

PAS: Paraminosalicylic acid

INH: Isoniazid

RIF: Rifampicin

EMB: Ethambutol

MOXI: Moxifloxacin

FOR: Frequency of resistance

MIC: Minimum inhibitory concentration

PptT: Phosphopantetheinyl transferase

CoA: Coenzyme A

PptH: Phosphopantetheinyl hydrolase

ppt: phosphopantetheine

AcpS: Acyl carrier protein synthase

AcpH: Acyl carrier protein hydrolase

ACP: Acyl carrier protein

SD3: Shine-Dalgarno initiation sequence 3

NTI: Native translation initiation site

MS: Mass Spectrometry

CHAPTER 1

INTRODUCTION

Mycobacterium tuberculosis (Mtb) has been a human pathogen for thousands of years. Mtb DNA has been amplified from archeological remains dating as far back as 9000 years[1], and some analysis has found evolutionary nodes in the Mtb genome that coincide with human migration out of Africa 40,000 years ago[2]. Archeological remains from almost any era tested have been found to contain forensic or genetic evidence of Mtb infection[3]. Degree of outbreak has waxed and waned over time, but it has been estimated that Mtb has killed more people throughout history any other microbial pathogen[3]. TB was especially lethal during the industrial revolution, with soaring population density in cities, notoriously terrible air quality, and rampant malnutrition, all at a time when epidemics were poorly understood[4–6]. Little was known about TB infection until 1865, when Jean Antoine showed that tuberculosis was infectious[7]. Knowledge was further increased in 1882, when Robert Koch presented on his discovery of bacilli and the Koch-Henle postulates. These findings helped shape modern understanding of bacteria and epidemics[3,8].

Based on the early research of Antoine and Koch, as well as research that came later, we now know that tuberculosis is very infectious, and primarily spread through aerosols produced from the coughing or sneezing of infected people. In classic TB infection, a host will inhale bacteria within aerosol droplets, and the bacteria will be deposited in the lungs[9]. Once inhaled, primary immune response involving macrophages may disseminate Mtb throughout the body, but pulmonary TB is the most common form of infection, and the majority of the bacteria are located in the lungs.

A major mechanism of immune response to Mtb infection is to sequester the

bacteria in granulomas[9]. Granulomas are formed as necrotic cavities in the lungs, and are relatively isolated from the rest of the body. The host immune system can contain Mtb within granulomas more or less indefinitely, and many people who are infected with Mtb may live their whole lives unaware that they have been infected. Granulomas are often asymptomatic, but can be detected by chest X-ray, and are considered indicative of Mtb infection especially in the presence of other signs of Mtb, such as persistent cough[10].

It is estimated that 1/3 of the world's population is infected with Mtb, and tuberculosis causes more deaths annually than any other infectious disease[11–13]. The WHO reported that there were about 1.7 million deaths from Mtb in 2016, and while this is a tragically large number, it is nowhere near estimates of the number of people infected worldwide. This is because although Mtb is extremely infectious and only a small number of bacteria are needed to establish an infection, about 90% of infected people never develop active TB[12]. When Mtb is sequestered within granulomas, it can enter a non-replicative state and remain dormant for the entirety of the host's life. This stage of infection is called latent TB, and patients are not usually contagious when their infection is being managed by their immune system in this way[12,14,15]. In about 10% of those infected, Mtb can reactivate, at which point the bacterial population is no longer being contained by the immune system and the bacterial burden of Mtb can get very high[12]. This rate can be higher in populations comprised of individuals who are malnourished or immunocompromised from HIV or diabetes, which are all risk factors for active TB infection. When people have active TB they are infectious and on average will infect 10-15 people per year of untreated infection[15]. Tuberculosis is challenging to treat now with modern drugs, but during the height of the "white plague" the only real option available was isolation in sanitoria[6,16].

Sanitoria were developed in the mid-late 19th century, and for about 100 years

were the only treatment for tuberculosis- and then, only for those who could afford them[17]. The premise was that by isolating "consumptives," or people infected with Mtb, sanatoria could help curb the spread of TB within cities, and could also provide better nutrition and ventilation, improving the outcomes of disease for infected patients[3,6,17]. We now know that clean/drier air, proper nutrition, and vitamin D exposure can improve the outcome for TB patients, but they are far less effective than antibiotics.

The first antibiotics discovered for TB treatment were streptomycin (1944) and para-aminosalicylic acid (PAS) (1946), closely followed by isoniazid (INH) and pyrazinamide in (PZA) 1952[18]. It was quickly discovered that monotherapy for TB treatment was ineffective and could rapidly result in the emergence of resistant strains- this is likely a result of high bacterial burden in active TB cases. If the bacterial burden is higher than the frequency of resistance (FOR), a patient undergoing treatment is likely to have a naturally occurring subpopulation of bacteria that are resistant to the drug. For this reason, a standardized multi-drug therapy has been developed, because when multiple drugs with different targets are combined, their FOR becomes far higher than the possible bacterial burden during infection. Standard recommended treatment for drug-susceptible TB from the 2016 WHO report includes 2 months of daily treatment with rifampicin (RIF), INH, PZA, and ethambutol (EMB) followed by 4 months of daily INH and RIF[10]. In the first 2 months of this treatment regime, the multi-drug therapy results in a conservative estimated FOR of 1 in 10^{18}. PZA is not very effective against Mtb alone but is synergistic with the drug regime.

Table 1 shows a summary of the 4 front line drugs for TB treatment and their activity, mechanism of action, and frequency of resistance. Streptomycin is not included but is sometimes used in place of EMB. Treatment targets active TB infection, as most of the targets are only essential in actively replicating cells. There is

some dispute as to the efficacy of treatment on latent TB, and in most countries where rates of TB are high, resources are focused on the treatment of active infection[14,19,20].

Table 1: Summary of the 4 front line drugs for treatment of Mtb infection[18,21]

Drug (year of discovery)	MIC_{90} (μg/ml)	Mechanism of action	Resistance genes	Gene function	FOR
Isoniazid INH (1952)	0.02-0.2	Inhibition of mycolic acid biosynthesis	*katG, inhA*	Catalase-peroxidase , Enoyl ACP reductase	10^{-5}-10^{-6}
Rifampicin RIF (1966)	0.05-1	Inhibition of RNA synthesis	*rpoB*	β subunit of RNA polymerase	10^{-7}-10^{-8}
Pyrazinamide PZA (1952)	16-50 (pH5.5)	Depletion of membrane potential	*pncA*	Nicotinamidase/ pyrazinamidase	10^{-5}
Ethambutol EMB (1961)	1-5	Inhibition of arabinogalactin synthesis	*embB*	Arabinosyl transferase	10^{-5}

Mtb treatment has been relatively effective at curbing outbreaks in modern Western cities. Unfortunately, resistance is on the rise. Despite the low frequency of resistance expected with standard treatment, there are a number of causes for the emergence of resistance. Many countries with the highest incidence of Mtb are developing countries with poor infrastructure, where people may have limited access to medical care. Diagnosis of TB may be low, and patients who are diagnosed with TB may not have a steady supply of drugs, or may not finish their course for other reasons. The minimum length of time for treatment is 6 months, and many people—even those with steady access to healthcare—begin treatment but do not finish the full course [22,23]. There can be many side effects from the TB treatment, including hepatotoxicity and gastrointestinal distress, which can cause patient noncompliance—especially as many of the symptoms of pulmonary TB may disappear in the first 2

months[24,25]. The CDC reported 500,000 new cases of multi drug-resistant (MDR) and extensively drug-resistant (XDR) TB in 2016, though most TB cases are not tested for drug sensitivity so this number is likely underestimating the true extent of resistance[23].

Once Mtb becomes MDR or XDR, it becomes much harder to treat. Second line drugs are not as effective and have much more severe side effects; additionally treatment time is expanded from 6-9 months to up to 32 months for XDR TB[10]. The lowered efficacy of the drugs also significantly reduces the chance of successful patient outcome; 50-60% success rate is common (**Figure 1A**), and the success rate for XDR TB treatment is even lower. In addition to the reduction in treatment success, MDR and XDR are exponentially more expensive to treat than drug-susceptible Mtb (**Figure 1B)**. Resources for the treatment of TB are already limited, and the added costs of treating MDR and XDR TB realistically mean that fewer people can receive treatment for their infection. Additionally, MDR or XDR patients should ideally be isolated for part of their treatment to avoid spreading the resistant bacteria, but this can be challenging to achieve even if facilities are available for the isolation[10,21]. With a lack of effective options for XDR TB treatment and the infectious nature of TB, XDR TB has already begun to spread, and it will be extremely challenging to stop with our current drug arsenal. Some doctors have even suggested bringing back sanitoria as viable treatment options, though their main benefit would be control, given the lack of alternatives[26].

Figure 1: WHO and CDC graphics on patient outcomes and costs associated with MDR and XDR TB. **(A)** WHO chart following patient outcome of MDR TB treatment in various countries[10]. **(B)** Adapted CDC infographic on the side effects and costs associated with MDR and XDR treatments[23].

A.

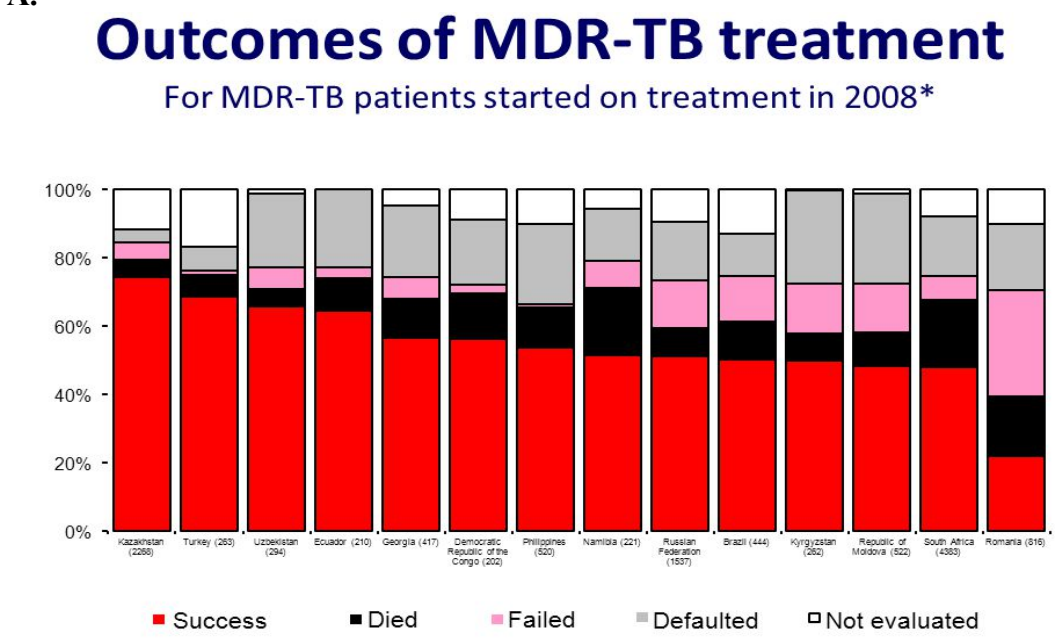

* In countries reporting outcomes for >200 MDR-TB cases with <20% unevaluated (cohort size shown below country names)

B.

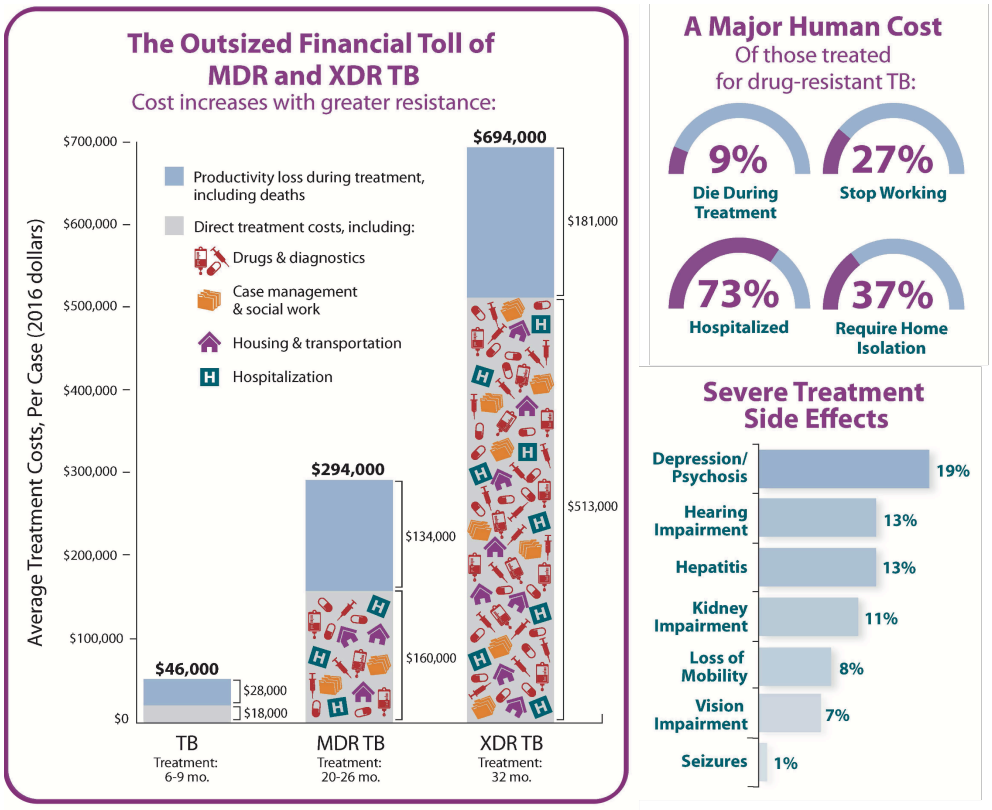

In the face of rising resistance rates, the global community needs to act sooner rather than later. One way to help prevent the spread of MDR or XDR TB is to introduce new drugs for treatment. With more frontline drugs that are as effective or better than current options, patients with MDR or XDR TB would not necessarily face a daunting multi-year battle for health. For these reasons we have focused our research on identifying new potential drug targets by studying the effects of drug-like molecules from chemical libraries.

REFERENCES

1. Hershkovitz, I. *et al.* Detection and Molecular Characterization of 9000-Year-Old Mycobacterium tuberculosis from a Neolithic Settlement in the Eastern Mediterranean. *PLoS One* **3,** e3426 (2008).
2. Wirth, T. *et al.* Origin, spread and demography of the Mycobacterium tuberculosis complex. *PLoS Pathog.* **4,** e1000160 (2008).
3. Daniel, T. M. The history of tuberculosis. *Respir. Med.* **100,** 1862–1870 (2006).
4. The Origin of Plagues: Old and New. *Science (80-.).* **257,** (1992).
5. Merker, M. *et al.* Evolutionary history and global spread of the Mycobacterium tuberculosis Beijing lineage. *Nat. Genet.* **47,** 242–249 (2015).
6. Kumar, D., Watson, J. M., Charlett, A., Nicholas, S. & Darbyshire, J. H. Tuberculosis in England and Wales in 1993: results of a national survey. Public Health Laboratory Service/British Thoracic Society/Department of Health Collaborative Group. *Thorax* **52,** 1060–7 (1997).
7. Daniel, T. M. Jean-Antoine Villemin and the infectious nature of tuberculosis. *Int. J. Tuberc. Lung Dis.* **19,** 267–268 (2015).
8. Barberis, I., Bragazzi, N. L., Galluzzo, L. & Martini, M. The history of tuberculosis: from the first historical records to the isolation of Koch's bacillus. *J. Prev. Med. Hyg.* **58,** E9–E12 (2017).
9. Rayasam, G. V. & Balganesh, T. S. Exploring the potential of adjunct therapy in tuberculosis. *Trends Pharmacol. Sci.* **36,** 506–513 (2015).
10. World Health Organization & Stop TB Initiative (World Health Organization). *Treatment of tuberculosis : guidelines.* (World Health Organization, 2010).
11. Gold, B. & Nathan, C. Targeting Phenotypically Tolerant Mycobacterium tuberculosis. *Microbiol. Spectr.* **5,** (2017).
12. Nathan, C. Fresh approaches to anti-infective therapies. *Sci. Transl. Med.* **4,**

140sr2 (2012).

13. WHO Model List of Essential Medicines 20th List WHO Model List of Essential Medicines (March 2017) Explanatory notes. (2017).
14. Barry, C. E. *et al.* The spectrum of latent tuberculosis: rethinking the biology and intervention strategies. *Nat. Rev. Microbiol.* **7,** 845 (2009).
15. WHO | Tuberculosis. *WHO* (2017).
16. Tuberculosis Sanitariums: Reminders of the White Plague | National Trust for Historic Preservation. Available at: https://savingplaces.org/stories/tuberculosis-sanitariums-reminders-of-the-white-plaque#.WiX6brSpn58. (Accessed: 4th December 2017)
17. John Frith. History of Tuberculosis. Part 2- the Sanatoria and the Discoveries of the Tubercle Bacillus. *J. Mil. Veterans. Health* **22,** 36–41 (2014).
18. Zhang, Y. & Yew, W. W. Mechanisms of drug resistance in Mycobacterium tuberculosis. *Int. J. Tuberc. Lung Dis.* **13,** 1320–30 (2009).
19. Bryk, R. *et al.* Selective killing of nonreplicating mycobacteria. *Cell Host Microbe* **3,** 137–45 (2008).
20. Morrison, J., Pai, M. & Hopewell, P. C. Tuberculosis and latent tuberculosis infection in close contacts of people with pulmonary tuberculosis in low-income and middle-income countries: a systematic review and meta-analysis. *Lancet Infect. Dis.* **8,** 359–368 (2008).
21. Fauci, A. S. Multidrug-Resistant and Extensively Drug-Resistant Tuberculosis: The National Institute of Allergy and Infectious Diseases Research Agenda and Recommendations for Priority Research. *J. Infect. Dis.* **197,** 1493–1498 (2008).
22. Optimizing Second-Line Therapy for Drug-Resistant Tuberculosis: the Additive Value of Sequencing for Multiple Resistance Loci. *Antimicrob. Agents Chemother.* **55,** 3968–3969 (2011).

23. HHS, CDC & NCHHSTP. THE COSTLY BURDEN OF DRUG-RESISTANT TB IN THE U.S.

24. Burman, W. J. *et al.* Noncompliance With Directly Observed Therapy for Tuberculosis: Epidemiology and Effect on the Outcome of Treatment. *Chest* **111,** 1168–1173 (1997).

25. Jaggarajamma, K. *et al.* REASONS FOR NON-COMPLIANCE AMONG PATIENTS TREATED UNDER REVISED NATIONAL TUBERCULOSIS CONTROL PROGRAMME (RNTCP), TIRUVALLUR DISTRICT, SOUTH INDIA. *Indian J. Tuberc. J Tuberc* **54,** 130–135 (2006).

26. Dheda, K. & Migliori, G. B. The global rise of extensively drug-resistant tuberculosis: is the time to bring back sanatoria now overdue? *Lancet (London, England)* **379,** 773–5 (2012).

27. Warrier, T. *et al.* Identification of Novel Anti-mycobacterial Compounds by Screening a Pharmaceutical Small-Molecule Library against Nonreplicating Mycobacterium tuberculosis. doi:10.1021/acsinfecdis.5b00025

Chapter 2:

A high throughput screen uncovered X-B016178918, a compound that selectively kills replicating *Mycobacterium tuberculosis*

Summary

One method of identifying potential drug targets is to screen chemical libraries for compounds which produce a desired phenotype (e.g. cell death)[1]. After compounds that can kill bacteria have been identified, cells can be exposed to lethal concentrations of the compound of interest, and resistant colonies grown. The DNA from these colonies can then be sequenced to determine genetic mutations that may cause the resistance, thereby indicating the mechanism of resistance and possibly the mechanism of action. After testing compounds from Sanofi's chemical library, one compound, X-B016178918 (8918) was identified as a potential hit. 8918 was an attractive compound because the parent compound, proguanil, is a well-established drug, and 8918 similarly did not have any major structural red flags. We found that 8918 was mycobacteria specific, and active on replicating *Mycobacteria tuberculosis*, as well as active in a highly acute mouse model of Mtb infection. We also observed that 8918 appeared to have a distinct target from Mtb drugs, and that 8918-resistant mutants had mutations in *rv2795c*, a non-essential enzyme of unknown function, as well as *rv2794c/pptT*, a relatively well-characterized and essential enzyme in the same operon as *rv2795c*.

Introduction

As part of a broad-scale effort to uncover potential new targets and drug classes, our lab has been engaged in high-throughput screening of chemical libraries. We have

screened around 840,000 compounds in replicating and non-replicating assays, where Mtb is exposed to a test compound at a single concentration for 7 days, and the impact the compound has on growth is determined. Of those 840,000 compounds, 7800 had been shown to have activity against *M. smegmatis* or *M. marinum* whole cells, with unknown targets. Among that set of 7800 compounds with whole cell anti-mycobacterial activity, we identified the compound X-B016178918 (8918). 8918 was initially considered a compound of interest in part due to its similarity to the parent compound proguanil, as shown in **Figure 1**. Proguanil is a well-established drug used to treat *Plasmodium falciparum* (malaria), and is considered a WHO essential medicine[2]. Proguanil is typically co-administered with atovaquone, as the two drugs synergize to disrupt the potential of the *Plasmodium* mitochondrial membrane[3]. This synergy and membrane potential disruption is considered the main mechanism of action of proguanil, but proguanil is also metabolized by the liver into cycloguanil, and cycloguanil can act as a *Plasmodium* dihydrofolate reductase inhibitor[4]. We hypothesized that 8918 may act as a dihydrofolate reductase (DHFR) inhibitor in Mtb.

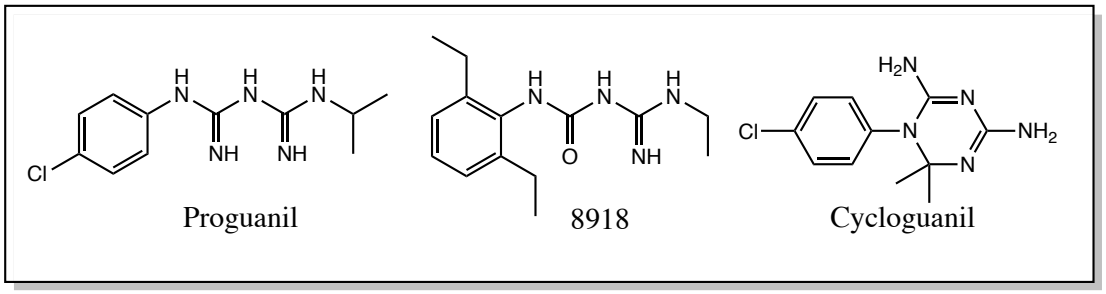

Figure 1: Structures of proguanil, 8918, and cycloguanil

8918 was also initially flagged as a compound of interest because of some apparent activity in non-replicating (NR) as well as replicating (R) conditions. The

vast majority of antibiotics are active on replicating bacteria, and compounds which can target cells that are not currently replicating are highly desired[5,6]. With potential dual activity and a hypothesized mode of action work was initiated to better understand the activity of 8918.

Results

The structure-activity relationship of 8918 against Mtb

After 8918 was selected as a compound of interest, Sanofi began to examine the structure and to generate similar compounds in order to expand information about the structure-activity relationship (SAR) of the family. They found a narrow SAR, as the structure could not be modified in many ways without reducing activity. Wild-type (WT) Mtb was exposed to decreasing concentrations of proguanil, lidamidine, and 8918 to determine the minimum inhibitory concentration (MIC) (**Figure 2A**). Lidamidine was of interest as it has a very similar structure to 8918, and is a commercially available anti-diarrheal drug[7] (**Figure 2B**).

A.

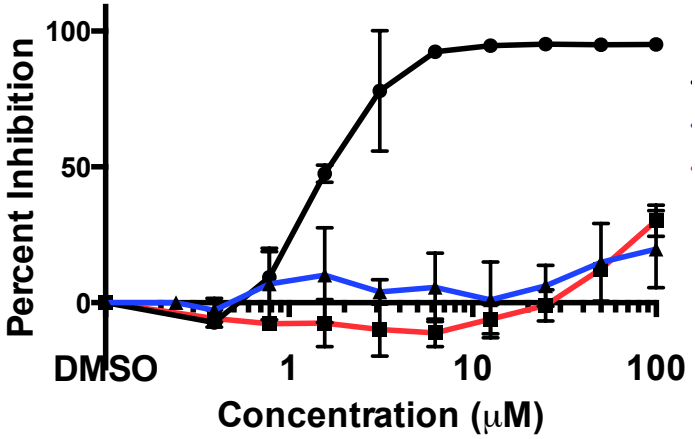

B.

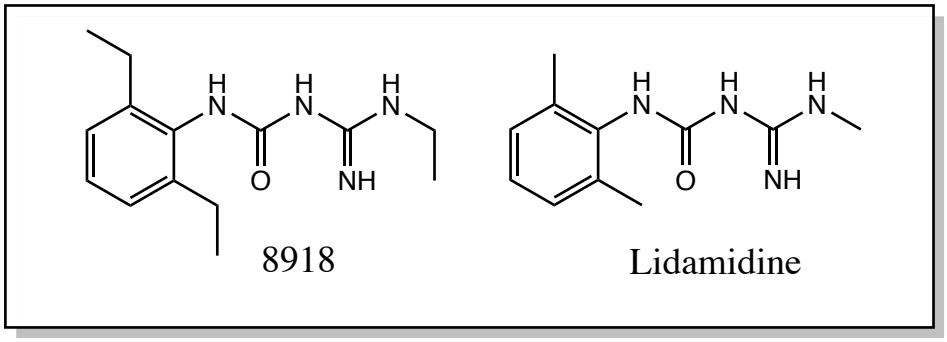

Figure 2: Activity and structure of 8918 and lidamidine (A) Activity of 8918 (black circles), lidamidine (blue triangles), and proguanil (red squares on wild-type Mtb. **(B)** Structures of X-B016178918 and lidamidine.

Because of the structural similarity between lidamidine and 8918, we decided to include it in future studies as an inactive control to 8918.

8918 activity is specific to Mycobacteria

Before attempting to determine the target of a compound, it is helpful to know if the

activity is specific, as non-specific activity can indicate general toxicity and be challenging to analyze. Additionally, it is helpful to have antibiotics that are as narrow spectrum as possible, so that incidental resistance does not occur. Because many people do not know they are infected with Mtb, if an antibiotic is active against other common infections it is likely a patient may take the drug to treat a non-mycobacterial infection, thus accidentally selecting for resistant Mtb in undiagnosed infection[8]. Additionally, standard treatment for Mtb infection is prolonged, and broad spectrum antibiotics can wreak havoc on the gut microbiome, dysbiosis of which has been linked to a number of health problems that can be exacerbated by the impact of antibiotic treatment[9,10]. 8918 was tested against *Candida albicans, Pseudomonas aeruginosa*, *Escherichia coli*, *Staphylococcus aureus*, *Mycobacterium smegmatis,* BCG (attenuated strain of Mtb) and *Mycobacterium tuberculosis*. We found that 8918 was only active against *Mycobacteria* species, and the MIC_{90} for non-mycobacterial strains was above 100 μM, as indicated in **Table 1**. This indicates a narrow spectrum of activity for 8918.

Table 1: Summary of MIC_{90} data for several bacterial species

MIC_{90} (μM) of 8918						
C. albicans	*P. aeruginosa*	*E. coli*	*S. aureus*	*M. smegmatis*	*BCG*	*M. tuberculosis*
>100	>100	>100	>100	**0.78**	**6.25**	**3.13**

Investigating the activity of 8918 against replicating and non-replicating Mtb

The potential dual activity of 8918 (active in both replicating and non-replicating conditions) was of great interest, and we investigated the activity of 8918 further. Beginning with replicating conditions, we saw that 8918 is very active against replicating Mtb, and after exposing cells to decreasing concentrations of 8918 we were

unable to recover any colonies at high concentrations to the limit of detection (**Figure 3A**). We also observed that cell death caused by 8918 was time dependent, though activity was observed after two days of treatment, more death was observed at later time points. Interestingly, we saw that when cells were grown on agar plates containing charcoal we were able to recover colonies at higher concentrations, and that there appeared to be a baseline population of cells that survive treatment regardless of 8918 concentration (**Figure 3B**). When charcoal is added to plates it can absorb compounds that may be carried over from treatment conditions into outgrowth conditions[11]. These results may indicate that 8918 is carried over when cells are transferred onto the outgrowth plates.

We next examined the activity of 8918 on cells that are non-replicating. Our lab typically uses an NR model which includes four stresses; hypoxia, butyrate as the main carbon source, acidic pH, and presence of reactive nitrogen species[6]. These stresses are similar when Mtb is inside of immunologically active macrophages, which is a critical process during Mtb infection, as discussed previously[12]. When cells in the 4-stress NR media were exposed to 8918 and then plated on standard 7H11 agar plates, a reduction in colony-forming units was observed (~1.5 $\log_{10}$), indicating that there was some activity against cells in this NR model (**Figure 3C**). However, when the experiment was repeated and the bacteria were plated on 7H11 containing charcoal this effect was ameliorated (**Figure 3D**). This again indicates that 8918 can be carried over by the cells when they are removed from treatment conditions, but that charcoal is effective in absorbing the compound and preventing cell death during outgrowth.

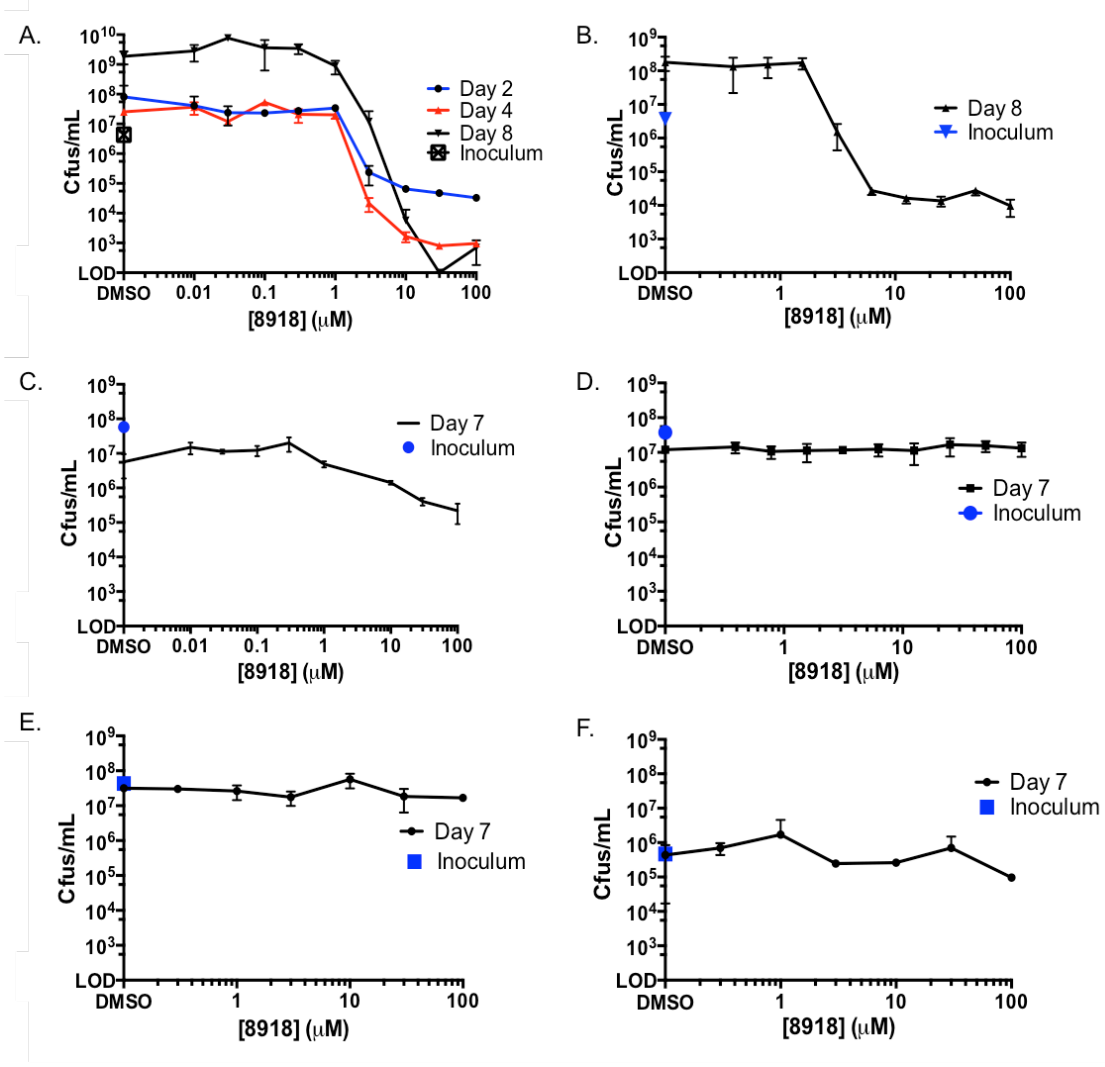

Figure 3: Activity of 8918 against Mtb in non-replicating conditions, and the impact of charcoal on outgrowth. (A) Colonies found after treating replicating Mtb with 8918 after 2, 4, and 8 days on standard 7H11 plates. **(B)** Colonies found after treating replicating Mtb with 8918, recovered on 7H11 plates containing charcoal. **(C)** Activity of 8918 on 4-stress non-replicating Mtb, recovered on standard 7H11 plates. **(D)** Activity of 8918 on 4-stress non-replicating Mtb, recovered on 7H11 plates containing charcoal. **(E)** Activity of 8918 on PBS starved non-replicating Mtb, recovered on 7H11 plates containing charcoal. **(F)** Activity of 8918 on hypoxic (O_2 < 0.1%) non-replicating Mtb, recovered on 7H11 plates containing charcoal**.**

There are many methods of inducing a non-replicating state, and 8918 was also tested against Mtb in severe hypoxia and Mtb which has been starved in phosphate buffered saline (PBS) for one month. In both cases, 8918 was not active. Taken together, these data indicate that 8918 is active in replicating conditions, but not non-replicating conditions.

Testing impact of 8918 on folate biosynthetic pathway

Proguanil toxicity against *Plasmodium* is achieved by inhibiting folate biosynthesis, through inhibition of dihydrofolate reductase (DHFR). We hypothesized that 8918 may be impacting the same pathway in Mtb. Para-aminosalicylic acid (PAS) is an antibiotic for Mtb, typically used as a second line drug in resistant infections[13]. PAS kills Mtb by inhibiting folate biosynthesis. It does so by mimicking the structure of p-aminobenzoate (PABA) thereby acting as a pseudo-substrate of dihydropteroate synthase (DHPS) as the PAS structure can be incorporated into downstream products that are inactive due to the substitution of PABA for PAS[14,15]. Additionally, PAS toxicity can be rescued by the addition of methionine, serine, and glycine, as the presence of an excess of these amino acids can bypass incorporation products of the toxic PAS metabolites[16]. Because proguanil and PAS are active in the same pathway, albeit different organisms (malaria vs Mtb), we tested if supplementing with methionine, serine, and glycine could rescue Mtb growth inhibition caused by 8918 treatment, as we hypothesize that 8918 inhibition would also be upstream of the amino acid rescue. We saw that although we could rescue the growth inhibition caused by PAS by supplementing with the three amino acids, there was no difference in toxicity of 8918 against Mtb (**Figure 4)**. This indicates that 8918 is not inhibiting folate biosynthesis in Mtb.

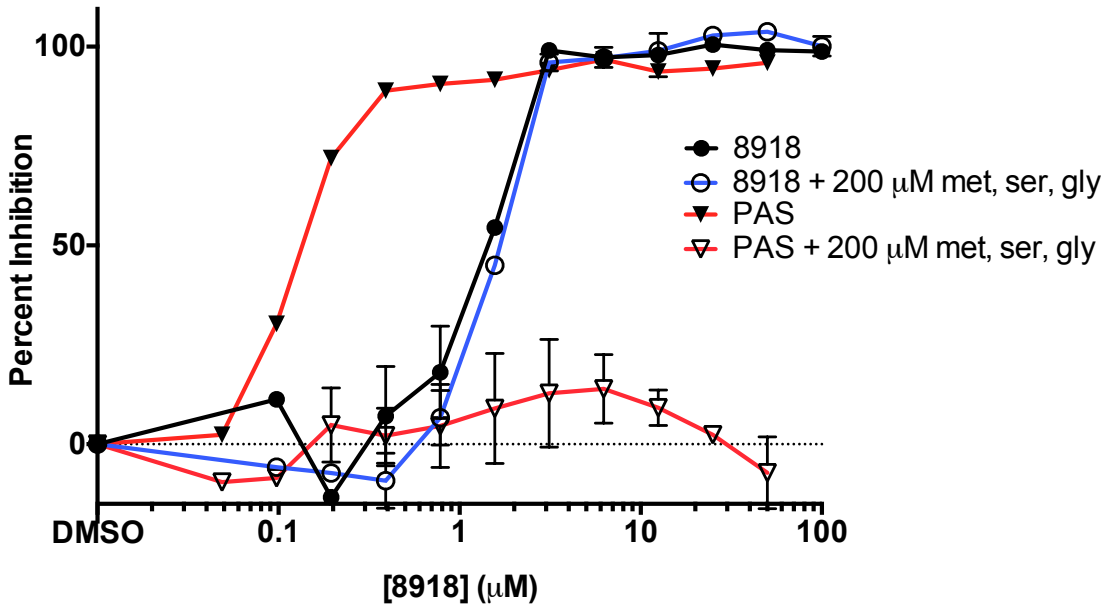

Figure 4: Impact of amino acid supplementation during 8918 treatment. Para-amino salicylic acid (PAS) inhibition of growth (closed triangle) can be rescued by the addition of methionine, serine, and glycine pH 7 (open triangle). 8918 growth inhibition (closed circle) is not impacted by the presence of methionine, serine, and glycine (open circle).

8918 is active in acute mouse model of Mtb infection, moderately active in chronic mouse infection. (Performed by Isabelle Blanc at Sanofi)

One challenge of drug development is that an active compound *in vitro* may not be active when it is used to treat infection with an *in vivo* model. Once a drug is administered, first- and second-pass metabolism may alter the drug, or distribution of the drug may never allow for concentrations to become inhibitory at the desired target. Enzymes may be essential *in vitro* and seem like good drug targets, but may not be essential *in vivo*. Finally, while compounds may be tested for toxicity on mammalian cell lines, such as liver originating HepG2 cells, toxicity may be impossible to predict

until tried in a live organism.

When 8918 was tested in mice acutely infected with Mtb (10^6 bacteria, via nasal innoculation), it was metabolized quickly, but activity was observed at higher doses. Co-administration with aminobenzotriazole (ABT), a CYP450 inhibitor which helps reduce metabolism, allowed for activity of 8918 at lower doses (**Figure 5**). This indicates that 8918 has favorable chemical properties allowing it to maintain concentrations sufficient for antibacterial activity at the site of Mtb infection, and that the target of 8918 is essential for the survival of Mtb during infection.

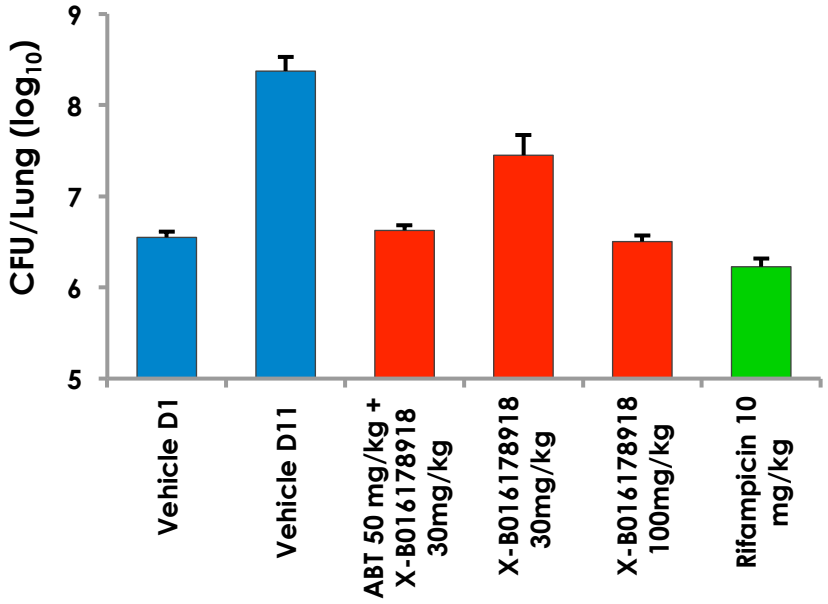

Figure 5: 8918 activity during acute mouse infection. Colony forming units (CFU) per lung of mice infected with high bacterial burden of Mtb after 10 days of treatment. *Experiment performed by Isabelle Blanc, Sanofi.*

8918 was also tested in a chronic mouse infection model, where mice are infected with a low number of bacteria and infection progresses for a longer period of time. In this model, 8918 normalized lung weight to the level of PZA treated mice

(**Figure 6A**). However, there was a modest (0.6 $\log_{10}$) reduction in CFUs recovered from lungs (**Figure 6B**).

A.

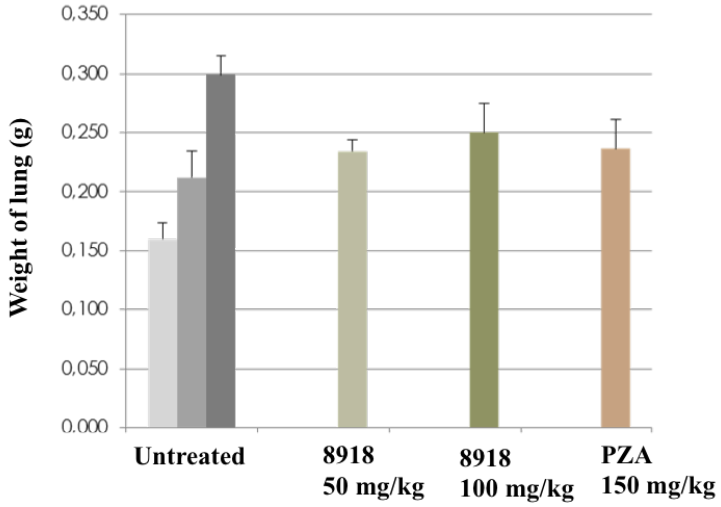

B.

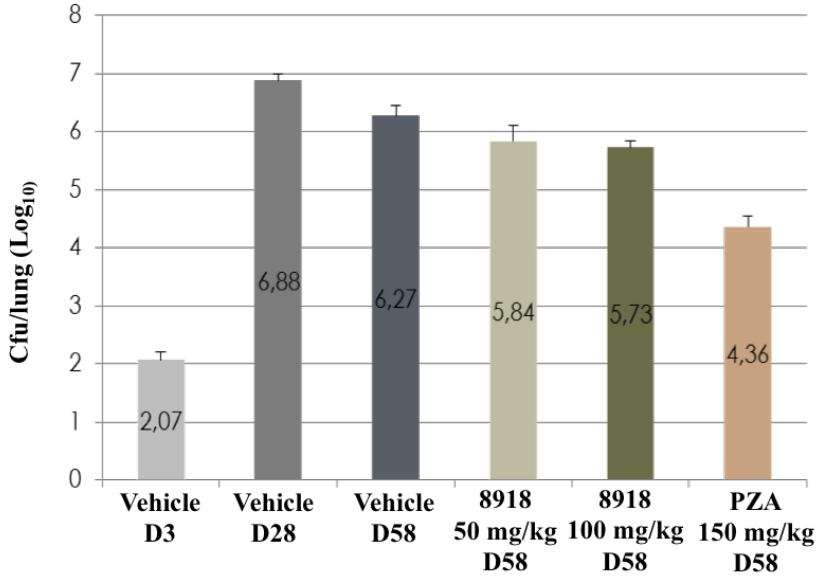

Figure 6: **8918 activity during chronic mouse infection (A)** treatment with 50 mg/kg and 100 mg/kg of 8918 normalized lung weight (g) to similar levels as PZA during chronic infection. **(B)** high doses of 8918 reduced recoverable CFUs modestly (0.6 $\log_{10}$) but to a lesser degree than PZA in the chronic mouse model. *Experiment performed by Isabelle Blanc, Sanofi.*

Selecting for resistant mutants to find genetic determinants of resistance

In order to determine how 8918 kills Mtb, we decided to generate and analyze resistant mutants. Bacteria have natural rates of mutation in all genes, which can vary depending on the fidelity of the species' DNA polymerase, and the impact the mutation has on cell viability. For this reason, a large population of bacteria tends to have a wide variety of mutations, some of which may confer resistance to a given stress or drug. This property of bacterial populations makes multi-drug therapy necessary for Mtb treatment, but it can be used advantageously to determine the mechanism of resistance to a compound. When Mtb is exposed to lethal concentrations of a compound, the members of the population that have a mutation that enables resistance will grow, and the genomes of these colonies can be sequenced to identify mutations which may have caused the resistance. This can implicate the mechanism of resistance, which in turn can elucidate the target, though sometimes resistance mutations are non-specific. We generated resistant mutants in Mtb as well as *Mycobacterium smegmatis* (Msm*),* which is a non-pathogenic and fast-growing species of *Mycobacteria*. 12 colonies were selected from each species and analyzed for mutations. The summary of these data is found in **Table 2** and **Table 3**. Interestingly, Msm mutant selection was done at 10x the MIC and it was possible to isolate resistant mutants. By contrast, Mtb mutant selection was done at 4x and 8x the MIC, but only the 4x MIC plates produced mutants. No Mtb colonies were observed at 8x the MIC of 8918.

Table 2: Summary of resistant Msm mutants isolated. Including MIC to 8918, RIF, and EMB, as well as the gene suspected to cause resistance. Asterisks denote strains which were whole genome resequenced; other mutations were found by PCR and sequencing of gene

	$MIC_{90}(\mu M)$			
	8918	Rif	EMB	Gene mutated
WT	0.78	6.25	1.56	none
A1	50	3.13	1.56	*msm_2647* G206V
A2*	25	3.13	1.56	*msm_2647* 9 bp deletion
A3*	50	3.13	1.56	*msm_2647* D161E
A4	50	3.13	1.56	*msm_2647* Y97D
A5	50	3.13	1.56	*msm_2647* D120N
A6	100	3.13	1.56	unknown
B1	25	3.13	1.56	*msm_2647* D120N
B2	>100	3.13	3.13	*msm_2647* 9 bp deletion
B4*	6.25	3.13	1.56	*msm_2647* Y97D
B5	>100	6.25	1.56	*msm_2647* D161E
B6*	>100	3.13	3.13	*msm_2647* 9 bp deletion

.

Table 3: Summary of resistant Mtb mutants isolated. Including MIC_{90} to PAS, INH, 8918, RIF, EMB and MOXI and the gene suspected to cause resistance. Clones denoted with an asterisk were whole genome resequenced; other clones were analyzed by PCR and sequencing of the genes of interest.

	MIC_{90} (μM)						
MT	PAS	INH	8918	RIF	EMB	MOXI	Gene mutated
WT	<.05	0.39	3.125	0.1	6.25	<.02	none
A1*	<.05	0.39	>100	0.2	3.125	<.02	*rv2795c* H246N
A2	<.05	0.39	>100	0.1	3.125	<.02	*rv2795c* H246N
A3	<.05	.39	>100	0.1	6.25	<.02	*rv2795c* H246N
A4	<.05	0.39	>100	0.1	6.25	<.02	*pptT (rv2794c)* W170S
A5	<.05	0.39	>100	0.2	6.25	<.02	*rv2795c* G266V
A6*	0.1	0.39	>100	0.2	6.25	<.02	*rv2795c* V203F
B1*	0.1	0.39	100	0.2	6.25	<.02	*pptT W170L*
B2*	.20	1.56	>100	0.2	6.25	<.02	*rv2795c* G266V
B3*	0.1	0.39	>100	0.1	6.25	<.02	*rv2795c* R321R, H246N
B4*	0.20	0.39	>100	0.2	6.25	0.04	*rv2795c D51E*
B5	0.1	0.39	>100	0.1	6.25	<.02	*rv2795c* D24N
B6	<.05	0.39	>100	0.1	6.25	<.02	*rv2795c* A41G

The frequency of resistance (FOR) found against 8918 was $7x10^{-7}$ in Msm and $3x10^{-7}$ in Mtb, a similar FOR for both species, and an FOR that is comparable to TB antibiotics[17]. Of note is that none of the 8918 resistant mutants had cross-resistance to standard Mtb drugs, which may indicate that 8918 is inhibiting a different target, and

that the resistance observed was specific to 8918. *rv2795c* (Mtb) and its Msm homolog *msm_2647* was by far the most commonly mutated gene, present in all Msm mutants and 10 out of 12 Mtb mutants. *pptT* was found to be mutated in 2 Mtb clones, with the same amino acid residue mutated in both. Later work with a summer student (Raphael Kirou) uncovered an 8918 resistant Msm mutant with a P67 mutation in the *pptT* homolog *msm_2648*. *rv2795c* and *pptT* are predicted to be in the same operon, and have a small overlap of sequences.

Discussion

Taken together, these data indicate that 8918 kills Mtb through a novel and Mtb-specific target. We observed that 8918 did not kill non-mycobacterial species in an antimicrobial spectrum screen. Further, clones resistant to 8918 had no cross resistance to any Mtb drugs tested, which led us to suspect that resistance to 8918 was specific, i.e. not caused by non-specific efflux or increased metabolism into a non-toxic structure. We also hypothesized that the target is different from the Mtb drugs tested, as otherwise mutations in the same target may have resulted in cross resistance. Initially 8918 was chosen as a compound of interest because of its structural similarity to proguanil, and the possibility that 8918 could be acting as a dihydrofolate reducase inhibitor. Because 8918 inhibition was not rescued by addition of methionine, serine, and glycine, as dihydrofolate synthesis inhibition caused by PAS can be, we also hypothesized that 8918 has a mechanism of action distinct from proguanil, despite their structural similarities. We therefore hypothesize that 8918 has a target distinct from RIF, EMB, INH, PAS, MOXI, and proguanil.

8918 appears to be active specifically on replicating Mtb. We tested a variety of conditions that induce non-replication and saw that 8918 did not kill in hypoxia, 4-stress, or PBS starved cells. It was interesting that there was a significant difference

when cells were grown on plates with or without charcoal after treatment. In replicating cells, outgrowth on standard 7H11 plates showed a strong reduction in CFUs, with no colonies recoverable to the limit of detection at high concentrations of 8918. By contrast, outgrowth of an identically performed exposure on 7H11 plates containing charcoal showed that although 8918 did lead to a multi-$\log_{10}$ reduction of CFUs, there was a concentration independent population of about 10^4 cells that were constant and not impacted by treatment. These cells may represent a persistent population, and the activity of 8918 specifically on replicating cells may indicate that these cells were non-replicating persisters in the original treatment conditions[18,19]. The large reduction of CFUs observed on regular 7H11 plates during outgrowth from NR exposure indicates that 8918 might stick to cell membranes or be taken into the cells at relatively high levels during non-replication. Then, when the cells are plated onto 7H11 without charcoal and start to replicate again, 8918 is present in sufficient concentrations to kill the cells and reduce the recoverable CFUs. When cells are plated on 7H11 with charcoal, the charcoal can absorb the 8918 that is carried over inside or on the cell membrane, and at higher doses the approximately 10^4 cells that are killed by carryover on regular 7H11 plates are able to grow. In the case of NR cells treated with 8918, it appears that any activity observed in the conditions tested may be attributed to the carryover of compound into outgrowth, and not any activity of the compound on non-replicating cells—again, because there appears to be no activity when the outgrowth is performed on 7H11 plates containing charcoal.

The results that 8918 is active in the highly acute mouse model and moderately active in the chronic model are encouraging. It is common for compounds to kill Mtb *in vitro* and then have no activity *in vivo*. It is also significant that 8918 is metabolized rapidly in mice, however, there is still a high enough concentration for a long enough time to reduce the bacterial burden in infected mice. This indicates that the target is

vulnerable to *in vivo* inhibition, and therefore is essential for *in vivo* survival of Mtb. Not all genes are essential in all conditions, and sometimes a gene essential *in vitro* is not essential during infection. The activity of 8918 in mice indicates that the target is vulnerable and druggable, and confirms that *pptT* is essential *in vivo*, which has been shown before by attenuated infection in mice with a conditional knockdown of *pptT*[20].

Finally, the mutations found in resistant clones were relatively consistent, indicating that Mtb and Msm had similar frequencies of resistance and that they tended to become resistant to 8918 through mutations in homologous genes. *rv2795c* encodes a gene of unknown function, which is predicted to be non-essential through transposon mutagenesis[21]. As a non-essential enzyme, we hypothesized that it was not the target of 8918, but most likely had a role in the mechanism of resistance of these resistant clones, especially as the Mtb resistant strains with *rv2795c* mutations were highly resistant to 8918, and many of the strains sequenced did not have other mutations which could logically have resulted in resistance. The frequency of mutations in *rv2795c* supports the inference that the enzyme is non-essential, as mutations in non-essential enzymes are less likely to cause growth defects or prevent growth, and therefore may persist in higher numbers throughout a cell population after they occur. Random mutations in non-essential enzymes are far more likely to be loss of function, as opposed to gain of function. Additionally most of the mutations we observed in *rv2795c* impacted amino acids located in the predicted active site and predicted to be involved with magnesium binding, which in turn was the predicted ion involved in catalytic activity, and so we hypothesize that mutations in *rv2795c* result in loss of function of the enzyme, which can enable the cells to become 8918 resistant.

By contrast, Phosphopantetheinyl transferase (PptT) is an essential enzyme, and has been a desired drug target for several years[21,22]. PptT uses Coenzyme A (CoA) to catalyze the activation of precursors for the synthesis of many essential cellular

products, including mycobactins and mycolic acids, which as the names suggest are characteristic mycobacterial products. The identification of mutations in *pptT* in 8918 resistant Mtb and Msm suggest that it likely may be the target. The frequency of mutations found in *pptT* was much lower; this is notable because it may indicate that although the frequency of resistance of 8918 was around 10^{-7}, the frequency of mutation of *pptT* may be closer to 10^{-8}, which is a very low frequency of resistance and is comparable to the FOR for RIF[17,23]. If it is possible to negate the mechanism of resistance caused by *rv2795c*, it may be possible to reduce the FOR of 8918 about 10 fold.

Materials and Methods

Antimicrobial spectrum:

Escherichia coli: Cells were grown in Middlebrook LB broth from a frozen stock at 37°C with shaking overnight. Cultures were then diluted to OD_{580} 0.01 and plated into 96 well plates for experimental groups to be added. Compound and control (meropenem, MIC_{90} = 3.13 μM) dissolved in DMSO were added at varying concentrations. The plates were incubated at 37°C with shaking for 3-5 hours, at which point the OD_{580} was taken.

Pseudomonas aeruginosa: cells were grown overnight in Middlbrook LB broth from a frozen stock at 37°C with shaking. Cultures were diluted to OD_{580} 0.01 and plated into 96 well plates, data collected after 4-5 hours. Moxifloxacin (MIC_{90}=0.8 μM) was used as a control.

Candida albicans: cells were grown in YM media (pH 4.0) at 30°C without shaking, in aerated tissue culture flasks for 36 hours. Cells were diluted to OD_{580} 0.01, plated into 96 well plates and exposed to compound. After 36 hours the cells were mixed and the OD_{580} taken, nystatin (MIC_{90}= 1.6 μM) was used as a control.

Staphylococcus aureus: Cells were grown from frozen stocks in Mueller Hinton media overnight at 37°C with shaking. After diluting to OD_{580}= 0.01 cells were exposed to compounds, and shaken at 37°C for 3-5 hours before again taking the OD_{580}. Moxifloxacin (MIC_{90}=0.1 μM) or Rifampicin (MIC_{90}=0.01 μM) were both used as controls.

Mouse infections

All mouse infection experiments were performed by Isabelle Blanc at Sanofi

Highly acute mouse model:

Balb/C 5 week old female mice were infected with $1x10^6$ colonies of H37Rv Mtb (Day 0). Infection method was via nasal inhalation of liquid Mtb culture. The next day (Day 1) lungs were harvested from some mice as Day 1 lungs. The remaining mice were treated with either the experimental compound (8918) or rifampicin as a control. Mice were treated every weekday by oral gavage, and lungs were harvested on Day 11 as the final endpoint for the experiments. Lungs were homogenized and plated for CFUs.

Chronic mouse model:

Balb/C 5 week old female mice were infected with 10^2 CFU of H37Rv Mtb. Lung samples were collected from small cohorts of mice at day 3 and day 28, at which point (day 28) treatment was initiated once a day on weekdays via oral gavage for an additional 25 days, at which point the experiment was ended and lungs collected for homogenization and plating for CFUs.

Replicating and non-replicating MIC or CFU

H37Rv Mtb was the strain used for all experiments. Replicating cultures were

grown in Middlebrook 7H9 media supplemented with 0.2% glycerol, 10% Middlebrook OADC growth supplement, and 0.02% tyloxapol. Cultures were grown at 37°C. Non-replicating cultures were produced by washing replicating cultures twice in an equal volume of PBS and 0.05% tyloxapol. Cells were then resuspended in a modified Sauton's minimal media (0.05% ammonium sulfate, 0.05% monopotassium phosphate, 0.005% ferric ammonium citrate, 0.05% magnesium sulfate, 0.01% zinc sulphate, 0.02% tyloxapol, and 0.05% butyrate at pH 5. To determine CFUs Mtb was plated on Middlebrook 7H11 plates supplemented with 10% OADC supplement and 0.5% glycerol, and with 5 g/L charcoal, if charcoal was required.

Mutant selection of 8918 resistant Mtb and Msm

Msm: 7H11 plates were prepared containing 0.2% glycerol and 19.3 μM 8918 (10x the MIC). Cultures were grown in Middlebrook 7H9 media supplemented with 0.2% glycerol and 0.02% tyloxapol, at 37°C with shaking. Cells were then spun down (4000 RPM) and resuspended at a high concentration, such that 10^8 cells could be plated in 100uL. This concentrated cell stock was then used to make a dilution such that 10^7 cells could be plated in 100uL. The original inoculum was plated on 7H11 plates not containing 8918 at the time of plating to calculate the FOR. After resistant colonies were selected, they were restreaked on plates containing the same concentration of 8918 the cells were originally selected on to confirm resistance, followed by testing the MIC_{90}.

Mtb: 7H11 plates were prepared containing 0.2% glycerol, 10% OADC, and 12.5 μM 8918, or 25 μM 8918 (4x and 8x the MIC, respectively) 10^8 and 10^7 cells were also used as the number of cells plated on each agar plate. Colonies selected for further testing were restreaked on plates containing 12.5 μM 8918 to confirm resistance, then grown in liquid 7H9 media and tested for MIC against 8918.

REFERENCES

1. Warrier, T. *et al.* Identification of Novel Anti-mycobacterial Compounds by Screening a Pharmaceutical Small-Molecule Library against Nonreplicating Mycobacterium tuberculosis. doi:10.1021/acsinfecdis.5b00025

2. Annex 1 19th WHO Model List of Essential Medicines (April 2015). *WHO* (2015).

3. Srivastava, I. K. & Vaidya, A. B. A mechanism for the synergistic antimalarial action of atovaquone and proguanil. *Antimicrob. Agents Chemother.* **43,** 1334–9 (1999).

4. Foote, S. J., Galatis, D. & Cowman, A. F. Amino acids in the dihydrofolate reductase-thymidylate synthase gene of Plasmodium falciparum involved in cycloguanil resistance differ from those involved in pyrimethamine resistance. *Med. Sci.* **87,** 3014–3017 (1990).

5. Sacchettini, J. C., Rubin, E. J. & Freundlich, J. S. Drugs versus bugs: in pursuit of the persistent predator Mycobacterium tuberculosis. *Nat. Rev. Microbiol.* **6,** 41–52 (2008).

6. Bryk, R. *et al.* Selective killing of nonreplicating mycobacteria. *Cell Host Microbe* **3,** 137–45 (2008).

7. Sninsky, C. A., Davis, R. H., Clench, M. H., Thomas, K. D. & Mathias, J. R. Effect of lidamidine hydrochloride and loperamide on gastric emptying and transit of the small intestine. A double-blind study. *Gastroenterology* **90,** 68–73 (1986).

8. Leekha, S., Terrell, C. L. & Edson, R. S. General principles of antimicrobial therapy. *Mayo Clin. Proc.* **86,** 156–67 (2011).

9. Langdon, A., Crook, N. & Dantas, G. The effects of antibiotics on the microbiome throughout development and alternative approaches for therapeutic modulation. *Genome Med.* **8,** 39 (2016).

10. Zaura, E. *et al.* Same Exposure but Two Radically Different Responses to Antibiotics: Resilience of the Salivary Microbiome versus Long-Term Microbial Shifts in Feces. doi:10.1128/mBio.01693-15

11. Gold, B. *et al.* Rapid, semiquantitative assay to discriminate among compounds with activity against replicating or nonreplicating Mycobacterium tuberculosis. *Antimicrob. Agents Chemother.* **59,** 6521–6538 (2015).

12. Sasindran, S. J. & Torrelles, J. B. Mycobacterium Tuberculosis Infection and Inflammation: what is Beneficial for the Host and for the Bacterium? *Front. Microbiol.* **2,** 2 (2011).

13. Optimizing Second-Line Therapy for Drug-Resistant Tuberculosis: the Additive Value of Sequencing for Multiple Resistance Loci. *Antimicrob. Agents Chemother.* **55,** 3968–3969 (2011)

14. Chakraborty, S., Gruber, T., Barry, C. E., Boshoff, H. I. & Rhee, K. Y. Para-Aminosalicylic Acid Acts as an Alternative Substrate of Folate Metabolism in Mycobacterium tuberculosis. *Science (80-.).* (2012).

15. Rengarajan, J. *et al.* The folate pathway is a target for resistance to the drug para-aminosalicylic acid (PAS) in mycobacteria. *Mol. Microbiol.* **53,** 275–282 (2004).

16. Nixon, M. R. *et al.* Folate Pathway Disruption Leads to Critical Disruption of Methionine Derivatives in Mycobacterium tuberculosis. *Chem. Biol.* **21,** 819–830 (2014).

17. Martinez, J. L. & Baquero, F. Mutation frequencies and antibiotic resistance. *Antimicrob. Agents Chemother.* **44,** 1771–7 (2000).

18. Brauner, A., Fridman, O., Gefen, O. & Balaban, N. Q. Distinguishing between resistance, tolerance and persistence to antibiotic treatment. *Nat. Publ. Gr.* **14,** (2016).

19. Nathan, C. Fresh approaches to anti-infective therapies. *Sci. Transl. Med.* **4,** 140sr2 (2012).

20. Leblanc, C. *et al.* 4′-Phosphopantetheinyl Transferase PptT, a New Drug Target Required for Mycobacterium tuberculosis Growth and Persistence In Vivo. *PLoS Pathog.* **8,** (2012).

21. Sassetti, C. M., Boyd, D. H. & Rubin, E. J. Genes required for mycobacterial growth defined by high density mutagenesis. *Mol. Microbiol.* **48,** 77–84 (2003).

22. Chalut, C., Botella, L., de Sousa-D'Auria, C., Houssin, C. & Guilhot, C. The nonredundant roles of two 4'-phosphopantetheinyl transferases in vital processes of Mycobacteria. *Proc. Natl. Acad. Sci. U. S. A.* **103,** 8511–6 (2006).

23. Lyu, L.-D. & Zhao, G.-P. Determination of Rifampicin-resistance Mutation Frequency and Analysis of Mutation Spectra in Mycobacteria. **4,** (2014).

Chapter 3

Metabolomics indicate 8918 can alter CoA metabolism

Summary

We used metabolomics as a tool to identify the pathway(s) targeted by 8918 activity. We also suspected the Rv2795c may be inactivating or metabolizing 8918 in some way, leading to high-level resistance when the gene is mutated. Thus, we wanted to know if 8918 was acting as a pro-drug, being metabolized to a significant degree, and if we could identify potential active metabolites as a result. We found that 8918 does not appear to be significantly metabolized in WT or the *rv2795c* mutant strain, and therefore is likely not a pro-drug. We also observed that the high MIC_{50} of lidamidine does not appear to be related to the ability of lidamidine to enter the cell. Finally, we saw that CoA biosynthetic pathways seemed to be most impacted by 8918 activity, which is consistent with the hypothesis that PptT is the target.

Introduction

Metabolomics can be an effective tool to understand what happens to cellular metabolism when inhibition from a drug is occurring. If a drug has a specific target, inhibition of this target can manifest itself by increases or decreases in metabolites around the impacted enzyme or enzymes. We wanted to examine metabolism of 8198 itself between WT and MT strains of Mtb, as well as the changes that occurred in cellular metabolites inside the cells. In order to study the way 8918 works, we first looked at compound uptake. To this end, we used a "swimming pool" assay method, in which cells are placed on filters that can then be exposed to compounds for a short period of time before being lysed and examined for metabolites (**Figure 1)**. We compared WT and MT Mtb, as well as the impact of 8918 on WT Mtb at a variety of

8918 concentrations.

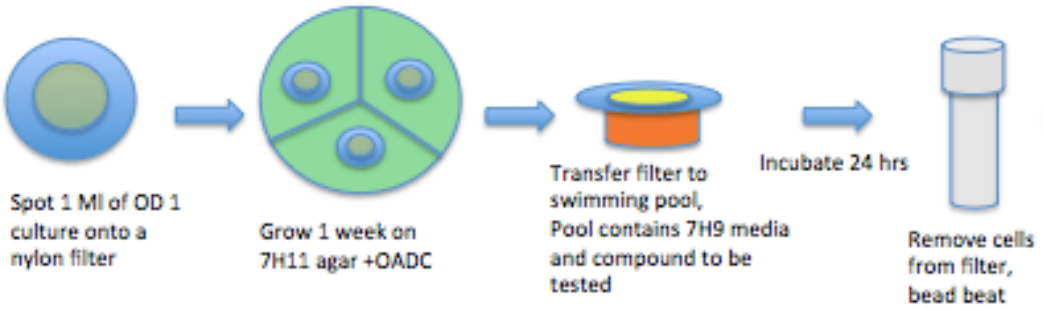

Figure 1: Overview of metabolomics experimental set-up. After lysate is generated it is injected for mass spectrometery (MS) analysis

Results

Determining appropriate concentration of 8918 for metabolomic experiments

Before setting up experiments to examine relative metabolite concentrations we wanted to ensure that we knew what concentrations of 8918 were likely to be sublethal or lethal on the filter setup. Because the filters are inoculated with 1 mL of OD_{580} 1 and are then grown on agar for a week, the inoculum for the experiment is very high, which is necessary to get metabolite concentrations high enough for detection. We had previously observed that 8918 had an inoculum effect at high concentrations of cells, which resulted in a much higher than normal MIC[1]. Additionally, the MIC in agar vs liquid media may be slightly different. We made agar plates with concentrations ranging from 10-50 μM 8918 and placed the filters with the 1 mL cell mat on the plates. We observed that 40 μM 8918 over a week was growth inhibitory to the cells, and selected 40 μM as our baseline concentration for experiments.

Examining metabolism of 8918 in WT vs MT cells

Initially we hypothesized that Rv2795c activates 8918, and therefore loss of function

mutations in *rv2795c* could lead to resistance from 8918 no longer being metabolized into its lethal form. To this end we set up a metabolomics experiment comparing uptake and metabolism of WT Mtb and the *rv2795c* H246N mutant strain of Mtb, with 40 μM 8918, and with 40 μM proguanil as an inactive control. We observed that both compounds seemed to be taken up readily into the cells, as demonstrated by high levels of compounds detected from the filter/cell fraction, and very little compound remaining in the swimming pool section of the experimental setup (**Figure 2A-B**). We also observed that there was not a significant difference in recoverable 8918 or proguanil between the WT and MT strains of Mtb. (**Figure 2C-D**). As there was no significant loss of recoverable 8918 between MT and WT strains, we hypothesized that the resistance mechanism was not related to loss of function of an activating enzyme. Additionally, no significant levels of 8918 metabolic products were detectable in the MS data, and only minor amounts of methylated and hydroxylated 8918 were observed in both WT and MT Mtb, further indicating that 8918 was not being significantly metabolized in either strain.

Figure 2: Detection of 8918 and proguanil in cells vs swimming pool fractions (A) Area under the curve (AUC) ion counts for 8918 and proguanil, in WT (blue) and MT (red) strains recovered from the Mtb cells. **(B)** AUC ion counts for 8918 and proguanil, in WT (blue) and MT (red) strains, recovered from the swimming pool section (separate from cells). **(C)** AUC ion counts for media (red) and cell (lysate)(blue) fractions together for 8918 in MT and WT strains. **(D)** AUC ion counts for media (red) and cell (lysate)(blue) fractions together for proguanil in MT and WT strains. *Experiment and analysis done with the help of Madhumitha Nandakumar.*

A.

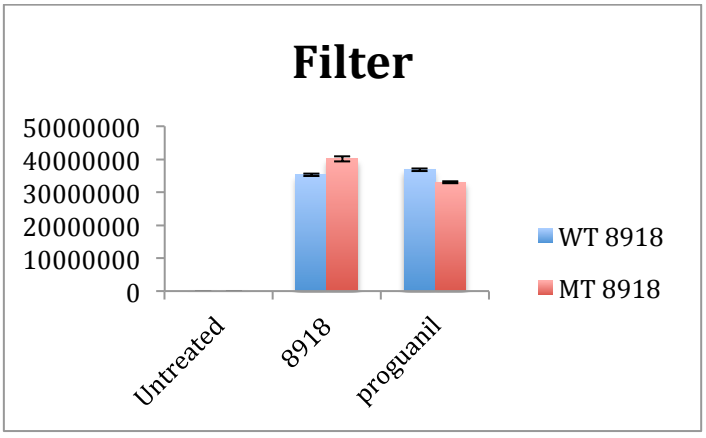
Filter
50000000
40000000
30000000
20000000
10000000
0
Untreated
8918
proguanil
WT 8918
MT 8918

B.

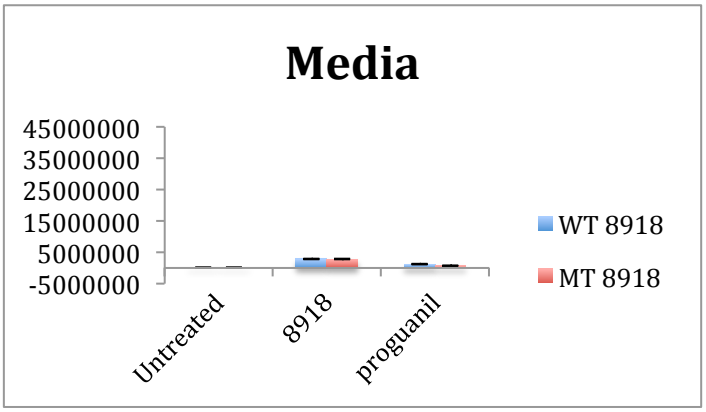
Media
45000000
35000000
25000000
15000000
5000000
-5000000
Untreated
8918
proguanil
WT 8918
MT 8918

C.

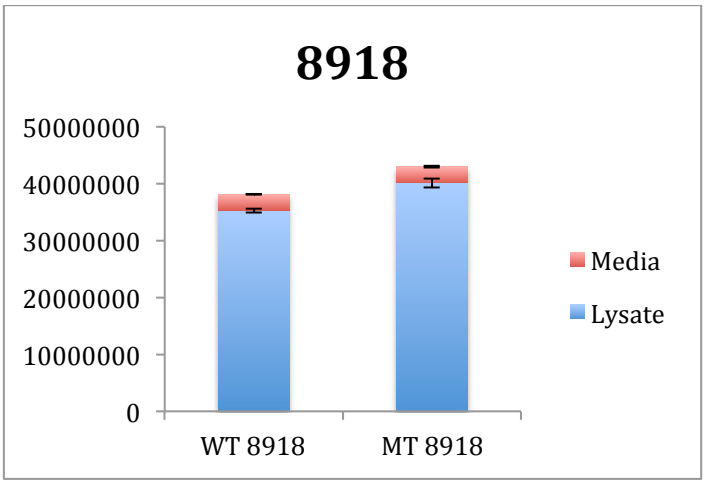
8918
50000000
40000000
30000000
20000000
10000000
0
WT 8918
MT 8918
Media
Lysate

Figure 2 continued

D.

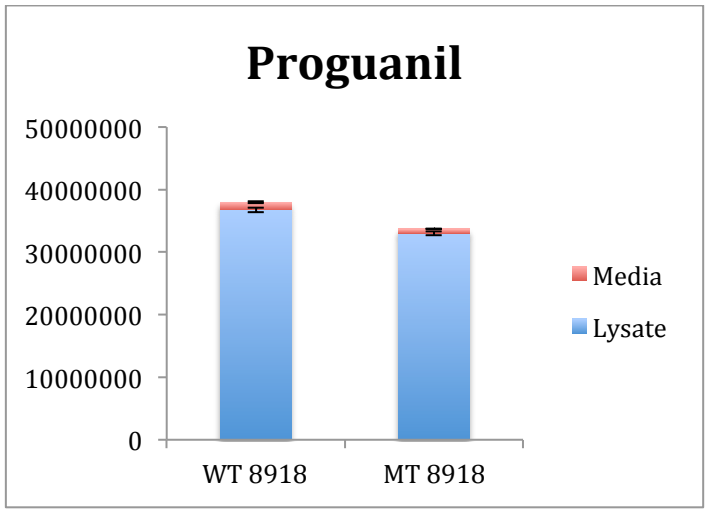

We next wanted to observe more broadly the impacts of 8918 on cell metabolism, to identify what pathway was being impacted. In this experiment we used 20, 40, 200, and 400 μM of 8918 as the active compound concentrations. A dose curve was performed as dose-dependent changes in metabolites provide evidence that any changes observed are related to the activity of the compound. Additionally, lidamidine and proguanil were selected in this experiment as inactive controls. Lidamidine has a more similar structure to 8918 than proguanil, and we wanted to test if it was also a good inactive control in metabolomics. We first observed that out of the 3 compounds, 8918 accumulates inside cells to a far lesser degree, again indicating that the inactivity of proguanil and lidamidine is not related to an inability to get inside Mtb (**Figure 3**). The amounts recovered were slightly lower but still comparable to the first metabolomics experiment tried (**Figure 2**).

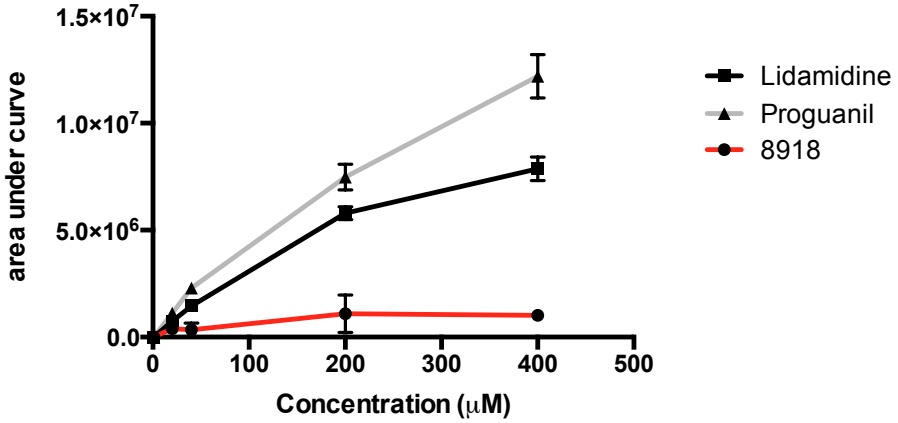

Figure 3: AUC at 0, 20, 40, 200, and 400 µM. AUC of lidamidine (black) proguanil (grey) and 8918 (red) recovered from cell lysates in metabolomics experiment.

When we moved into a more general analysis, we were looking to see if we could find peaks which were dose-dependently accumulated or depleted after 8918 treatment, but not in lidamidine or proguanil treated cells. Metabolites that are accumulated across all treatment groups may be related to the compound structure (off target effects) but not the actual activity of the compound. We found that while a number of metabolites were recoverable, only a small number were modified dose dependently by 8918 alone (**Figure 4**).

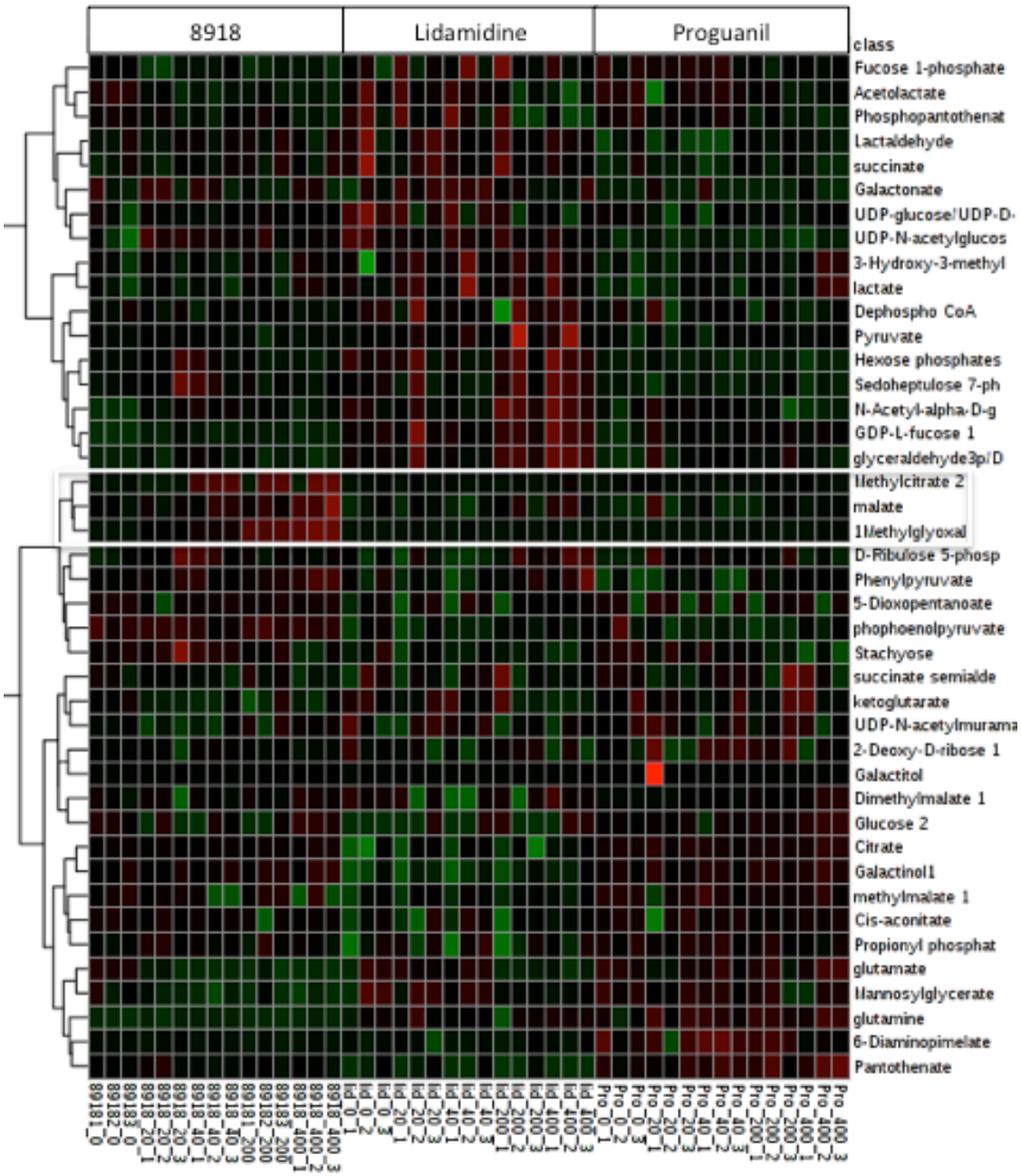

Figure 4: Heatmap of metabolites observed in this experiment. Concentrations are in triplicate, increasing in concentration starting with 8918, followed by lidamidine, then proguanil. (normalized to untreated cells). Color gradient are scaled by Log_2 and range from -6 to +6 based on color intensity, with green representing depletion (down to -6 log_2 and red representing accumulation up to 6 log_2.

Upon further analysis of compounds that were dose dependently impacted by 8918 treatment, we found methyl citrate, malate, propionyl CoA, and 2-dehydropantolactone as the only significant accumulations after 8918 treatment (**Figure 5 A-C**). Methyl citrate and propionyl CoA in particular had striking accumulations, increasing from barely detectable in untreated cells. We also observed depletion of some metabolites: 3-hydroxypropionyl-CoA and R-pantoate showed depletions after 8918 treatment.

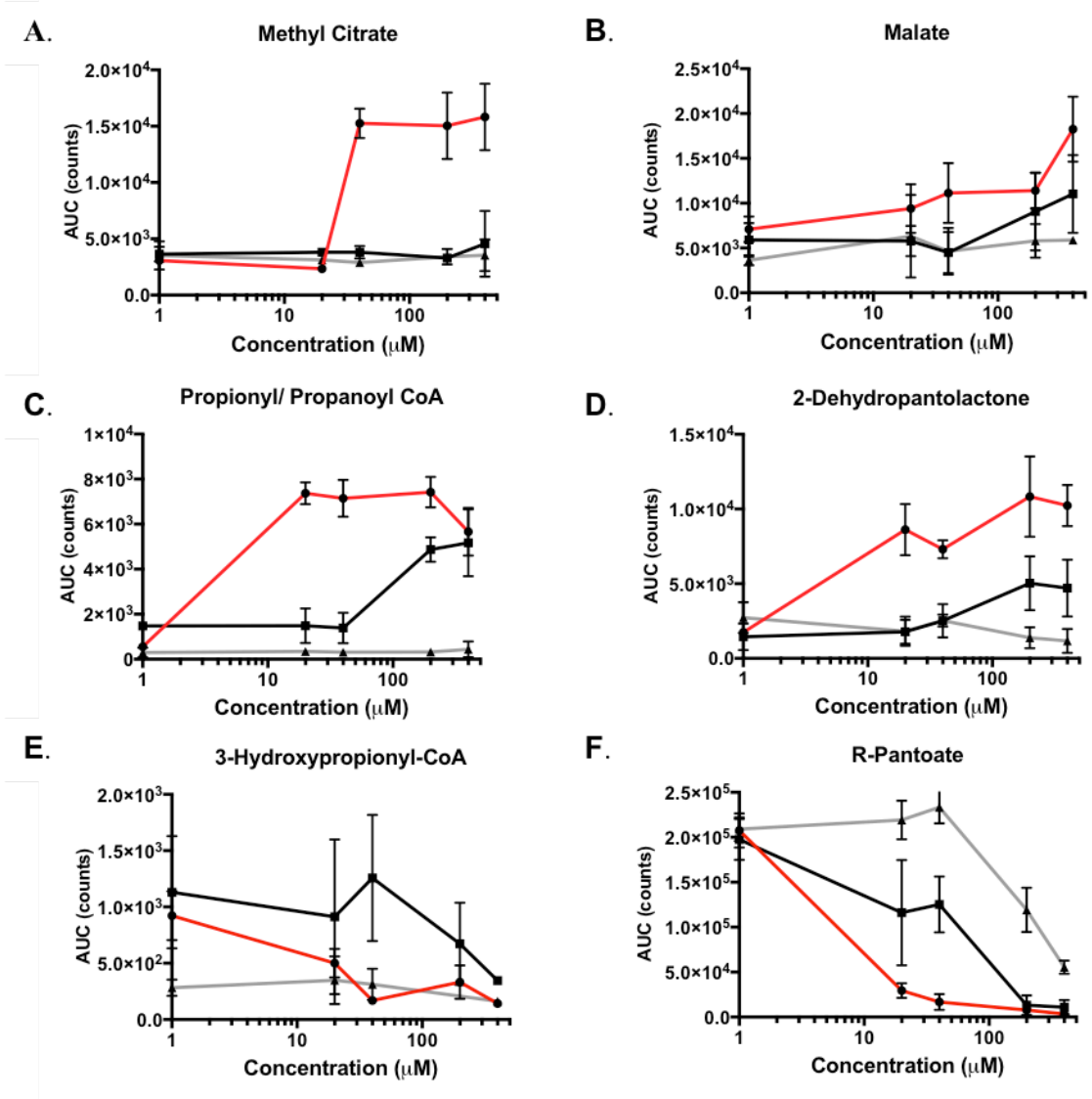

Figure 5: Graphs of dose-dependent and 8918-induced metabolite changes. AUC graphs of 8918 (red line; black circles), lidamidine (black line; black squares), and proguanil (grey line; black triangles). These metabolites represent all the metabolites found which were measureable and dose-dependently impacted by 8918 treatment.

We were interested to see that lidamidine appeared to generate an intermediate metabolic profile, between proguanil and 8918, and hypothesized that lidamidine might inhibit the same target as 8918 but to a lesser degree. We tested the MIC of

lidamidine at a higher concentration, and saw that high concentrations of lidamidine could inhibit cell growth of WT Mtb (**Figure 6**). Lidamidine may be a relatively poor inhibitor, but the high degree of accumulation within the cell may be sufficient to inhibit the target at very high doses.

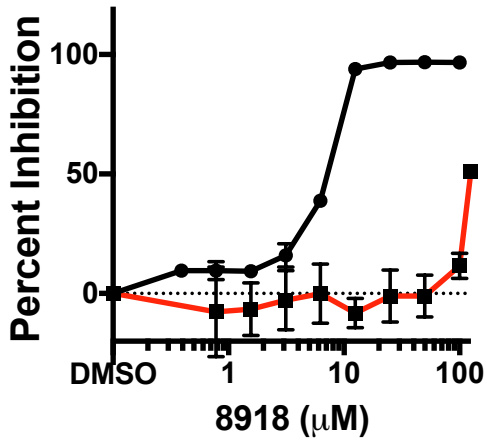

Figure 6: Inhibition of WT Mtb by 8918 (black circles) and lidamidine (red squares). At 100 μM lidamidine does not appear to inhibit Mtb at all, but at 125 μM lidamidine has an MIC_{50}

When the dose-dependently altered metabolites are placed in a connected metabolic map, it becomes apparent that while they may not complete a metabolic pathway, they can be placed relatively near each other. Most notably, they can all be related within a few metabolic steps of CoA (**Figure 7**). This is significant because PptT, the gene of which was found mutated in 8918-resistant Mtb, uses CoA as a substrate, and we hypothesize that inhibition of PptT would result in downstream or upstream changes to CoA precursors.

Figure 7: Schematic overview of all dose-dependent and 8918-specific metabolite changes observed. Green represents depletion of metabolites, and red represents accumulation. CoA is indicated in fuchsia.

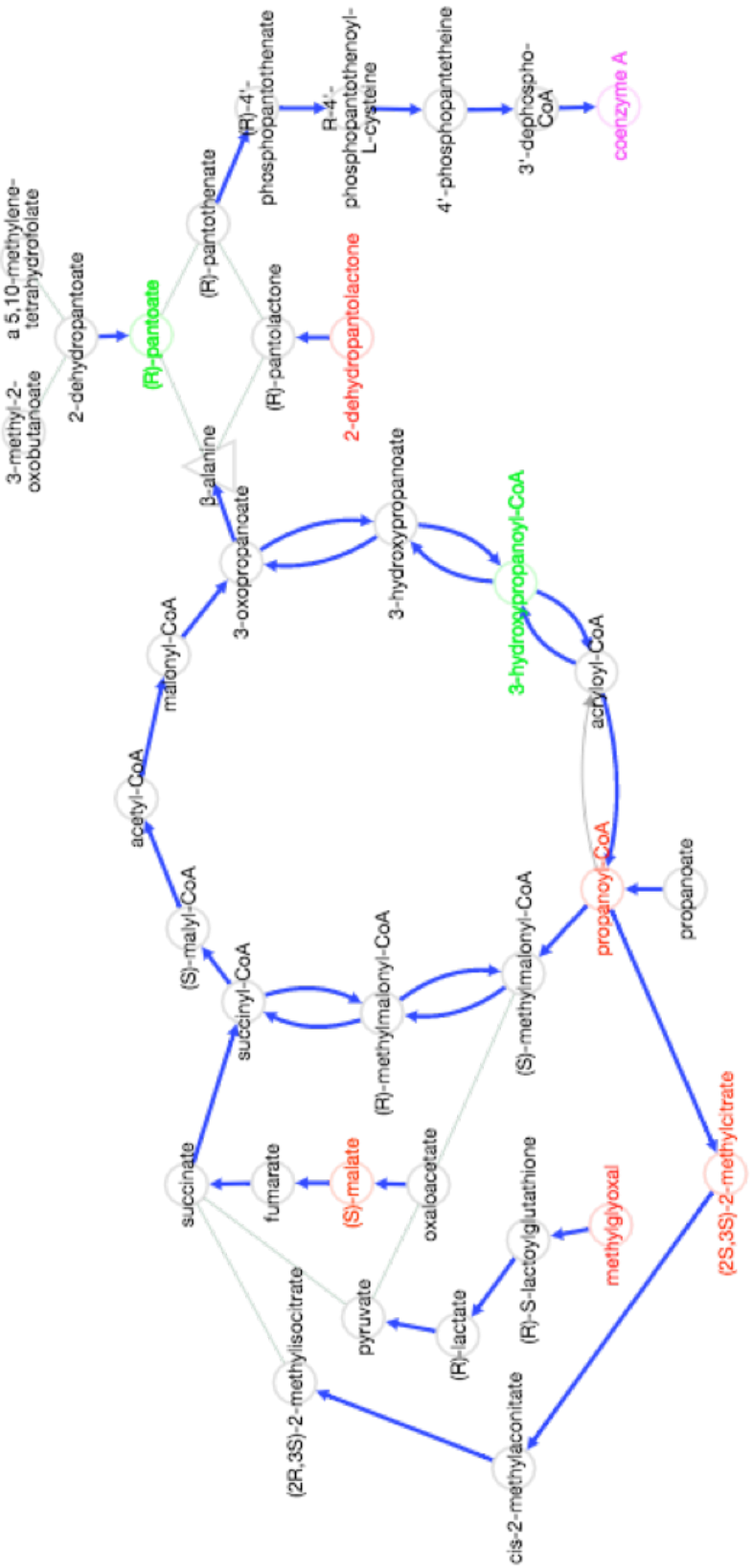
3-methyl-2-oxobutanoate
a 5,10-methylene-tetrahydrofolate
2-dehydropantoate
(R)-pantoate
(R)-pantothenate
(R)-4'-phosphopantothenate
R-4'-phosphopantothenoyl-L-cysteine
4'-phosphopantetheine
3'-dephospho-CoA
coenzyme A
(R)-pantolactone
2-dehydropantolactone
β-alanine
3-oxopropanoate
3-hydroxypropanoate
3-hydroxypropanoyl-CoA
acryloyl-CoA
malonyl-CoA
acetyl-CoA
(S)-malyl-CoA
succinyl-CoA
(R)-methylmalonyl-CoA
(S)-methylmalonyl-CoA
propanoyl-CoA
propanoate
succinate
fumarate
(S)-malate
oxaloacetate
(R)-S-lactoylglutathione
methylglyoxal
(2S,3S)-2-methylcitrate
pyruvate
(R)-lactate
(2R,3S)-2-methylisocitrate
cis-2-methylaconitate

Discussion

At this point it seemed as though Rv2795c was not metabolizing 8918, as mutations causing high levels of resistance to 8918 did not result in any changes in the metabolism of 8918. The fact that proguanil and lidamidine also appear to accumulate within cells at high concentrations indicates that the lack of bactericidal activity from the compounds is most likely due to lack of engagement with the target, though growth inhibition at high concentrations and the intermediate metabolic profile observed with lidamidine indicates that lidamidine may be a weak inhibitor of PptT. Similarly, the high degree to which the compounds enter the cells (or at least are associated with the cells, perhaps stuck in the membrane) also supports the finding that there appears to be a large degree of carryover during outgrowth experiments, as shown by the differences between standard and charcoal CFUs in chapter 2. If 8918 (and similarly structured proguanil and lidamidine) accumulate inside the cells, it could explain why charcoal is necessary to get accurate CFU counts in outgrowth experiments. We also saw that 8918 appeared to accumulate within cells to a lesser degree than lidamidine or proguanil; this may be due to 8918 being mycobactericidal while the other compounds are not, as there may be no benefit to metabolizing or pumping out non-toxic compounds. One caveat to this observation is that due to the experimental setup, the cells were lysed but there was no distinction between membrane and intracellular areas, so we hypothesize that uptake was high but compounds may also just be associating with the cell membrane. We observed high amounts of lidamidine associated with cells but it is possible this accumulation is a combination of membrane association and intracellular concentration. Either way, 8918 is found in lower concentrations, but lidamidine may stick to the cellular membrane to a higher degree.

While 8918 did cause significant dose-dependent changes in metabolites,

Figure 5 also shows that lidamidine sometimes had an intermediate change compared to 8918. This may indicate that although lidamidine does not kill Mtb, it may partially inhibit the target. If lidamidine is less inhibitory than 8918, and it does appear that effects can only be seen at very high concentrations, it may be possible that lidamidine would not cause the cells to die. By contrast, proguanil did not have any dose-dependent metabolic profile, indicating that proguanil does not cause any significant changes in metabolites even at high concentrations.

When placed on a metabolic map showing CoA conversions and precursors, it is notable that the metabolites with significant and dose-dependent changes after 8918 exposure are observed relatively close together, and are related to CoA metabolism. However, many CoA metabolites were not observed or were not significantly changed upon 8918 treatment. Some metabolites (such as CoA) may degrade quickly and be difficult to observe in the experiment as it was done. Some metabolites are challenging to capture with this method, and may not be detectable by this method. Additionally, some metabolites have no standards available, and definitive or confident identification of a peak may be impossible without a proper standard to use as a control. Other metabolites may be present in concentrations too low to detect, and accumulations or depletions, while significant if they occur, may still not be large enough to be detected at our level of sensitivity when run through mass spectrometry analysis. In those cases it may be possible to detect changes with a much higher mass of cells than were used in this experiment.

Ultimately, metabolic changes may not be easily predictable. Because cellular metabolism exists as an interchanging system of pathways, it is very possible for inhibition of an enzyme to manifest in accumulations or depletions further upstream or downstream of the target than may be easily rationalized. Some metabolites may be toxic, and accumulation exacerbates problems initiated by the activity of the toxic

compound. As a result, the toxic metabolite may be rapidly metabolized into something that is less toxic when accumulated. Subject to these caveats, these data support that 8918 activity impacts metabolism related to CoA, and generally causes accumulation of CoA precursors, which fits our hypothesis that PptT is the target of 8918.

Materials and Methods

Metabolomics

H37Rv Mtb was grown to OD_{580} 1 in standard 7H9, and then 1 mL was added to a nylon Durapore 0.22 μm nylon filter. Once the media had been filtered out, the filter with Mtb was placed on top of Middlebrook 7H11 plates supplemented with 0.2% glycerol and 10% OADC. Filters were incubated at 37°C for 1 week, until biomass had significantly increased. Filters were then transferred onto swimming pools containing 3 mL of 7H9 media with 0.2% glycerol (no tyloxapol), and 0, 20, 40, 200, or 400 μM 8918, lidamidine, or proguanil. Swimming pools were constructed from sterile 15 mL falcon tube caps glued inverted into Corning costar 6 well plates. Filters and swimming pools were incubated at 37°C for 24 hours, at which point the filters were placed into chilled bead beating tubes containing 1 mL 40:40:20 methanol:acetonitrile:water and approximately 250 μL bead beating beads. Filters were immediately removed after sloughing the cell mat into the bead beating tube, and the filters were discarded. Tubes were beaten at 4°C for 8 rounds of 30 seconds on, 1 min off. Lysates were filtered using costar Spin-X centrifuge tube filters (0.22 μM nylon) to remove any remaining whole cells. Lysates were then removed from the BSL3 and mixed 1:1 with acetonitrile containing 0.2% formic acid before being run on the mass spectrometer in both positive and negative ion settings. Experiments were performed with the assistance of Madhumitha Nandakuma, Roxanne Morris, and Travis Hartman.

REFERENCES

1. Brook, I. Inoculum effect. *Rev. Infect. Dis.* **11,** 361–8
2. Nandakumar, A. Kumar, R. Liao, T. Rustad, J. C. Sacchettini, K. Y. Rhee, J. S. Freundlich and D. R. Sherman (2014). "Folate pathway disruption leads to critical disruption of methionine derivatives in *Mycobacterium tuberculosis*." Chem Biol **21**(7): 819-830.
3. Nandakumar, M., G. A. Prosser, L. P. de Carvalho and K. Rhee (2015). "Metabolomics of *Mycobacterium tuberculosis*." Mycobacteria Protocols 105-115.

Chapter 4

8918 inhibits Phosphopantetheinyl transferase (PptT)

Summary

After analyzing Mtb mutants resistant to 8918 for genetic changes that could explain their resistance, we identified PptT as a likely candidate for the target. Two mutations in the same tryptophan (W) residue were identified in the screen, indicating that PptT may be the target and W170 may be important for 8918 binding. We therefore decided to investigate the role of PptT in 8918 resistance by expressing recombinant PptT and testing for 8918 inhibition of its it *in vitro* activity. We showed that in an *in vitro* enzymatic assay, 8918 could inhibit the activity of PptT in a non-competitive manner. The indication of non-competitive binding seemed contrary to our finding of the active site mutation, but we found that heterologously expressing MT PptT in WT background Mtb could confer high-level resistance to 8918. The co-crystal of PptT with 8918 indicated that 8918 did bind in a pocket near the suspected W170 residue, but that CoA can bind simultaneously with 8918; this may have been the cause of the non-competitive inhibition result from the *in vitro* assays. Finally, we investigated the changes in lipids that occurred after sublethal concentrations of 8918, and saw that treatment caused depletion of downstream PptT products including PDIMs, sulfolipids, cardiolipins, and mycolic acids.

Introduction

The production of active acyl carrier proteins is an extremely common and essential cellular process. Phosphopantetheinyl transferase (PptT) catalyzes the activation of acyl carrier proteins (ACPs) by transferring the 4'-phosphopantetheine (ppt) moiety from Coenzyme A (CoA) onto apo-ACPs, thereby transforming them into holo-ACPs, as shown in **Figure 1**. Holo-ACPs are active and are essential for the synthesis of

precursors for a number of cellular products, including mycolic acids and mycobactins[1]. Mycolic acids are significant in Mtb biology as they are essential for the bacteria's ability to evade host immune cells, which plays a large role in the ability of the cells to remain viable and virulent[2]. Mycobactins are siderophores Mtb produces and are associated with the cell wall or secreted and can sequester iron; thus they represent a crucial mechanism by which Mtb can acquire iron in iron-deficient environments, such as within a granuloma or macrophage[3,4].

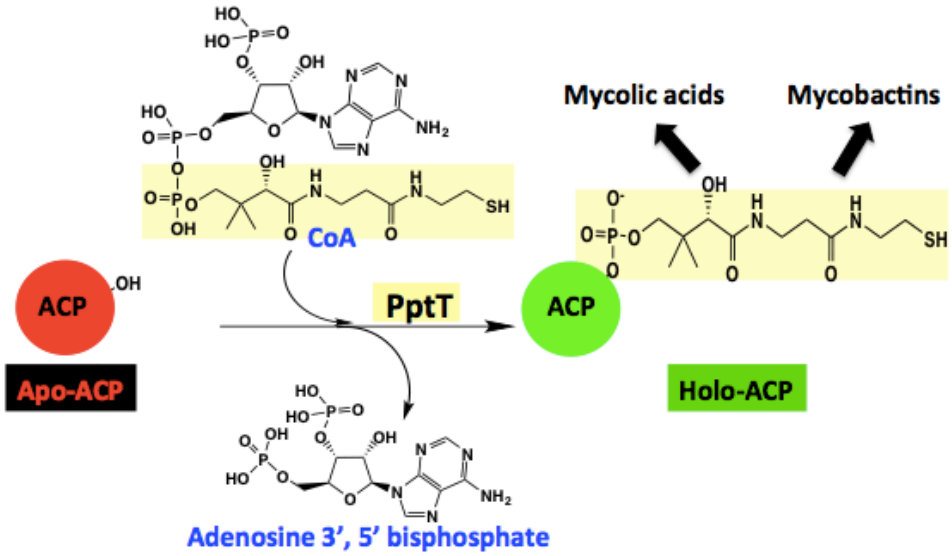

Figure 1: Schematic of reaction catalyzed by PptT and products of PptT

PptT catalyzes the conversion of apo-ACPs to holo-ACPs by transferring the phosphopantetheine arm of CoA onto the acyl carrier protein, releasing adenosine 3', 5' bisphosphate as a product.

PptT has been an attractive drug target for some time and was shown by Leblanc, et al. 2012 to be essential for infection *in vivo*; it was therefore hypothesized that a PptT inhibitor would work to kill Mtb during treatment[5]. Further, Mtb *pptT* is distinct from acyl carrier protein synthases in other bacterial species, and also distinct

from human equivalent enzymes. It was therefore hypothesized that an inhibitor may be narrow spectrum and have few if any on-target effects on mammalian cells.

Results

When PptT was identified as a potential target of 8918, we first were interested in investigating how PptT differs from other phosphopantetheinyl transferases, especially since 8918 appeared to have narrow specificity in our microbial screen. PptT in Mtb is distinct from other enzymes of similar function, however, in that Mtb has two enzymes that may catalyze the formation of holo-ACPs: PptT and acyl carrier protein synthase or AcpS. AcpS and PptT have distinct substrates, and AcpS is not essential for Mtb survival[1]. It is possible that even though the two enzymes have distinct substrates, in the absence of AcpS, PptT can phosphopantetheinylate the substrates of AcpS, though AcpS cannot activate PptT substrates[6]. We hypothesized that AcpS has structural similarity to other bacterial acyl carrier protein synthases, but that PptT was distinct, which would rationalize the narrow/mycobacteria specific activity of 8918. After using T-Expresso to align sequences of Mtb PptT and AcpS from a variety of bacterial species, we saw that AcpS from Mtb has strong structural similarities to other bacterial AcpS proteins, but that PptT is more distinct despite a few regions of similarity **(Figure 2A)**[7,8]. We also saw that PptT has closer structural alignment with mammalian PptT-like enzymes than it does with AcpS, though it still does not have significant homology with these non-bacterial PptT enzymes **(Figure 2B)**. Finally, we saw that the tryptophan 170 residue is highly conserved among mycobacteria species, indicating another explanation of 8918 specificity **(Figure 2C)**.

Figure 2: T-Expresso analysis of Pptases from several species (A) structural alignment based on sequence of Mtb AcpS and *Escherichia coli* AcpS, *Pseudomonas alcaligense* AcpS (*P. aeruginosa* gene information unavailable), *Staphylococcus aureus* AcpS, and Mtb PptT **(B)** Structural alignment based on sequence for Mtb PptT, *Candida albicans* PptT, and human PptT. **(C)** Structural alignment based on sequence for *Mycobacteria* species PptT, W170 highlighted by box.

A.

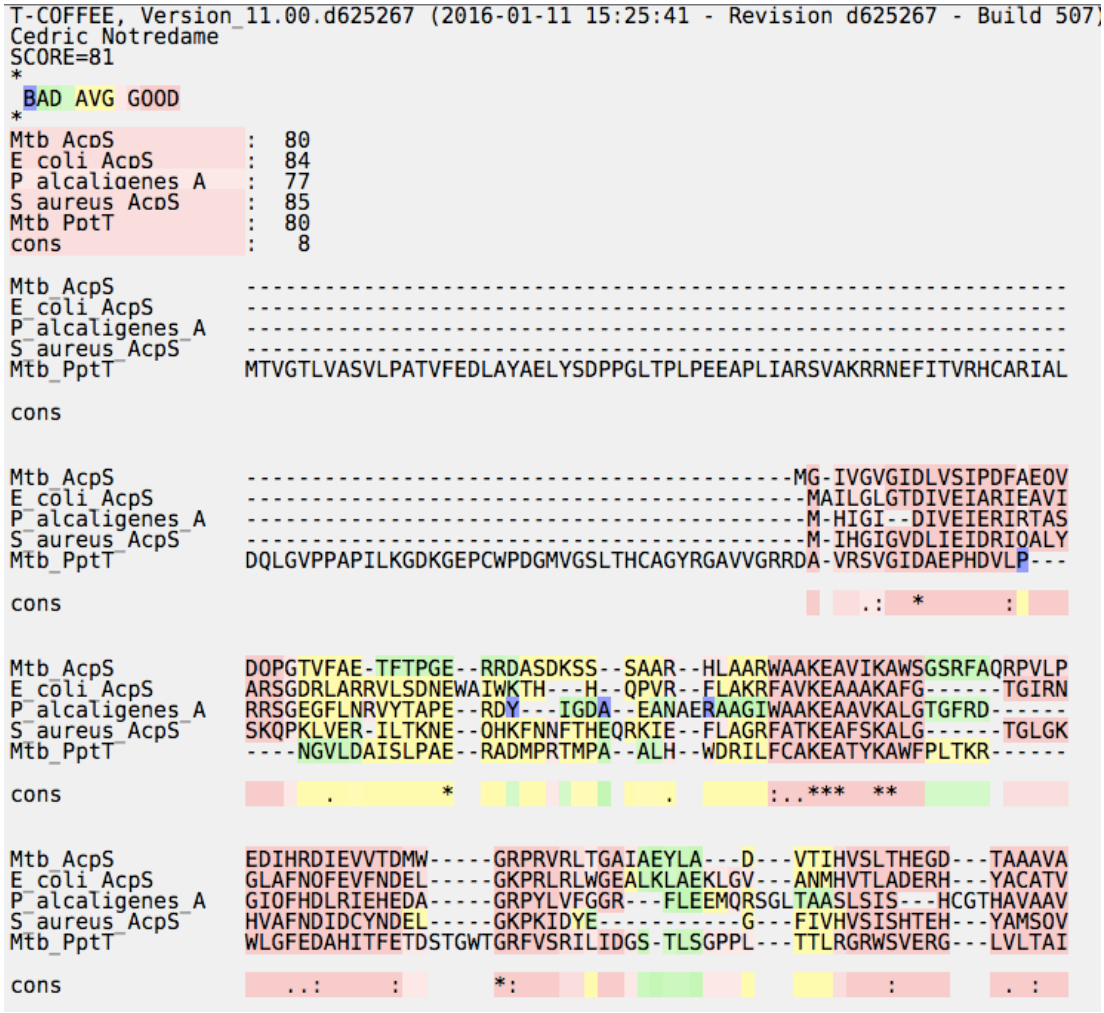
T-COFFEE, Version_11.00.d625267 (2016-01-11 15:25:41 - Revision d625267 - Build 507)
Cedric_Notredame
SCORE=81
BAD AVG GOOD
Mtb_AcpS : 80
E_coli_AcpS : 84
P_alcaligenes_A : 77
S_aureus_AcpS : 85
Mtb_PptT : 80
cons : 8
Mtb_AcpS ----------
E_coli_AcpS ----------
P_alcaligenes_A ----------
S_aureus_AcpS ----------
Mtb_PptT MTVGTLVASVLPATVFEDLAYAELYSDPPGLTPLPEEAPLIARSVAKRRNEFITVRHCARIAL
cons
Mtb_AcpS ----------MG-IVGVGIDLVSIPDFAEQV
E_coli_AcpS ----------MAILGLGTDIVEIARIEAVI
P_alcaligenes_A ----------M-HIGI--DIVEIERIRTAS
S_aureus_AcpS ----------M-IHGIGVDLIEIDRIQALY
Mtb_PptT DQLGVPPAPILKGDKGEPCWPDGMVGSLTHCAGYRGAVVGRRDA-VRSVGIDAEPHDVLP---
cons
Mtb_AcpS DQPGTVFAE-TFTPGE--RRDASDKSS--SAAR--HLAARWAAKEAVIKAWSGSRFAQRPVLP
E_coli_AcpS ARSGDRLARRVLSDNEWAIWKTH---H--QPVR--FLAKRFAVKEAAAKAFG------TGIRN
P_alcaligenes_A RRSGEGFLNRVYTAPE--RDY---IGDA--EANAERAAGIWAAKEAAVKALGTGFRD------
S_aureus_AcpS SKQPKLVER-ILTKNE--QHKFNNFTHEQRKIE--FLAGRFATKEAFSKALG------TGLGK
Mtb_PptT ----NGVLDAISLPAE--RADMPRTMPA--ALH--WDRILFCAKEATYKAWFPLTKR------
cons
Mtb_AcpS EDIHRDIEVVTDMW-----GRPRVRLTGAIAEYLA---D---VTIHVSLTHEGD---TAAAVA
E_coli_AcpS GLAFNQFEVFNDEL-----GKPRLRLWGEALKLAEKLGV---ANMHVTLADERH---YACATV
P_alcaligenes_A GIQFHDLRIEHEDA-----GRPYLVFGGR---FLEEMQRSGLTAASLSIS---HCGTHAVAAV
S_aureus_AcpS HVAFNDIDCYNDEL-----GKPKIDYE----------G---FIVHVSISHTEH---YAMSQV
Mtb_PptT WLGFEDAHITFETDSTGWTGRFVSRILIDGS-TLSGPPL---TTLRGRWSVERG---LVLTAI
cons

Figure 2 continued

B.

Figure 2 continued

C.

```
T-COFFEE, Version_11.00.8cbe486 (2014-08-12 22:05:29 - Revision 8cbe486 - Build 477)
Cedric Notredame
SCORE=98
*
 BAD AVG GOOD
*
tb          :  99
smeg        :  98
m.leprae    :  99
m.avium     :  98
m.bovis     :  99
cons        :   9

tb          MTVGTLVASVLPATVFEDLAYAELYSDPPGLTPLPEEAPLIARSVAKRRNEFITVRHCARIALDQLGVPPAP
smeg        MT-DSLLSLVLPD----RVASAEVYDDPPGLSPLPEEEPLIARSVAKRRNEFVTVRYCAROALGELGVGPVP
m.leprae    MTVSMLVSSVLPDYASODLEYAELYSDPPGLTPLPEEELLIAKSVAKRRNEFITARYCARIALGRLRVPPVP
m.avium     MT-GTLVSSVLPAS--DGLAYSEVYSDPPGLAPLPEEEPLIARSVAKRRNEFITVRHCARIALGELGLPPAP
m.bovis     MTVGTLVASVLPATVFEDLAYAELYSDPPGLTPLPEEAPLIARSVAKRRNEFITVRHCARIALDQLGVPPAP

cons        ** . *:: ***   ***  :  :*:*.*****:*****  ***:*********:*.*:*** **..* : *.*


tb          ILKGDKGEPCWPDGMVGSLTHCAGYRGAVVGRRDAVRSVGIDAEPHDVLPNGVLDAISLPAERADMPRTMPA
smeg        ILKGDKGEPCWPDGVVGSLTHCOGFRGAVVGRSTDVRSVGIDAEPHDVLPNGVLDAITLPIERAEL-RGLPG
m.leprae    ILKGDKGEPCWPDGVVGSLTHCSGYRGAVVGRSAAVRSVGIDAEPHEMLPNGVLDVISLPEERSEMRRKLPS
m.avium     ILKGEKGEPRWPDGVVGSLTHCTGYRGAVVGRTGAVRSVGIDAEPHDVLPDGVLNAISLPAERSEIPSVLPG
m.bovis     ILKGDKGEPCWPDGVVGSLTHCAGYRGAVVGRRDAVRSVGIDAEPHDVLPNGVLDAISLPAERADMPRTMPA

cons        ****:**** ****:******* *:*******   ***********::**:***:.*:** **:::   :*.


tb          ALHWDRILFCAKEATYKAWFPLTKRWLGFEDAHITFETDSTGW-TGRFVSRILIDGSTLSGPPLTTLRGRWS
smeg        DLHWDRILFCAKEATYKAWYPLTHRWLGFEDAHITFEVDGSGT-AGSFRSRILIDPVAEHGPPLTALDGRWS
m.leprae    VLYWDRILFCAKEATYKAWFPLTKRWLGFEDAHITFDVDNLGS-SGGFVSRILVDGSALSGPPLTVLTGRWS
m.avium     DLHWDRILFCAKEATYKAWFPLTRRWLGFEDAHITFEADHPGATTGGFVSRILIDPAALCGPPLTALSGRWS
m.bovis     ALHWDRILFCAKEATYKAWFPLTKRWLGFEDAHITFETDSTGW-TGRFVSRILIDGSTLSGPPLTTLRGRWS

cons        *:****************:***:************:.*  *  :* * ****:*  :  *****.* ****


tb          VERGLVLTAIVL
smeg        VRDGLAVTAIVL
m.leprae    VDRGLVLTAIVL
m.avium     VARGLVLTAIVL
m.bovis     VERGLVLTAIVL

cons        *  **.:*****
```

In vitro enzymatic examinations indicate PptT is inhibited by 8918

With heterologous expression of MT PptT in WT Mtb conferring resistance, we wanted to test 8918 and PptT *in vitro* in an enzymatic assay to see if we could characterize the degree of inhibition of PptT by 8918. We collaborated with John Mosior and Jim Sacchettini at TAMU for these results.

PptT was heterologously expressed in *E. coli* and purified. The enzyme was then used in a BpsA assay, which is a frequently used assay to test the activity of

phosphopantetheinylating enzymes[9,10]. BpsA can be expressed in the apo form, and when it is combined with an enzyme capable of phosphopantetheinylation (such as PptT) and CoA as a cofactor, it can be activated into the holo form, and subsequently convert 2 glutamate molecules into indigoidine[9]. Indigoidine is colored and production can be observed at 590 nm, therefore the assay was set up with PptT, CoA, BpsA, and glutamate. Indigoidine was used as the readout of productivity of PptT. We observed that 8918 inhibited PptT at 5 μM, a fatal dose to Mtb *in vitro*, but we also observed that fatal doses did not fully abolish the activity of PptT, even up to 80 μM (**Figure 3A**). The maximum inhibition observed was about 87% at the highest dose tested (**Figure 3A**), despite the relatively high potency indicated by the low IC50 of 2.5 μM (**Figure 3B**). This observation indicates that PptT may be a hypervulnerable target, if less than 100% activity may be lethal to cells. It also may indicate that PptT inhibition alone is not sufficient to explain the lethality observed from 8918 treatment.

We also observed that while Vmax was reduced, Km did not change significantly, increasing only from 0.601 to 0.867 over the course of 75 μM 8918. A reduction in Vmax and static Km generally indicate non-competitive inhibition, and indeed the Whitely plot of fractional velocity vs the reciprocal of inhibitor concentration shows that inhibition of PptT by 8918 was non-competitive (**Figure 3C**).

Figure 3: Impact of 8918 on recombinant PptT (A) Activity of 8918 against heterologously expressed PptT *in vitro*. Uninhibited PptT activity (circles) reaches a Vmax of about 11.9, while 5 μM (squares), 10 μM (triangles), 20 μM (inverted solid triangle), 40 μM (inverted empty triangle) and 80 μM (stars) 8918 treatment inhibit PptT in a dose-dependent manner. Vmax and Km are shown +/- the standard error at each concentration of 8918 in μM. (**B)** Inhibition of 8918 on PptT. The IC50 was about 2.5 μM. (**C)** plot of V/V0-V +1/I for PptT and 8918. *Experiment performed by John Mosior, TAMU.*

A.

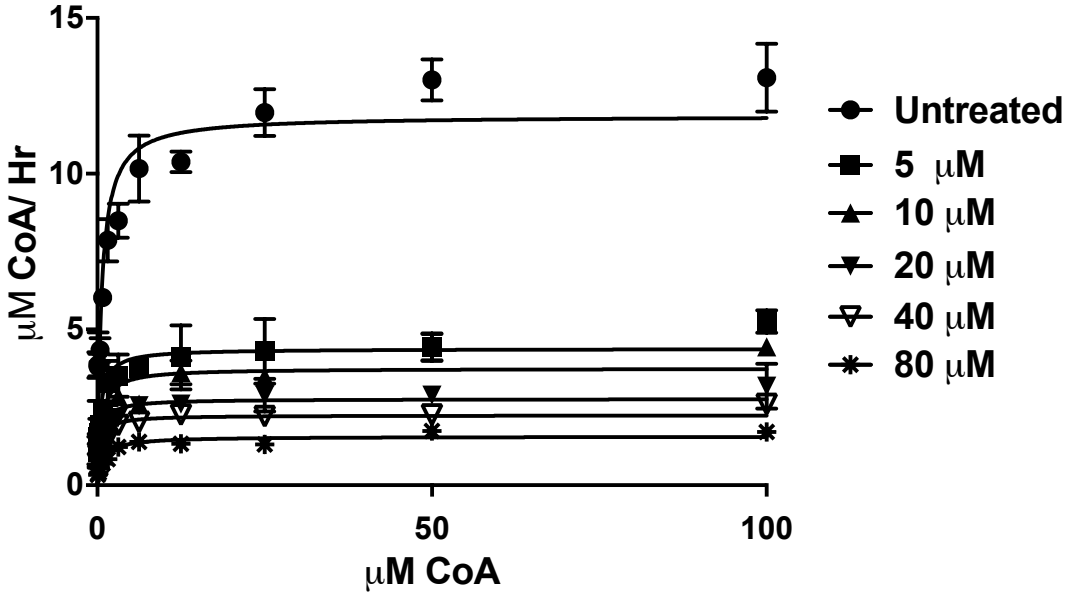

	0	5	10	20	40	80
Vmax	11.9 ± 4.24	4.38 ± 0.174	3.75 ± 0.180	2.77 ± 0.123	2.24 ± 0.098	1.56 ± 0.055
Km	0.601 ± 0.112	0.419 ± 0.090	0.541 ± 0.129	0.425 ± 0.102	0.399 ± 0.095	0.867 ± 0.152

B.

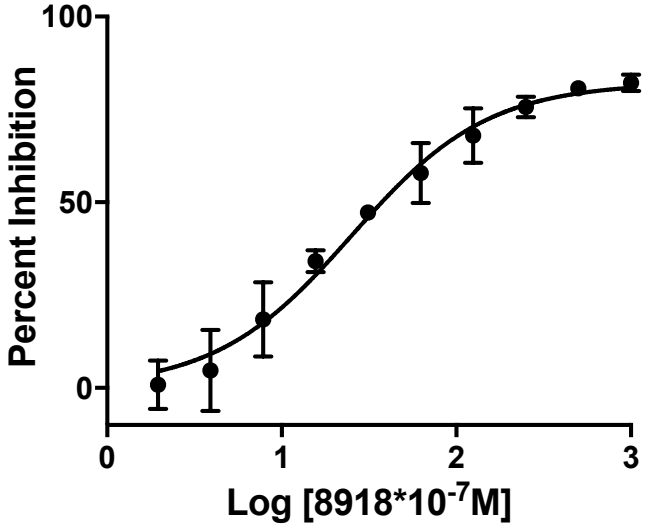

Figure 3 continued

C.

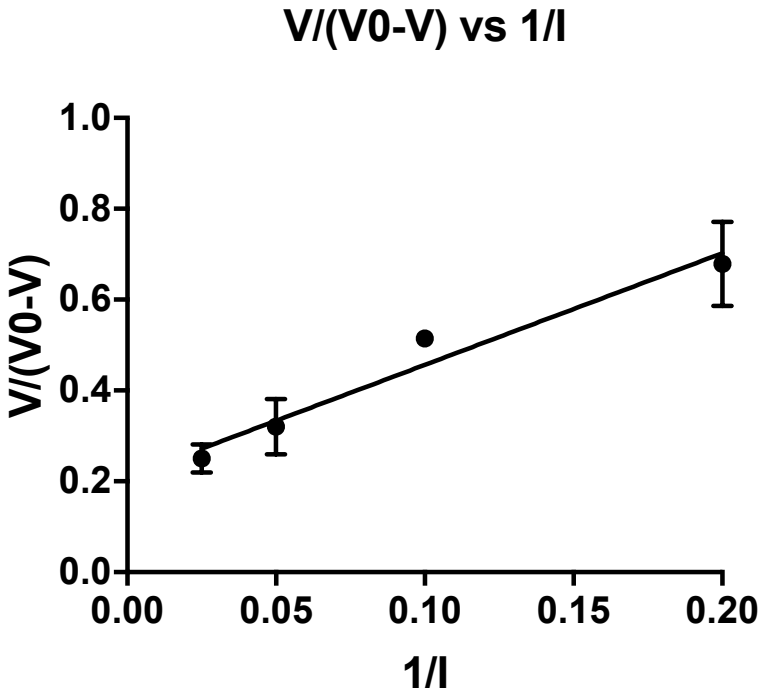

Lidamidine is a weak inhibitor of PptT

Consistent with our previous findings that lidamidine can cause similar metabolic changes to 8918 and is growth inhibitory at very high doses *in vivo*, we observed that lidamidine can inhibit PptT but to a lesser degree than 8918. Lidamidine similarly reached a max inhibition of about 88% but had an IC50 around 15 μM (**Figure 4**). It is interesting that lidamidine is not lethal to Mtb anywhere near comparable levels to 8918, given that its IC50 is only about 6 times higher than 8918, and lidamidine appears to associate with the cells 10x more than 8918. It may be that lidamidine sticks to the membrane more than 8918, thereby appearing to have a cellular association, but that little accumulates truly within the cells. It may also be possible that intracellular segregation of lidamidine from PptT is possible, but not for 8918.

The MIC_{90} of lidamidine is at least 31 times higher than the MIC of 8918. We also

observed that lidamidine appears to act as a non-competitive inhibitor of PptT, albeit a much weaker one than 8918.

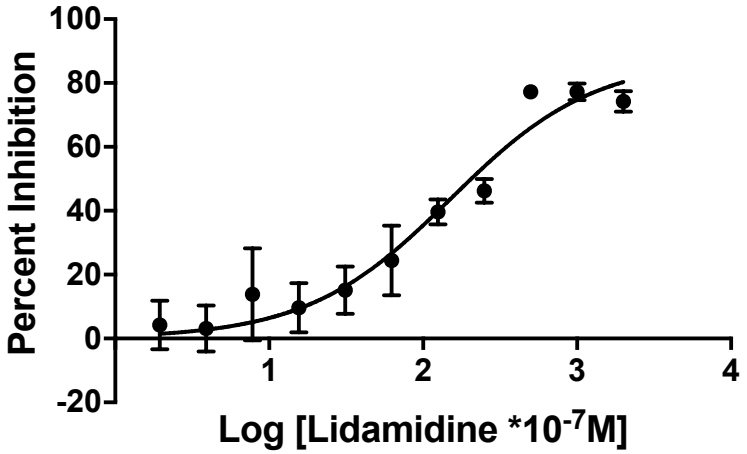

Figure 4: **Inhibition of PptT by lidamidine**, IC50 was 15.1 μM. *Experiment performed by John Mosior, TAMU.*

The finding of non-competitive inhibition was unexpected, given that the PptT W170S and W170L mutants we observed were highly resistant to 8918, and this residue projects over the phosphopantetheine pocket of the PptT active site. The location of the mutation in the target implied that the resistance was a result of a change in the ability of 8918 to bind to the target. When we tested the W170S mutant *in vitro* we observed that the mutant PptT was in fact resistant to inhibition by 8918, though not completely (**Figure 5**). The lowest Vmax observed for the MT W170S mutant after 8918 exposure was 3.77 μM CoA/Hr at 80 μM, as compared to the Vmax for the WT after 8918 exposure which was 1.56 μM CoA/Hr at 80 μM. We also observed that the mutant PptT seemed to show non-competitive inhibition as well, with Vmax reducing during inhibition but no significant change occurring in Km.

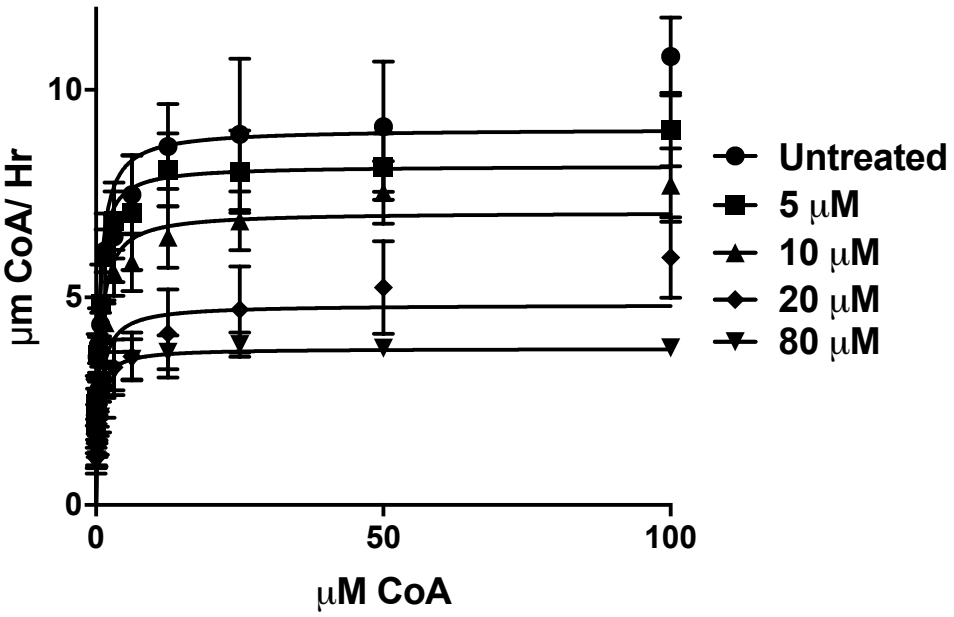

	0	5	10	20	40	80
Vmax	9.06 ± 3.65	8.17 ± 0.243	7.05 ± 0.225	4.82 ± 0.237	4.82 ± 0.237	3.77 ± 0.108
Km	0.568 ± 0.120	0.422 ± 0.071	0.632 ± 0.104	0.643 ± 0.163	0.643 ± 0.163	0.460 ± 0.071

Figure 5: **Activity of 8918 on MT W170S PptT.** Untreated Mt PptT (circles) compared to 5 μM (squares), 10 μM (triangles), 20 μM (inverted solid triangle), 40 μM (inverted empty triangle) and 80 μM (stars). Vmax and Km are shown +/- the standard error at each concentration of 8918 in μM. *Experiment performed by John Mosior, TAMU.*

Another potential explanation for the apparent non-competitive inhibition kinetics could be that 8918 inhibits PptT uncompetitively. In uncompetitive inhibition, an inhibitor binds specifically to the enzyme-substrate complex, and so could produce kinetics that appear non-competitive. The location of the mutated W170 residue deep within the PptT CoA binding pocket seems to refute this hypothesis, as the

hydrophobic binding pocket that holds the phosphopantetheine arm is not large enough for simultaneous binding of Ppt and 8918. Further, the W170 residue caps the end of the pocket, indicating that modulation of the binding site that interferes with 8918 binding occurs deep within the pocket, indicating that 8918 is present fully inside the pocket when bound.

Heterologous expression of mutant PptT in WT cells confers high level resistance to 8918

Given that 8918 didn't inhibit MT PptT as much as we anticipated, we decided to overexpress WT and MT *pptT* in WT Mtb. We hypothesized that if PptT is the target of 8918, overexpression of the target would result in an increase in the MIC. Similarly, we thought that introducing the MT PptT into WT cells could confer resistance to the WT, since the cells would be able to produce 8918 resistant PptT that could replace the inhibited PptT function. pMV261 was selected as the vector, which would put *pptT* under hsp60 control. pMV261 is often used to overexpress proteins in Mtb. When WT Mtb was transformed with WT *pptT,* however, no change in MIC was observed **(Figure 6A).** Similar results were observed with Msm. When *pptT* MT W170L in pMV261 was introduced into WT Mtb, however, an approximately 30-fold shift in resistance was observed. The level of resistance was the same as the original W170L mutant (**Figure 6B**). Similar results were observed in Msm, and no cross resistance to major antibiotics (PAS, EMB, MOXI, RIF) occurred, indicating that the resistance associated with the *pptT* W170L mutant was specific to 8918, and that the mutation was sufficient to cause high level resistance to 8918 even in the presence of WT *pptT*. It is possible that overexpression of *pptT* is toxic and therefore overexpression of WT *pptT* sufficient to cause resistance is impossible, but a small number of MT PptT enzymes are sufficient to confer resistance to 8918. Western

blotting of overexpression was inconclusive; native levels of PptT were not high enough to be visible on a western blot, nor were the concentrations of WT or MT PptT in the overexpression strain.

A.

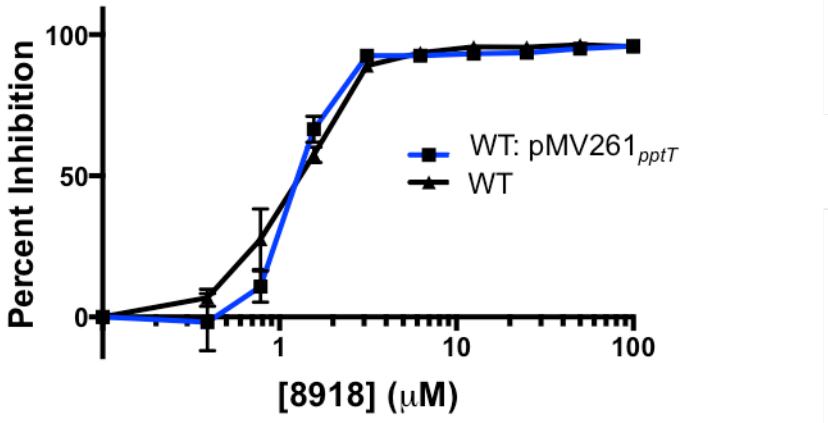

B.

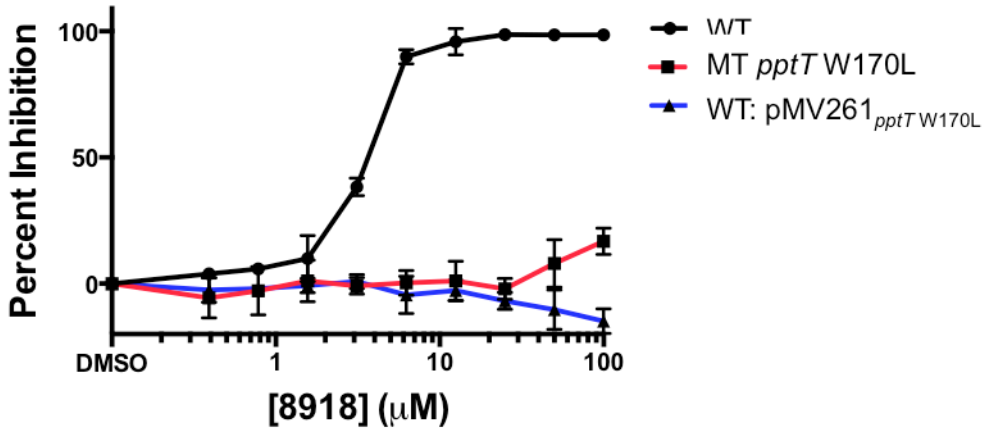

Figure 6: Expressino of WT or MT PptT in Mtb. (A) MIC of 8918 against WT Mtb (black) and WT Mtb with pMV261:*pptT* (blue) **(B)** MIC of 8918 against WT Mtb (black), MT Mtb (W170L) and WT Mtb with pMV261:*pptT*:W170L

Crystallization of PptT shows 8918 binds in the active site

We were confident that 8918 could inhibit PptT, and that mutation in PptT could prevent cells from dying during treatment with 8918, but we were uncertain how a presumed active site mutation (W170) could result in resistance if 8918 were a non-competitive inhibitor. John Mosior (TAMU) produced the co-crystal of 8918 and PptT at 1.76 Å, using the protocols for PptT crystallization previously reported as guidelines[10,11], and saw that 8918 does appear to bind in the active site of PptT (**Figure 7A-C**). The structure revealed that PptT formed a dimer with 8918 bound in the active site (**Figure 7A**). 8918 was also observed in some interstitial space between the two proteins, but is believed to be an artifact of high concentration of 8918 in the crystallization conditions (**Figure 7A**). It appeared that 8918 bound in a pocket with key interactions with K156, Y160, L171, and that W170 capped off the bottom of the pocket, (**Figure 7B**) indicating a rationalization for the resistance observed in the mutants.

We observed that CoA co-crystalized in the protein (**Figure 7C**). CoA was not added during the purification, but PptT likely co-purified with CoA due to high affinity between PptT and CoA[12]. Interestingly, while the adenosine 3', 5' bisphosphate portion of CoA appeared stable in the protein crystal, the phosphopantetheine (ppt) arm of CoA was not able to be resolved, possibly due to a very low degree of electron density such that it could not be concretely placed in the structure, which could mean the ppt arm is mobile and not stabilized by binding. This suggests that 8918 binds the active site concurrently with CoA and can disrupt the placement of the ppt arm of CoA (**Figure 7C**). Published crystal structures of PptT bound to CoA do indicate that normally the ppt arm of CoA binds where we observed 8918 in these crystals[10,12].

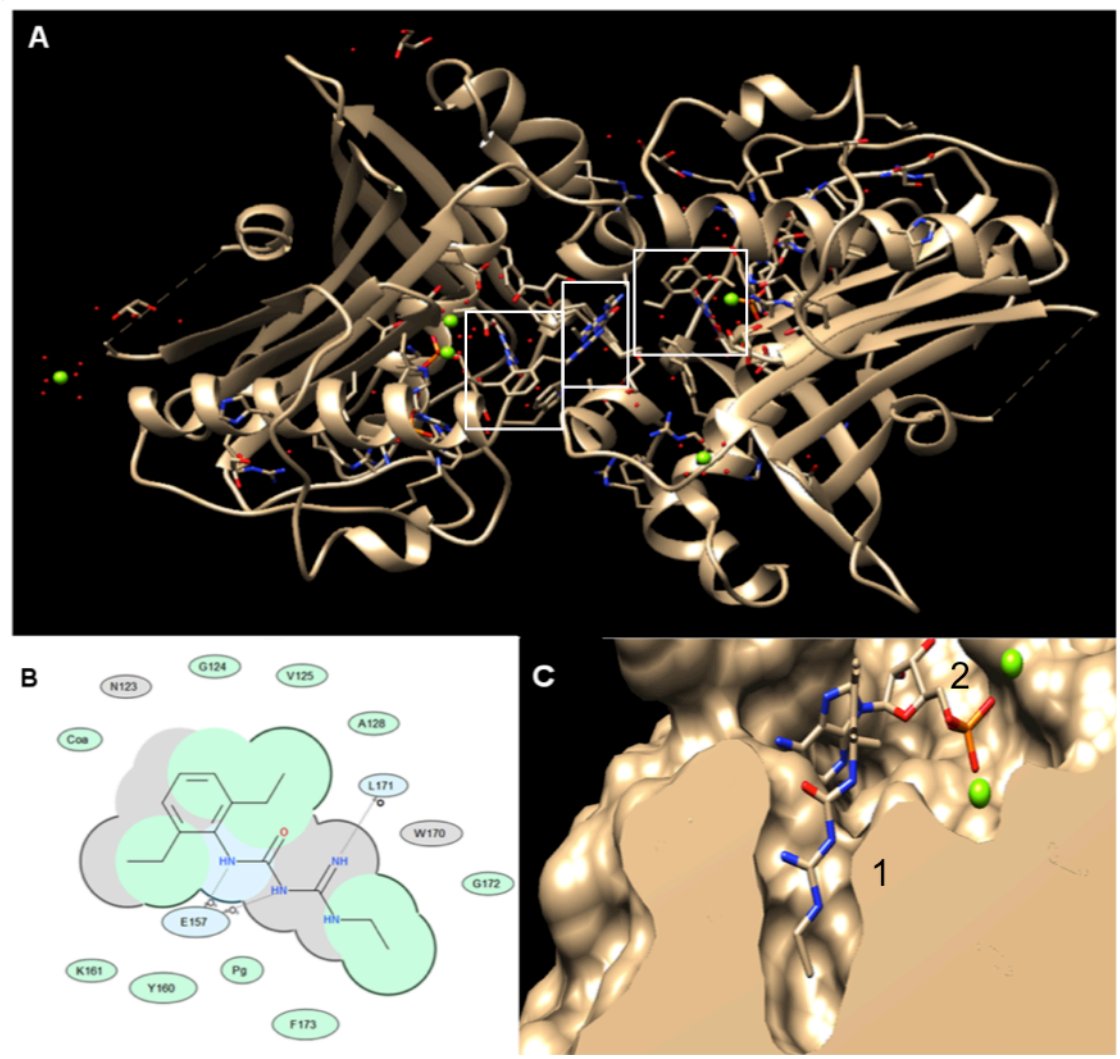

Figure 7: **Crystallographic analysis of PptT bound with 8918**

(**A**) The 1.76 Å model of PptT bound with CoA and 8918, as produced from the electron density in the PptT crystal. 8918 molecules identified are shown inside white boxes. Amino acids involved in water binding are shown as sticks rather than protein cartoon. (**B**) 8918 shown in the pocket with relevant stabilizing residues especially K156, Y160, L171, P173, and W170 at the bottom of the pocket. (**C**) 8918 (**1**) shown bound as well as the adenosine 3', 5' bisphosphate (**2**) region of CoA. Magnesium ions (green) were also identified in this pocket, likely as artifacts of the crystallization conditions. *Structure produced by John Mosior (TAMU)*

With the crystal structure in hand, uncompetitive inhibition of PptT by 8198 seems unlikely, as the 8918 molecule binds tightly into the Ppt binding pocket, and Ppt is not present in the binding structure. While non-competitive inhibition kinetics are possible with inhibitors that bind the active site[13], it may be possible that in this case non-competitive inhibition was observed despite the presence of 8918 in the active site because 8918 does not displace CoA, but rather can displace the relatively mobile phosphopantetheine arm and prevents catalysis without full displacement of the cofactor. As a result, inhibition would appear non-competitive because CoA cannot compete with 8918 for the binding pocket, since both molecules can bind simultaneously.

Lipidomic analysis of Mtb treated with 8918 supports PptT inhibition

With the knowledge that 8918 can bind in the active site of PptT, we wanted to examine what downstream effects PptT inhibition would have on lipid biosynthesis. Because PptT is a crucial enzyme for the activation of enzymes involved in the synthesis of a wide number of lipid precursors, we expected that inhibition of PptT, even partial inhibition as we observed *in vitro,* would result in far reaching depletions of a variety of lipid species. In collaboration with Dr. Travis Hartman in the Rhee lab, we used a lipidomics assay, similar to the metabolomics platform previously described. We examined what impact sublethal concentrations of 8918 would have on live Mtb over a relative short time frame of 24 hours. We observed that a number of lipid species directly downstream of PptT were indeed decreased in 8918-treated cells as compared to untreated WT Mtb (**Figure 8A-B**). There were a number of isoforms within a lipid species—these represent lipids with various acyl chain lengths or oxidation states within the same species. It was clear that even modest reduction of PptT activity can result in strong depletions of lipid species downstream of PptT.

Figure 8: **Heatmap of lipids observed depleted in 8918 treated cells after 24 hours**. Cells were compare to untreated cells, and normalized to glucose monomycolates which were statistically determined to be the species with the least variation between untreated and treated cells. Color gradient represents decreases on a Log_2 scale, with green representing a decrease as compared to untreated cells. *This experiment was performed by Travis Hartman*.

A.

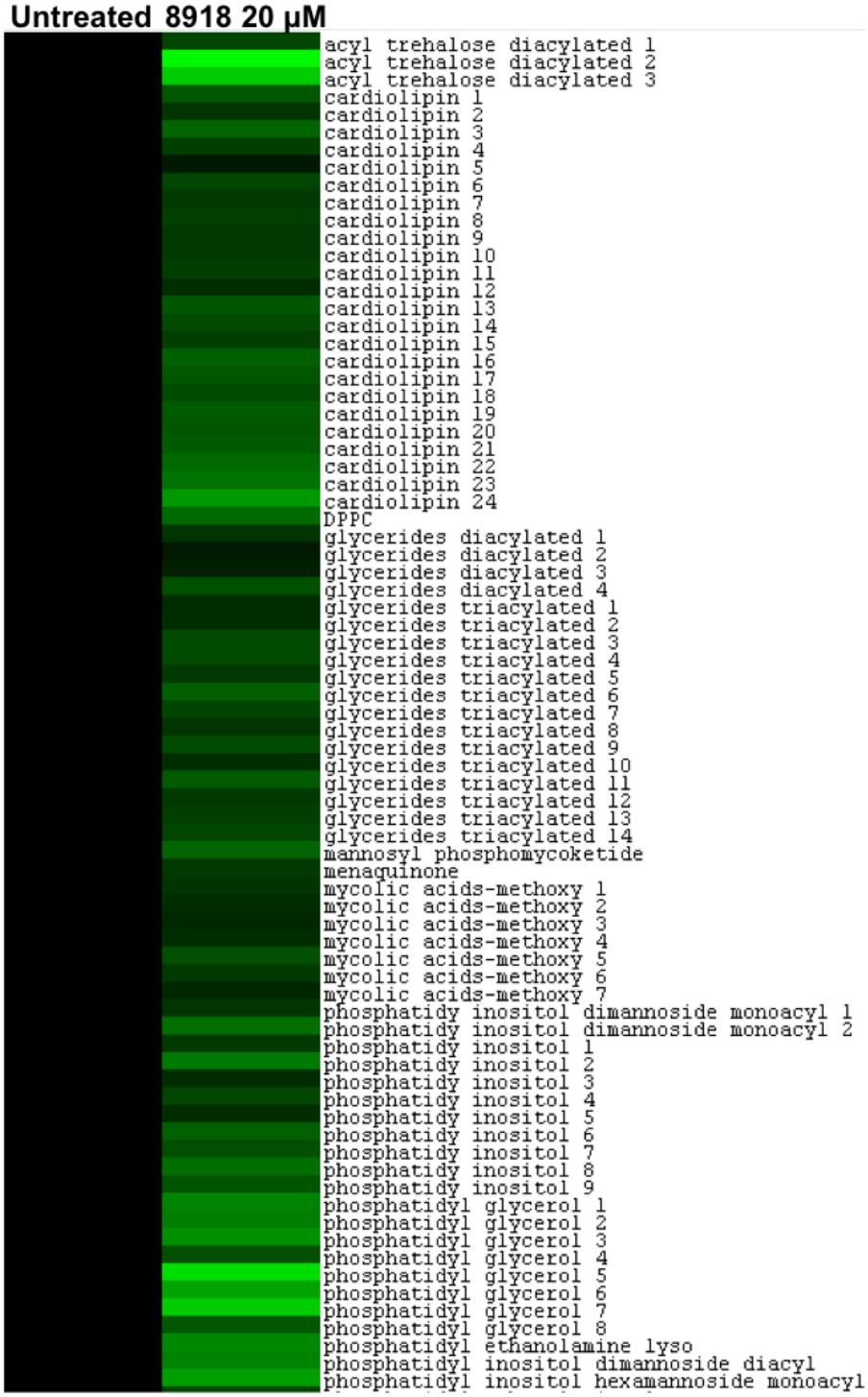
Untreated
8918 20 µM
acyl trehalose diacylated 1
acyl trehalose diacylated 2
acyl trehalose diacylated 3
cardiolipin 1
cardiolipin 2
cardiolipin 3
cardiolipin 4
cardiolipin 5
cardiolipin 6
cardiolipin 7
cardiolipin 8
cardiolipin 9
cardiolipin 10
cardiolipin 11
cardiolipin 12
cardiolipin 13
cardiolipin 14
cardiolipin 15
cardiolipin 16
cardiolipin 17
cardiolipin 18
cardiolipin 19
cardiolipin 20
cardiolipin 21
cardiolipin 22
cardiolipin 23
cardiolipin 24
DPPC
glycerides diacylated 1
glycerides diacylated 2
glycerides diacylated 3
glycerides diacylated 4
glycerides triacylated 1
glycerides triacylated 2
glycerides triacylated 3
glycerides triacylated 4
glycerides triacylated 5
glycerides triacylated 6
glycerides triacylated 7
glycerides triacylated 8
glycerides triacylated 9
glycerides triacylated 10
glycerides triacylated 11
glycerides triacylated 12
glycerides triacylated 13
glycerides triacylated 14
mannosyl phosphomycoketide
menaquinone
mycolic acids-methoxy 1
mycolic acids-methoxy 2
mycolic acids-methoxy 3
mycolic acids-methoxy 4
mycolic acids-methoxy 5
mycolic acids-methoxy 6
mycolic acids-methoxy 7
phosphatidy inositol dimannoside monoacyl 1
phosphatidy inositol dimannoside monoacyl 2
phosphatidy inositol 1
phosphatidy inositol 2
phosphatidy inositol 3
phosphatidy inositol 4
phosphatidy inositol 5
phosphatidy inositol 6
phosphatidy inositol 7
phosphatidy inositol 8
phosphatidy inositol 9
phosphatidyl glycerol 1
phosphatidyl glycerol 2
phosphatidyl glycerol 3
phosphatidyl glycerol 4
phosphatidyl glycerol 5
phosphatidyl glycerol 6
phosphatidyl glycerol 7
phosphatidyl glycerol 8
phosphatidyl ethanolamine lyso
phosphatidyl inositol dimannoside diacyl
phosphatidyl inositol hexamannoside monoacyl

Figure 8 continued

B.

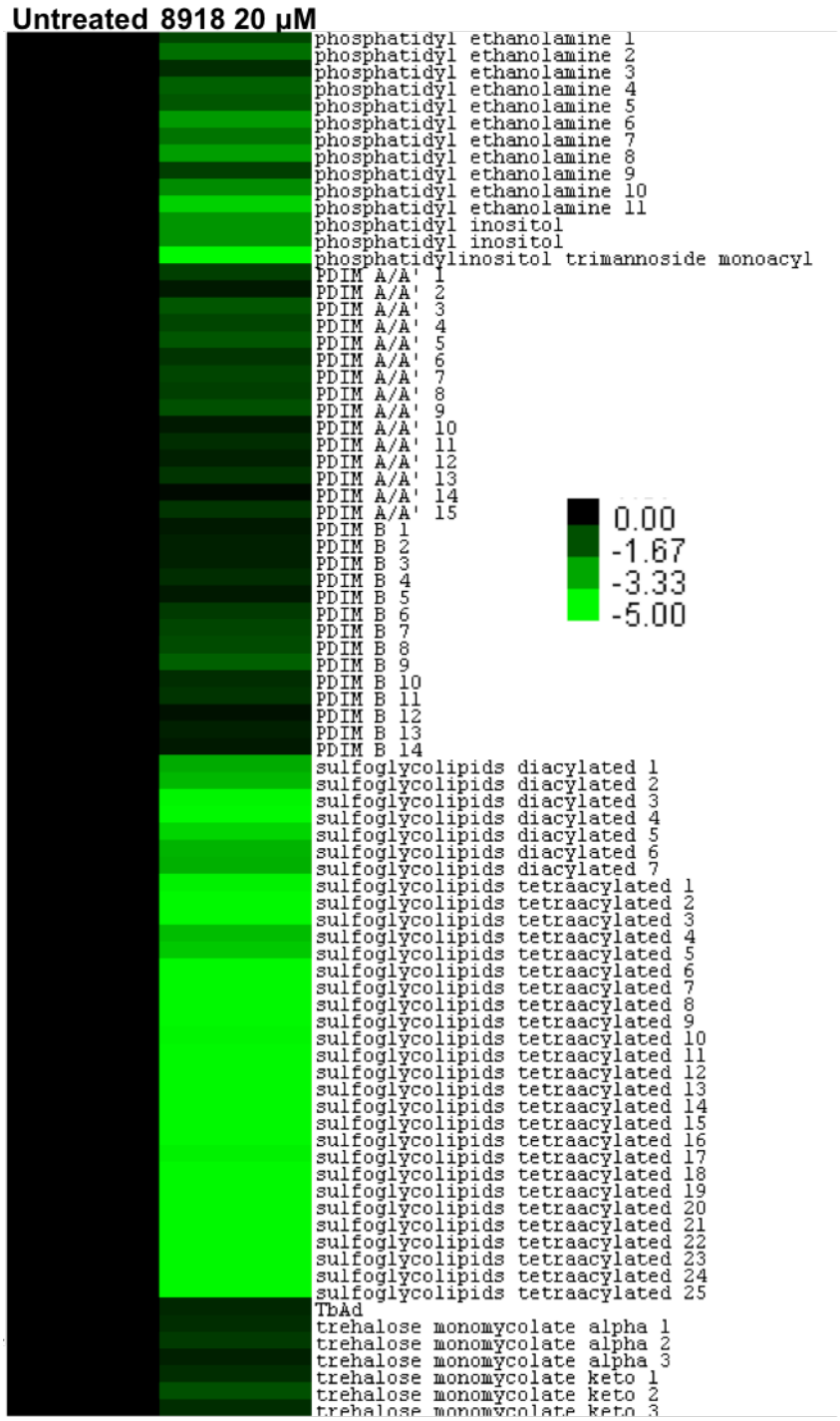

We noted that mycolic acids and phthiocerol dimycocerosates (PDIMs) were depleted as expected, but unexpectedly menaquinone was also significantly depleted in treated cells (**Figure 8**)

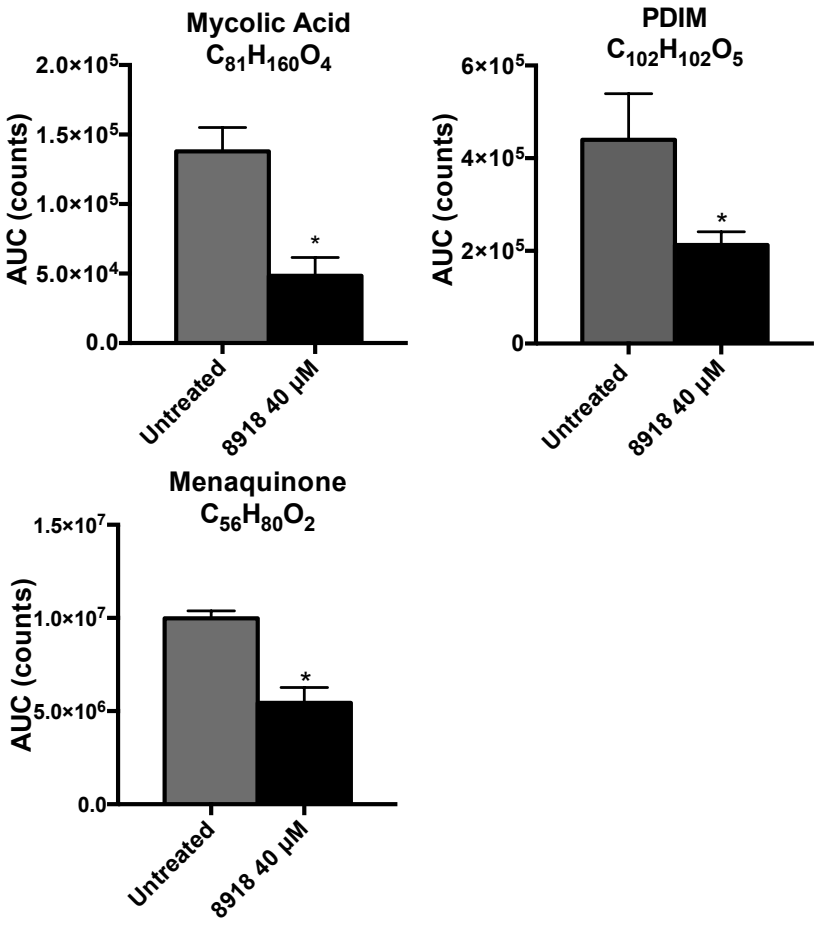

Figure 9: Illustrative changes in lipid levels in Mtb grown on a filter 24 hours after the filter was transferred to a fluid reservoir containing 8918 (40 µM). Means ± SD of triplicates in 1 experiment representative of 2. *p* values for depletion in unpaired two-tailed t tests = 0.02 for mycobactin, 0.002 for PDIM, 0.02 for mycolates, and 0.001 for menaquinone.

Discussion

Crystallization of the PptT enzyme indicated that 8918 binds to the active site within the pocket normally occupied by the phosphopantatheine portion of CoA, despite *in vitro* enzymatic data which indicated that 8918 was a non-competitive inhibitor, though this data could be a result of concurrent binding of CoA and 8918 in the active site. The structure of the ppt binding pocket supports the hypothesis that 8918 inhibits PptT by preventing catalysis of the ppt transfer onto apo-ACPs. The pocket structure as well as the highly conserved W170 residue that appears to be integral to the activity of 8918 makes a strong argument for the specificity of 8918. Because Mtb treatments are typically very long, antibiotics that are as narrow spectrum as possible are desirable. Current standard Mtb treatment typically results in profoundly disrupted gut microbiota, because the standard antibiotics (especially RIF) can kill a wide variety of normal gut flora, and the effects of the treatment related dysbiosis can be extremely long lasting[14-16]. Host microbiota have been shown to have widespread impact on the immune system, and some have postulated that the relatively high TB relapse rate of patients who have been treated for Mtb may be partially due to microbiota dysbiosis[17-18]. Accelerated HIV[18] and diabetes[14,19] disease progression have been associated with microbiota dysbiosis, and both conditions are risk factors for active TB infection. Dysbiosis is also associated with diarrhea and discomfort which can be a contributing factor to patient noncompliance with MTB treatment regimes[14,20]. Therefore, a drug that only targets Mtb could have the benefit of reducing gut microbiota dysbiosis and its associated problems. Because PptT in Mtb is structurally dissimilar from other bacterial acyl carrier protein synthases, we hypothesize that a PptT inhibitor would be reasonably narrow spectrum, and likely would not be able to inhibit normal gut bacteria, thereby preventing dysbiosis.

In addition, a drug that is only used to treat Mtb would have the benefit of not

generating incidental resistance. Some current TB drugs are used to treat a number of different infections, and if a patient is treated for a non-TB infection, but is concurrently and unknowingly infected with MTB they may accidentally generate mono-resistant Mtb, which would make their infection harder to treat if they develop an active TB infection in the future. Finally, the generation of our crystal structure bound to 8918 may facilitate simulation-driven, rational design of better PptT inhibitors.

Lipidomic analysis also supported the finding that 8918 inhibited PptT, as downstream products of enzymes activated by PptT were found to be decreased after 8918 treatment. Some of the depleted lipids were expected; PDIMs and mycolic acids require PptT activity for their synthesis. Mycolic acids are essential for Mtb membrane function, as they help provide structure, fluidity, and barrier to extracellular conditions[21]. Inhibition of mycolic acid synthesis is the main mechanism of action of INH, which is a very effective frontline Mtb drug[22,23]. PDIMs have been implicated in virulence; loss of PDIMs occurs often during laboratory passaging of cultures but is directly related to a loss of Mtb virulence[24]. Sulfolipids and cardiolipins are downstream products of PptT via activation of the PKS13 system as well, and reductions may have impacts on Mtb's ability to manipulate the host immune system or regulate cell division[25,26]. The finding of depleted menaquinone was unexpected, but we believe that a reduction in menaquinone can be explained by a bottleneck in isochorismate and salicylate availability; mycobactin is also a downstream product of PptT and requires salicylate as a substrate for synthesis[4,27]. Mtb synthesizes isochorismate from salicylate, and isochorismate is a necessary substrate for menaquinone synthesis. We were unable to determine with confidence the identity of mycobactin in our lipidomic analysis, but it is possible that during PptT inhibition Mtb prioritizes some processes over others, and may reserve salicylate for mycobactin

synthesis and deprioritize menaquinone. Menaquinone is an essential electron transport chain electron carrier, and many reactions depend on it for shuttling electrons; as a result inhibitors of menaquinone synthesis have been studied or desired for many years[28-30]. We were not able to detect salicylate in our metabolomics studies but it may be worth pursuing later, as the actual mechanism that causes Mtb to die in the presence of 8918 may be directly related to the reduction in menaquinone and the inability of the cells to properly shuttle electrons.

Lipidomics provided evidence of *in vivo* PptT inhibition, and our enzymatic experiments also provided strong evidence that the cidality of 8918 on Mtb was mediated by inhibition of PptT. It was interesting to discover that 8918 could not fully abolish PptT activity *in vitro*, and it was also unexpected that the mutant PptT enzyme was inhibited by 8918 to a surprising degree *in vitro*. While that finding may indicate that PptT is not the target, we observed that expression of the PptT W170 mutant conferred high level resistance to WT cells. This was despite the *in vitro* data indicating that mutant PptT was inhibited by 8918 to a degree that should be lethal at much lower concentrations than we observed *in vivo*. The implication is that PptT is being inhibited by 8918, but that there may nuances in the way that 8918 reaches the target *in vivo*. It's possible that the mutant Mtb strain is in some way more effective at sequestering 8918 away from PptT than the WT, but it may also be possible that PptT is even more susceptible to inhibition *in vivo* than the *in vitro* results would suggest. We did not observe any other mutations in the W170 mutant strains that could explain a complementary genetic component to the W170 mutant resistance. Given PptT's role in the production of membrane lipids, it is possible that the reduced efficiency of the uninhibited PptT mutant enzyme (Vmax 9.06 for the mutant vs 11.9 for the WT) may somehow slightly alter the formation of the mutant Mtb membrane that can help increase resistance beyond the simple active site mutation, and may provide additional

protection to the susceptible target.

The finding that 8918 does not fully abolish activity of PptT at lethal concentrations was very interesting, as it indicates that Mtb is hypersusceptible to PptT inhibition. PptT may represent an even more attractive drug target than before; if only partial inhibition (around 37%, the max reduction in Vmax at 5) is sufficient to cause cell death, Mtb may be more reliant on PptT for cellular processes than previously thought, and it may be possible to produce a wider range of inhibitors if relatively low levels of inhibition can cause cell death. It may also indicate that Mtb death from PptT inhibition is exceptionally sensitive because of additional processes that occur beyond PptT inhibition. Because we observed so many mutations in another gene, *rv2795c*, that seemed to cause high-level resistance, we hypothesized that Rv2795c may be involved in the hypersusceptibility of Mtb to PptT inhibition.

Materials and Methods

Primers to express *pptT* in Pmv261

For: caagcagctggcccagttccgggaacgattg (PvuII restriction)

Rev: caagaagctttcatagcacgatcgcggtcag (HindIII restriction)

Lipidomics:

Filters were prepared with cell mats as for metabolomics, and placed on swimming pools containing 40 μM 8918 or lidamidine for 24 or 48 hours. Filters were removed from the swimming pools and placed into 13x100 mM glass screw-top vials with 5 mL 1:2 chloroform:methanol and quickly removed. Vials were shaken overnight at room temperature, then spun at 2000 g for 30 min at 4° C. Supernatant was decanted and cells resuspended in 1:1 chloroform:methanol, vortexed vigorously, and spun at

2000 g for 30 min, 4° C. The wash/vortex/spin cycle was repeated with 2:1 chloroform:methanol. Supernatants for each sample were pooled, evaporated under nitrogen, and resuspended in 1/10 starting volume 70:30 [v/v] hexane:isopropanol, 0.02% formic acid [m/v], ammonium hydroxide 0.01% [m/v]. *Lipidomics analysis performed by Travis Hartman.*

Purification of PptT

E. coli BL21 cells were grown to OD_{580} 0.6-0.8 and induced with 0.5 mM IPTG overnight at 15 °C. Cells were resuspended in lysis buffer (50 mM $NaPO_4$ pH 6.5, 0.5 M NaCl, 1 mM $MgCl_2$, 5 mM imidazole and 25% glycerol) and lysed in a French press. Lysates were spun at 35000 G for 45 min and lysate passed over Ni-NTA resin. Resin was washed with 600-800 mL lysis buffer and eluted with elution buffer (50 mM $NaPO_4$ pH 6.5, 0.5 M NaCl, 1 mM $MgCl_2$, 250 mM imidazole and 25% glycerol). Tobacco etch virus (TEV) 1:30 w/w ratio was added and samples dialyzed overnight at 4°C in 25 mM $NaPO_4$ pH 6.5, 0.5 M NaCl, 1 mM $MgCl_2$, 1 mM DTT, 25% glycerol. Protein was passed back over Ni-NTA column and concentrated on 10000 MW Centricon.

Purification of Apo-BpsA

Protein was expressed in BL21 DE3 cells grown to OD_{540} 0.6-0.8 and induced with 0.5 mM IPTG overnight at 18°C, no longer than 17-18 hrs. Cells were resuspended in lysis buffer (50 mM Tris-HCl pH 7.9, 0.5 M NaCl, 5 mM imidazole, 12.5% glycerol) and French pressed. Lysate was spun down at 35000 G for 45 minutes, supernatant passed over Ni-NTA column, and washed with 600-800 mL lysis buffer. Protein was eluted with elution buffer (50 mM Tris-HCl pH 7.9, 0.5 M NaCl, 250 mM imidazole, 12.5% glycerol). TEV was added 1:30 w/w ration and dialyzed overnight at 4°C in 50

mM $NaPO_4$ pH 7.8, 1 mM DTT, 12.5% glycerol. Protein was passed over Ni-NTA column and concentrated on 100000 MWCO centricon.

PptT-BpsA Reaction Method

75 uL of buffer 1 (75 mM Tris-HCl pH 7.8, 15 mM $MgCl_2$, 16 mM L-glutamine, 10 mM ATP, 2.5 nM PptT, 0.5 mM DTT, and a 2-fold dilution series of CoA from 200-0.09 μM) were added to a 96 well plate. Reaction was initiated by adding 75 uL of buffer 2 (75 mM Tris-HCl pH 7.8, 15 mM $MgCl_2$, 3.4 uM Apo-BpsA, and inhibitor if applicable) and absorbance was recorded at 590 nM.

Crystallization of PptT

PptT was incubated with excess 8918 and screened against Hampton research crystallization conditions. The most promising condition (100 mM bis tris propane, pH 6.7, 1.8 M $MgSO_4$) was optimized by varying the pH and precipitant concentration using vapor diffusion (hanging drop, 5-10 uL, 50:50 protein:condition). Crystals formed within 6 days and generally grew to maximum size within 2 weeks. Crystals were cryoprotected by dipping them into mother liquor solution containing 30% glycerol. X-ray diffraction data was collected at 19-ID (APS Argonne National Labs) using a cdd ADSC Quantum 315r detector at a wavelength of 0.9253 Angstroms. The on-site HKL3000 package (HKL research, Inc., Charlottesville, VA) was used for data reduction (indexing, integration and scaling).

Structure Determination and Refinement of the PptT CoA 8918 complex

Molecular replacement using Phenix PHASER was used to phase the PptT-CoA-8918 structure using the reported PptT structures 4QJK and 4QVH as search models (having removed all heteroatoms). The PptT CoA 8918 complex crystallized in the C2

space group, with unit cell dimensions a=134.9, b=63.4, c=79.3; A=90, β=123.15, γ=90. Refinement consisted of iterative cycles of rigid body, reciprocal space, individual ADP, and simulated annealing using Phenix refine and manual model building in COOT. Final R factors were 19.90% R free, 16.24% R work, Bond Dev: .007, Angle Dev: .960.

REFERENCES

1. Leblanc, C. *et al.* 4′-Phosphopantetheinyl Transferase PptT, a New Drug Target Required for Mycobacterium tuberculosis Growth and Persistence In Vivo. *PLoS Pathog.* 8, e1003097 (2012).

2. Quigley, J. *et al.* The Cell Wall Lipid PDIM Contributes to Phagosomal Escape and Host Cell Exit of Mycobacterium tuberculosis. *MBio* **8,** e00148-17 (2017).

3. Reddy, P. V. *et al.* Disruption of Mycobactin Biosynthesis Leads to Attenuation of Mycobacterium tuberculosis for Growth and Virulence. *J. Infect. Dis.* **208,** 1255–1265 (2013).

4. De Voss, J. J. *et al.* The salicylate-derived mycobactin siderophores of Mycobacterium tuberculosis are essential for growth in macrophages. *Proc. Natl. Acad. Sci. U. S. A.* **97,** 1252–7 (2000).

5. Leblanc, C. *et al.* 4′-Phosphopantetheinyl Transferase PptT, a New Drug Target Required for Mycobacterium tuberculosis Growth and Persistence In Vivo. *PLoS Pathog.* **8,** (2012).

6. Chalut, C., Botella, L., de Sousa-D'Auria, C., Houssin, C. & Guilhot, C. The nonredundant roles of two 4'-phosphopantetheinyl transferases in vital processes of Mycobacteria. *Proc. Natl. Acad. Sci. U. S. A.* **103,** 8511–6 (2006).

7. Di Tommaso, P. *et al.* T-Coffee: a web server for the multiple sequence alignment of protein and RNA sequences using structural information and homology extension. *Nucleic Acids Res.* **39,** W13–W17 (2011).

8. Armougom, F. *et al.* Expresso: automatic incorporation of structural information in multiple sequence alignments using 3D-Coffee. *Nucleic Acids Res.* **34,** W604–W608 (2006).

9. Brown, A. S., Robins, K. J. & Ackerley, D. F. A sensitive single-enzyme assay system using the non-ribosomal peptide synthetase BpsA for measurement of L-glutamine in biological samples. *Sci. Rep.* **7,** 41745 (2017).

10. Vickery, C. R. *et al.* Structure, Biochemistry, and Inhibition of Essential 4′-Phosphopantetheinyl Transferases from Two Species of *Mycobacteria*. *ACS Chem. Biol.* **9,** 1939–1944 (2014).

11. Beld, J., Sonnenschein, E. C., Vickery, C. R., Noel, J. P. & Burkart, M. D. The phosphopantetheinyl transferases: catalysis of a post-translational modification crucial for life. *Nat. Prod. Rep.* **31,** 61–108 (2014).

12. Jung, J. *et al.* Crystal structure of the essential Mycobacterium tuberculosis phosphopantetheinyl transferase PptT, solved as a fusion protein with maltose binding protein. *J. Struct. Biol.* **188,** 274–278 (2014).

13. Blat, Y. Non-competitive inhibition by active site binders. *Chem. Biol. Drug Des.* **75,** 535–540 (2010).

14. Langdon, A., Crook, N. & Dantas, G. The effects of antibiotics on the microbiome throughout development and alternative approaches for therapeutic modulation. *Genome Med.* **8,** 39 (2016).

15. Hong, B.-Y. *et al.* Microbiome Changes during Tuberculosis and Antituberculous Therapy. *Clin. Microbiol. Rev.* **29,** 915–26 (2016).

16. Wipperman, M. F. *et al.* Antibiotic treatment for Tuberculosis induces a profound dysbiosis of the microbiome that persists long after therapy is completed. *Sci. Rep.* **7,** 10767 (2017).

17. Namasivayam, S. *et al.* Longitudinal profiling reveals a persistent intestinal dysbiosis triggered by conventional anti-tuberculosis therapy. *Microbiome* **5,** 71

(2017).

18. Vujkovic-Cvijin, I. *et al.* Dysbiosis of the gut microbiota is associated with HIV disease progression and tryptophan catabolism. *Sci. Transl. Med.* **5,** 193ra91 (2013).

19. Wen, L. *et al.* Innate immunity and intestinal microbiota in the development of Type 1 diabetes. *Nature* **455,** 1109–1113 (2008).

20. Gareau, M. G., Sherman, P. M. & Walker, W. A. Probiotics and the gut microbiota in intestinal health and disease. *Nat. Rev. Gastroenterol. Hepatol.* **7,** 503–514 (2010).

21. Liu, J., Barry, C. E., Besra, G. S. & Nikaido, H. Mycolic acid structure determines the fluidity of the mycobacterial cell wall. *J. Biol. Chem.* **271,** 29545–51 (1996).

22. World Health Organization & Stop TB Initiative (World Health Organization). *Treatment of tuberculosis : guidelines.* (World Health Organization, 2010).

23. Blanchard, J. S. Molecular Mechanisms of Drug Resistance in Mycobacterium Tuberculosis. *Annu. Rev. Biochem.* **65,** 215–239 (1996).

24. Reed, M. B. *et al.* A glycolipid of hypervirulent tuberculosis strains that inhibits the innate immune response. *Nature* **431,** 84–87 (2004).

25. Maloney, E., Madiraju, S. C., Rajagopalan, M. & Madiraju, M. Localization of acidic phospholipid cardiolipin and DnaA in mycobacteria. *Tuberculosis (Edinb).* **91 Suppl 1,** S150-5 (2011).

26. Maloney, E. *et al.* Alterations in phospholipid catabolism in Mycobacterium tuberculosis lysX mutant. *Front. Microbiol.* **2,** 19 (2011).

27. Manos-Turvey, A. *et al.* Inhibition Studies of Mycobacterium tuberculosis Salicylate Synthase (MbtI). *ChemMedChem* **5,** 1067–1079 (2010).

28. Kurosu, M. & Crick, D. C. MenA is a promising drug target for developing novel lead molecules to combat Mycobacterium tuberculosis. *Med. Chem.* **5,** 197–207 (2009).

29. Debnath, J. *et al.* Discovery of selective menaquinone biosynthesis inhibitors against Mycobacterium tuberculosis. *J. Med. Chem.* **55,** 3739–55 (2012).

30. Dhiman, R. K. *et al.* Menaquinone synthesis is critical for maintaining mycobacterial viability during exponential growth and recovery from non-replicating persistence. *Mol. Microbiol.* **72,** 85–97 (2009).

Chapter 5

Rv2795c contributes to the activity of X-B016178918 on *Mycobacterium tuberculosis* by antagonizing the activity of PptT: loss of function of Rv2795c contributes to a mechanism of resistance to X-B016178918

Summary

rv2795c is a gene of previously unknown function. It is highly conserved among mycobacteria species but has very little structural or sequence homology to proteins in other bacterial families. We observed that loss of function mutations or KO of *rv2795c* conferred high level resistance to 8918. We also saw that Rv2795c could convert holo-ACP to apo-ACP, liberating phosphopantetheine in the process. We therefore hypothesized that during 8918 treatment, partial inhibition of PptT was not sufficient to cause cell death without the additional activity of Rv2795c antagonizing PptT by de-phosphopantetheinylating the holo-ACPs produced by PptT. We propose naming Rv2795c PptH for its **P**hospho**p**ante**t**heinyl **H**ydrolase activity.

Introduction

As previously discussed, antimicrobial resistance may arise in response to drug treatment in a number of ways. While mutation of the site targeted by the antimicrobial agent is a common mechanism of resistance, bacteria may also become resistant to a compound if activity of the compound is dependent on activation or transport mediated by a second enzyme. We found 2 different mutations in W170 of PptT which were logical sources of resistance, and were confirmed to confer resistance. We also found 7 different mutations in *rv2795c* that seemed to confer high level resistance to 8918; this finding was replicated in 8918 resistant Msm mutants. It

seemed apparent that this non-essential enzyme was related to 8918 activity in some way. Generally, loss of function mutations are more likely than gain of function mutations, therefore, we suspected that the mutations observed in *rv2795c* were inactivating, especially as Rv2795c is a non-essential enzyme, and complete loss of function could impact the activity of 8918 without having an effect on the viability of the cell. With this in mind, along with the vulnerability observed in PptT as exhibited by cell death with relatively incomplete inhibition of PptT, we thought that Rv2795c may be involved in a new mechanism of resistance. We had shown by metabolomics that 8918 was not significantly modified in WT Mtb or the MT strain with a putative Rv2795c active site mutation. We know that 8918 can bind directly to the PptT active site. We also observed that 8918 accumulated to a similar degree in WT and $Rv2795c_{H246N}$ mutant cells- these findings together suggested that Rv2795c was not acting as an activating enzyme or effecting transport of 8918 into the cells. We posited that Rv2795c may be antagonizing PptT, such that when 8918 partially inhibits PptT, Rv2795c may convert the PptT product- holo-ACPs- into an unusable form.

Structure analysis of Rv2795c classifies it as a metallophosphoesterase that uses magnesium as a cofactor for catalysis: this is a class of enzymes that can carry out a wide variety of reactions including hydrolysis[1]. We hypothesized that Rv2795c may be carrying out a homologous reaction to an enzyme found in *E. coli* called Acyl carrier protein hydrolase (AcpH). AcpH hydrolyzes the phosphopantetheinyl arm off of holo-Acps, liberating free phosphopantetheine and generating Apo-Acp, as summarized in **Figure 1**. AcpH has been discovered and its mechanism characterized, but the actual purpose of an enzyme with a relatively futile and toxic reaction is not known[2-4]. Further, AcpH has been purified but activity *in vivo* has not been confirmed[2]. Rv2795c does not share significant structural homology with AcpH, but may carry out a similar reaction.

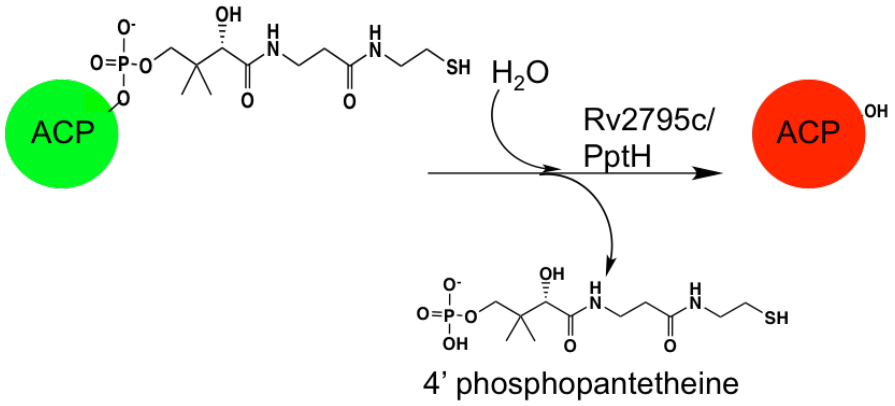

Figure 1: Reaction catalyzed by AcpH and hypothesized reaction catalyzed by Rv2795c.

Rv2795c is a non-essential enzyme, but it is highly conserved among mycobacteria and does not have significant structural homology with any protein outside of the mycobacteria genus. This may indicate that while the enzyme is not essential for growth *in vitro,* it could have an important role in some conditions, including infection. It is unknown if Rv2795c is essential for Mtb infection. We therefore were interested in confirming; **1)** if Rv2795c had a role in 8918 resistance and **2)** what reaction Rv2795c catalyzed, and how that might fit into the biochemical processes of growing Mtb.

Results

Attempts to overexpress WT or MT Rv2795c had no impact on 8918 MIC

We first determined whether overexpressing WT or MT *rv2795c* could confer resistance to 8918. We observed many putative active site mutations in Rv2795c, but the H246N mutation was the most common and also predicted by Phyre to have a high impact on catalytic activity so we selected it as our tool MT strain. We hypothesized that overexpressing an antagonistic enzyme could result in hypersensitivity to 8918,

and that overexpressing the MT gene may not result in a measurable phenotype, since the MT protein was most likely inactive. Because of the high degree of similarity between *rv2795c* and the Msm homologue gene *msm_2647*, we decided to make plasmids with *rv2795c* WT or H246N MT under the hsp60 promoter and transform both WT and the H246N MT Mtb and Msm.

When WT *rv2795c* was transformed into WT *M. smegmatis,* we observed that in most strains there was no change in sensitivity to 8918, but that one strain tested was hypersensitive (**Figure 2A**). The hypersensitive strain showed about a 3-fold change in sensitivity and was dependably hypersensitive even after freezing and reculturing. By contrast, the vast majority of other strains tested were similar to strain 1 in **Figure 2A**, and had no change in 8918 sensitivity. We predict that overexpression of Rv2795c may be toxic, as overexpression of AcpH in *E. coli* is toxic, and while the promotion of Rv2795c was under hsp60 expression, the levels of protein were too low to be assayed by western blot, indicating that overexpression of Rv2795c may not have been achieved. We also observed that expressing the WT *rv2795c* gene in a Msm strain with a presumed loss of function (LOF) mutation in *msm_2647* (Y97D) did not result in any change in sensitivity to 8918 (**Figure 2B**). We expected that this transformation would result in a strain that was more sensitive to 8918, but it may be possible that the gene is not being overexpressed, or that the mutation and loss of function of the gene is somehow dominant and the phenotype from the introduction of the WT gene is not observable. We believe that the toxicity of Rv2795c may have resulted in regulation or mutation of the promoter to protect the cells from the deleterious effects of overexpression of Rv2795c.

A.

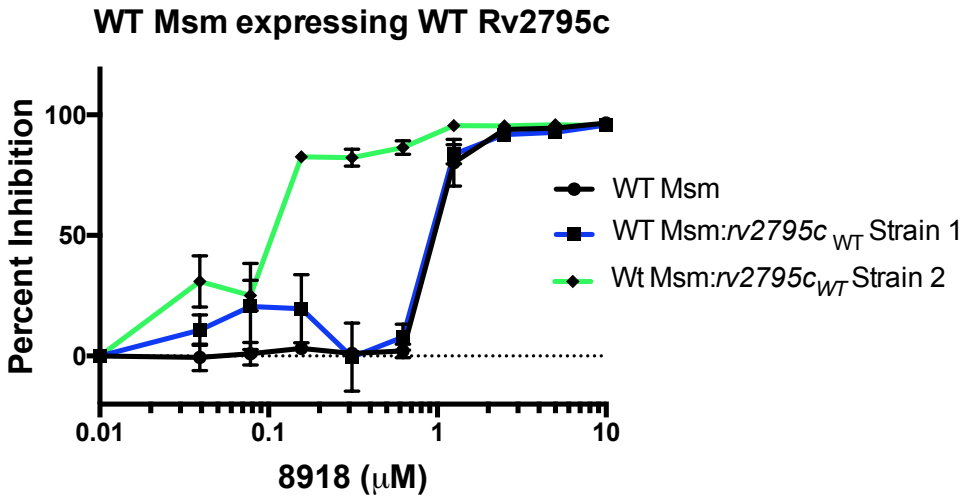

B.

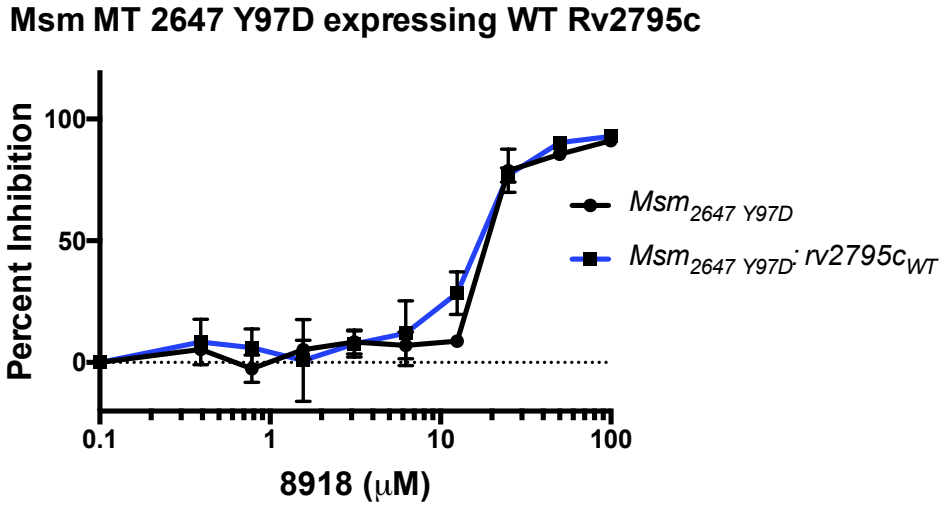

Figure 2: **Impact of Rv2795c expression on Msm sensitivity to 8918.**

(**A**) Expression of WT Rv2795c in WT Msm cells resulted in one strain that was repeatably hypersensitive to 8918, but many strains that had no change in sensitivity. (**B**) Expression of WT *rv2795c* in a strain of Msm with a predicted loss of function (LOF) mutation (Y97D) in the *rv2795c* homologue Msm_2647 resulted in no change in sensitivity to 8918.

While the homology between *msm_2647* and *rv2795c* is high, we knew that the results of testing in Msm may not correlate to results in Mtb. We tested the transformation products of the same plasmids described above in Mtb. We observed that when WT Rv2795c was introduced into WT Mtb there was no change in sensitivity to 8918 (**Figure 3A**) and that expressing the MT H246N *rv2795c* in the WT Mtb also did not have any impact on sensitivity to 8918. A major caveat to this experiment is that we are unsure if the gene was actually being overexpressed; while the gene was under the hsp60 promoter neither the WT nor the transformed strain containing the plasmid contained enough protein to be visible in western blot. Our antibodies for detecting Rv2795c were raised in rabbits against a synthesized peptide fragment of the last 20 amino acids of Rv2795c. The antibodies were able to bind to the peptide fragment they were raised with, as well as recombinant Rv2795c, so we inferred that the levels of Rv2795c in the volume of culture we were able to use were too low for detection. We suspect that *rv2795c* overexpression is toxic and that these strains are not actually overexpressing the protein.

We also transformed MT Mtb with a plasmid that encodes *rv2795c* with the H246N mutation (*rv2795c*$_{H246N}$). This strain is highly resistant to 8918 but transforming with WT or MT *rv2795c* had no impact on sensitivity (**Figure 3B**).

A.

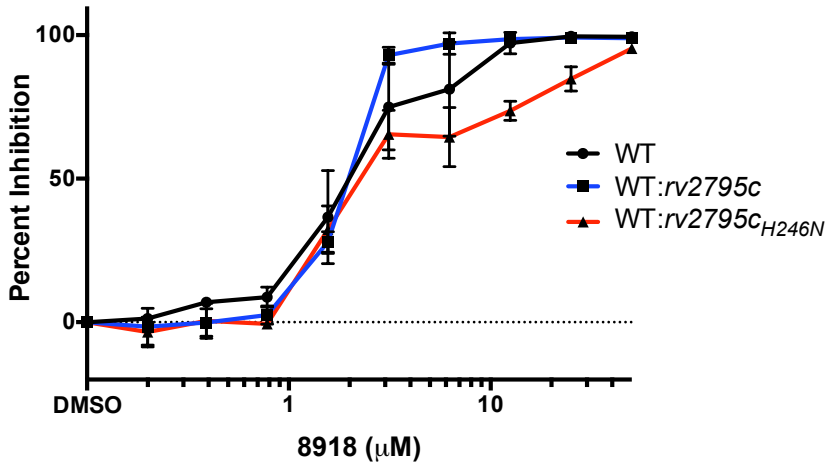

B.

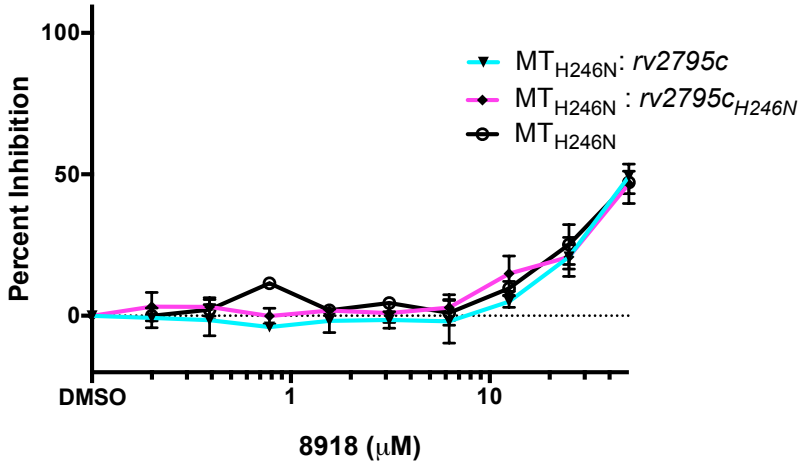

Figure 3: Mtb sensitivity to 8918 when expressing WT or MT *rv2795c*

(**A)** WT Mtb is sensitive to 8918 (black circles) but WT Mtb expressing WT *rv2795c* (blue line, black squares) on a new plasmid does not have any change in sensitivity to 8918; WT Mtb expressing *rv2795c* MT H246N also does not have any change in sensitivity to 8918 (red line black triangles). **(B)** MT Mtb with mutation H246N in *rv2795c* is highly resistant to 8918 (black) but introducing the WT *rv2795c* (cyan line inverted black triangles) does not restore sensitivity. Introducing MT $rv2795c_{H246N}$ to the mutant strain also does not impact sensitivity (purple line, black diamonds).

We again suspect that overexpression is toxic, as we expected that overexpression of WT *rv2795c* in either WT or MT strain would have result in hypersensitivity to 8918. By contrast, the presence of active Rv2795c in the WT Mtb would most likely be dominant, and in the WT:*rv2795c*$_{H246N}$ heterologous strains we would have no reason to suspect that the mutant LOF Rv2795c would be dominant, and these strains we would expect to have no change in sensitivity to 8918. Despite the fact that mutant inactive *rv2795c* would presumably not be toxic to cells, Rv2795c levels in this strain were also not high enough to be detectable by western blot.

Knocking out rv2795c confers high level resistance to 8918

With little information gained from heterologous expression of *rv2795c* in Mtb, we decided to knock out (KO) the gene in order to probe the activity of *rv2795c* in relation to 8918 activity. We expected that knocking out *rv2795c* would result in resistance to 8918, as we suspected that the *rv2795c* mutations we had observed in the resistance screen were LOF, so the KO would likely behave the same as the mutant. Because *rv2795c* is in an operon upstream of *pptT* with a few nucleotides of overlap, we wanted to be careful not to disrupt the expression of *pptT* when we removed *rv2795c,* as the essentiality of *pptT* means that any disruption of the gene would result in non-viable cells and the KO would be unsuccessful. The overlap of the two genes indicated that the translation initiation site for *pptT* was potentially contained within *rv2795c*, so we decided to generate 2 strains with different translation initiation sites for *pptT*.

For the first strain we decided to insert a Shine-Dalgarno sequence (SD3)[5,6] for *pptT* at the end of the hygromycin resistance (HygR) cassette which would be replacing the *rv2795c* gene; this construct was named KO1. For the second strain we decided to use the predicted native translation initiation (NTI) sequence for *pptT,*

which is a short (~20 bp) segment of *rv295c*. We inserted a stop codon after the hyg insertion followed by the NTI, hopefully to avoid disruption of *pptT* expression. This construct was named KO2. We hoped that of these two options at least one would preserve the translation of *pptT* such that we would have viable cells with an *rv2795c* KO. The summary of these constructs is shown in **Figure 4**.

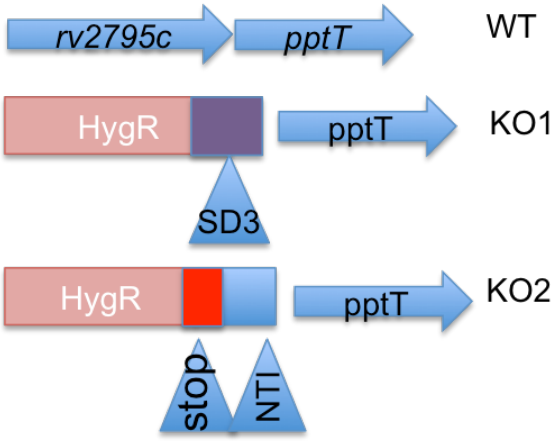

Figure 4: Summary of KO constructs. HygR is hygromycin resistance cassette, SD3 is Shine-Dalgarno 3, and NTI is native translation initiation.

After generating these knockouts and verifying the presence of the HygR cassette in the correct location by PCR and whole-genome resequencing, it appeared that the SD3 KO (KO1) and the NTI KO (KO2) were both resistant to 8918, but that KO1 was much more resistant than KO2. KO1 was about as resistant as the original *rv2795c* mutant H246N, while KO2 was only marginally more resistant than WT to 8918, and was less resistant than the H246N mutant (**Figure 5A and B**). We hypothesized that the SD3 translation initiation site may result in a strain that is slightly overexpressing *pptT* as compared to WT, and the NTI strain may have slightly lower *pptT* expression than WT. It's possible that the predicted NTI was not complete,

or that expression of *pptT* is in some way dependent on the expression of *rv2795c*.

A.

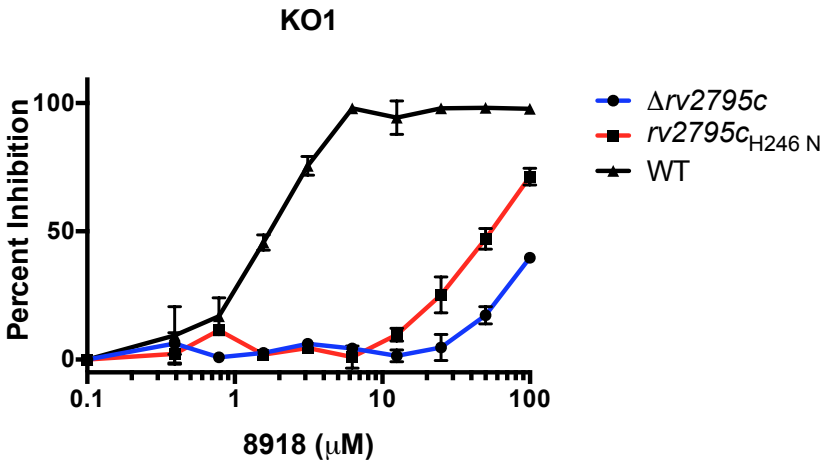

B.

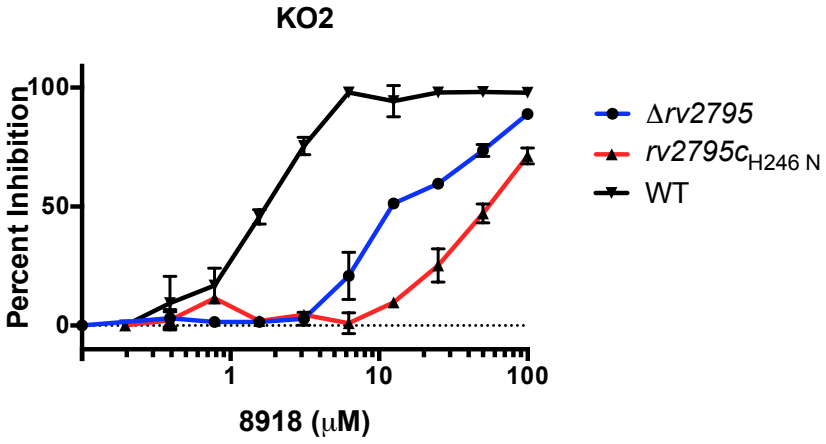

Figure 5: Effect of 8918 on the different knockout strains. (A) Δ*rv2795c* with Shine-Dalgarno translation initiation site for *pptT* (KO1) (blue) is highly resistant to 8918, comparable to the original $rv2795c_{H246N}$ mutation (red) and both are much more resistant than WT (black). **(B)** The Δ*rv2795c* strain made with the predicted NTI site (KO2) (blue) is less resistant to 8918 than KO1 or the MT H246N (red), but is still much more resistant than WT (black).

PCR of the HygR cassette and surrounding sequence confirmed that HygR was present in the correct region for 12 out of 16 mutants selected for further studies. Whole genome resequencing was conducted on four strains, two each of KO1 and KO2, all of which had been confirmed by PCR. One each of the constructs contained a silent SNP in *pptT* which may have some impact on the expression of *pptT*; this may be of interest for further studies, as the level of PptT expressed in the cell may be dependent on the levels of Rv2795c present, and this SNP may have some effect on the expression of *pptT*. For the purpose of this study however, the other strains tested were found to have minimal SNPs present in other genes, and were selected as the representative strains for their respective constructs. The summary of the SNPs identified in these strains can be found in **Table 1.**

Table 1: Summary of SNPs found in KO1 and KO2.

	Position	Gene	Description	AA Change	SNP
KO1	132415	*rv0109*	PE_PGRS1	R346G	C
	608334	*rv0516c*	anti-anti-sigma factor	M69L	T
	837036	*rv0746*	PE_PGRS9	T445A	A
	3250670	***rv2931***	**ppsA**	**frameshift at N1287**	**C**
	3381807	*rv3021c*	PPE47 (pseudogene)	frameshift at A5	G
KO2	132415	*rv0109*	PE_PGRS1	R346G	C
	608334	*rv0516c*	anti-anti-sigma factor	M69L	T
	837036	*rv0746*	PE_PGRS9	T445A	A
	3249676	***rv2931***	**ppsA**	**frameshift at E958**	**A**
	3381807	*rv3021c*	PPE47 (pseudogene)	frameshift at A5	G

Several of the mutations observed were identical between strains, indicating that these mutations may have been present in the parent strain used to generate the KOs. These mutations are not hypothesized to have any impact on 8918 activity, though the *ppsA*

mutations may be relevant. PpsA is involved with PDIM synthesis, and a frameshift mutations is most likely loss of function. PDIMs are important for Mtb virulence, but are non-essential *in vitro* and mutate rapidly during culture passaging[7].

As knocking out *rv2795c* did confer resistance to 8918, next we wanted to see the effect of complementing the Δ*rv2795c* strain with the WT *rv2795c* gene to determine if sensitivity to 8918 could be restored. We also wanted to test which of the 2 KO constructs and complement combination could restore 8918 sensitivity closest to WT levels. Our hypothesis was that complementing the KO would restore the activity of 8918, but due to our previous failure to overexpress *rv2795c* we were concerned that overexpression could be toxic. After initial attempts to complement using Ptb21 and Ptb38 promoters on *rv2795c* resulted in very low transformation efficiency and strains that did not appear to have any change in 8918 MIC, we decided to try a panel of promoters for *rv2795c.* We predicted that with a variety of promoter strengths we would be able to get some mutants that were expressing a level of *rv2795c* that would not be incompatible with viability.

Table 2 summarizes the strength of a variety of promoters tested with *rv2795c* expression. The promoters were tested by the amount of luciferase expression they induced when placed in front of the *luxAB* gene, as measured by the amount of fluorescence generated by LuxAB. PTB-21, PTB-38 and P16 were not tested in this assay, though are predicted to be as strong or stronger than P200.

Table 2: Summary of promoter strengths as measured by luciferase fluorescence.

	P200	P766-10A	P200-7A	P200-33T	P200-35A	pTB	pTB	P16

						21	38	
LuxAB (RFU)	28991	13492	10471	1094	381	Not tested	Not tested	Not tested

All promoters and luciferase measurements were generated and performed by the Schnappinger lab.

We observed that in general stronger promoters resulted in very low transformation efficiency, indicating that the expression may have been toxic and colonies may not have been viable. The transformation efficiency was low enough to be within the margin of natural kanamycin frequency of resistance. Colonies from strong promoter complements tended to show no sensitivity to 8918 (**Figure 6A-C**). This may be a result of mutation in the promoter impacting *rv2795c* expression, as we hypothesized was the reason for previous (failed) *rv2795c* overexpression attempts, though western blots could not detect Rv2795*c* to confirm expression levels. These strains also may not have the complementation plasmids and just be kanamycin resistant. If the expression of *rv2795c* is toxic at the levels these promoters generate, then the colonies that grew may not have the plasmid. For each strain and promoter, 2 candidates were chosen and tested for the MIC to 8918, and in all cases the 2 candidates had equivalent MICs.

In strains that showed sensitivity to 8918 when complemented with WT *rv2795c* and not MT, P766-10A in the KO1 strain was selected as the promoter most likely to result in expression of *rv2795c* closest to WT, based on 8918 MIC_{90} (**Figure 6F**). Interestingly, we observed that the KO2 background complements almost universally resulted in hypersensitivity to 8918 as compared to the WT, which has an MIC_{90} around 3 μM (**Figures 6 A, B, D, E, F**). We hypothesize that in normal cell

metabolism, *pptT* and *rv2795c* exist in balance, and when PptT is inhibited by 8918 the MIC_{90} is around 3 μM. By contrast, the KO2 strains where *pptT* is under the predicted (but possibly not accurate) native translation initiation site, *pptT* is being functionally underexpressed as compared to WT, and therefore most of the promoters are too strong and *rv2795c* is being functionally overexpressed, even if protein levels are quantitatively less than in WT. These strains may be of future interest in lieu of a successful *rv2795c* overexpression strain, as the balance between PptT and Rv2795c seems to have been pushed toward Rv2795c. As expected, when knockouts were complemented with mutant H246N *rv2795c*, sensitivity was not restored in any strains (**Figure 6F**). This confirms that resistance mutations in *rv2795c* are LOF. All strains were tested against INH, RIF, PAS, and EMB, but none had altered susceptibility to these drugs, indicating that the changes in MIC to 8918 as a result of the genetic manipulation were specific.

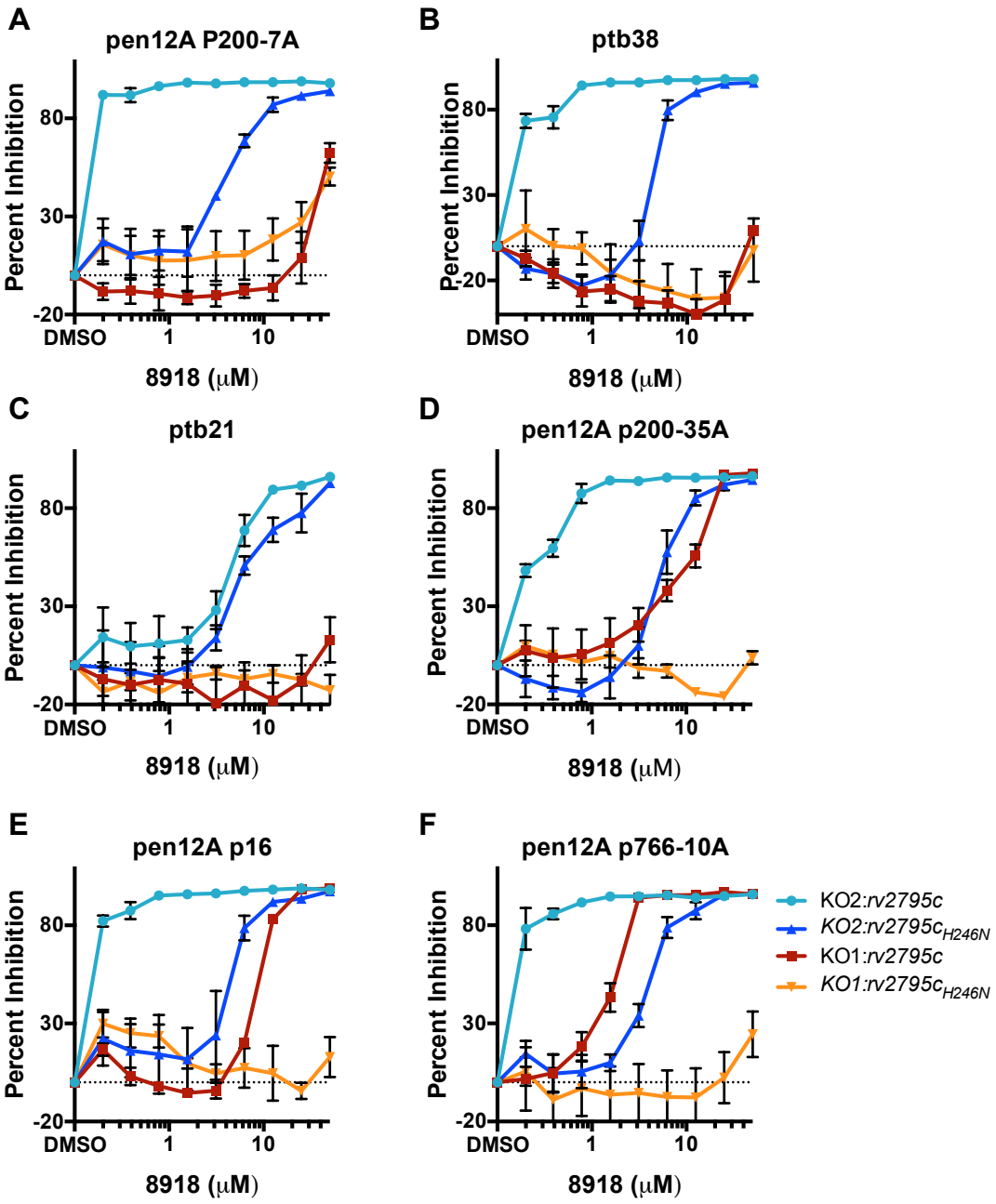

Figure 6: MIC_{90} from complementation of *rv2795c* KO under the control of promoters of different strengths. KO2 (native translation initiation *pptT* background) with *rv2795c* (teal circles), KO2 with $rv2795c_{H246N}$ (blue triangles), KO1 (Shine-Dalgarno *pptT* initiation) with *rv2795c* WT (red squares) and KO1 with $rv2795c_{H246N}$ (orange inverted triangles).

The results from the knockout and complement of *rv2795c* confirmed that while *rv2795c* is non-essential, the loss of the gene results in high level and specific resistance to 8918, implicating loss of function of *rv2795c* as a mechanism of resistance to 8918. We learned that *rv2795c* is involved in 8918 resistance, but because *rv2795c* was uncharacterized we lacked understanding of what reaction Rv2795c carried out in the cell, and how this related to PptT inhibition.

We next wanted to determine what reaction Rv2795c catalyzes, and decided to try to heterologously express and purify Rv2795c and carry out enzymatic reactions to probe its function. We knew from metabolomics studies that Rv2795c was not likely to be an activating enzyme, as no major conversion products were observed in WT but not MT Mtb. Additionally, we did not think Rv2795c was related to transport of 8918, as MT and WT strains both appeared to contain similar amounts of 8918 when examined during metabolomics experiments. Rv2795c is classified as a metallophosphoesterase, which means that it likely uses a metal as a cofactor and could carry out a number of reactions including hydrolysis, phosphorylation, dephosphorylation, or esterification. Amino acid analysis of the putative active site using Phyre[8,9] indicated that Rv2795c likely used magnesium as a metallic cofactor. When considering possible explanations for how loss of function could result in resistance that wasn't derived from structural modification or export, we hypothesized that Rv2795c may be antagonizing PptT. In this case, loss of function of an enzyme that is antagonistic to the target could theoretically result in resistance to a drug. We hypothesized that Rv2795c may be acting as a phosphopantetheinyl hydrolase, and may dephosphopantetheinylate holo-acps and convert them back into apo-ACPs (**Figure 7**). We know that magnesium can often be used as a cofactor for hydrolysis reactions[10-12]. We also know *E. coli* has an enzyme named named acyl carrier hydrolase, AcpH, which uses magnesium and performs hydrolysis[2]. While Rv2795c

does not have significant structural homology to AcpH, they may still be functionally homologous. The existence of AcpH has been confirmed from *in vitro* purifications but the activity has never been demonstrated *in vivo*, and the presence of a futile cycle that is antagonistic to an essential process has been described as an enigma[2].

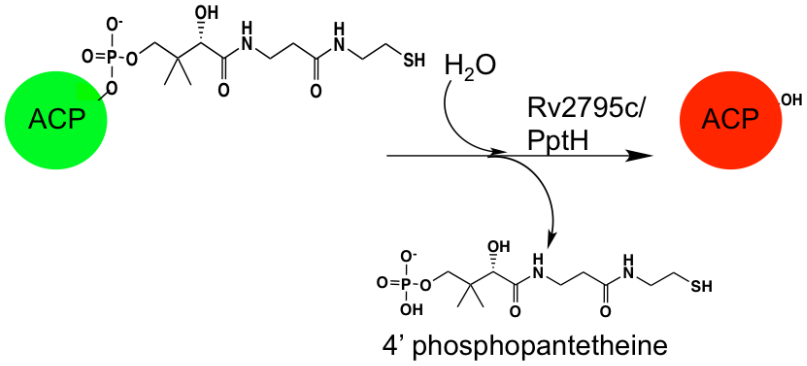

Figure 7: **Summary of putative reaction carried out by Rv2795c**. Rv2795c may be able to hydrolyze the phosphopantetheinyl group from holo-ACPs and generate apo-ACP and 4' phosphopantetheine in the process.

We attempted to express Rv2795c in *E. coli*, and found that expression was challenging, largely due to problems with solubility and toxicity. The inability of *E. coli* to express Rv2795c supported the hypothesis that previous attempts to overexpress in Mtb failed because overexpression of the protein is toxic. We also discovered that the protein was extremely insoluble. The solubility was largely improved by terminating the protein at amino acid 304, and deleting the last 20 amino acids ($Rv2795c_{304T}$). We also determined that only BL21 AI strains would express the protein, though yields were still low as compared to non-toxic proteins. BL21 AI *E. coli* differ from other expression strains in that the T7 polymerase is under *arab*BAD

control, and induction is obtained through addition of arabinose instead of IPTG[13]. This strain therefore results in less leaky expression of any gene on a T7 plasmid. Our first plasmid (generated by John Mosior at TAMU) contained *rv2795c* in pMCSG9 with ampicillin resistance. We observed that protein expression decreased substantially in cultures grown from frozen stock; we determined that pet28 (kanamycin resistance) induced much higher expression of Rv2795c than pMCSG9, and that highest protein yields were obtained from freshly transformed cells rather than frozen stocks.

Eventually, we were able to obtain pure His-tagged $Rv2795c_{304T}$ using a Ni-NTA agarose column, as confirmed by MS of the excised gel bands (**Figure 8**). The truncated protein is about 34 kDa, but we observed several bands around 60-70 KDa. When the bands were excised and tested by MS, one was found to be ArnA, which is an arabinose related membrane protein, and may be expressed as a result of arabinose induction, though we are unsure why it would co-purify with $Rv2795c_{304T}$. The other band was found to be GroL, a folding cofactor, which may be associated with Rv2795c as a result of instability or toxicity. Finally, a dimer of $Rv2795c_{304T}$ was also identified in the region.

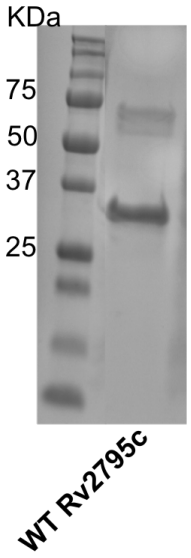

Figure 8: Gel image of recombinant Rv2795c (~34 KDa)

After numerous unsuccessful attempts to purify MT H246N Rv2795c, we hypothesized that the mutant protein may be too unstable to purify with similar methods used for the WT. We observed that while some stabilizing protein (GroL) copurified with WT Rv2795c, Rv2795c was the majority species present. By comparison, attempts to purify MT Rv2795c from the same *E. coli* strain and the same plasmid as the WT Rv2795c resulted in large amounts of SlyD and GroL, both of which are stabilizing/folding factors, but amounts of $Rv2795c_{H246N}$ were negligible and only detectable by western blot. By contrast, induction and purification of BL21 AI cells alone with the same protocol did not produce these proteins, and we concluded that the MT Rv2795c may be very unstable.

With the purified Rv2795c enzyme in hand, we wanted to test its activity against an acyl carrier protein. *In vivo* AcpM (acyl carrier protein meromycolate) is a native substrate of PptT, and is an enzyme that produces a precursor to mycolic acids[14]. We received the *acpM* expression plasmid as a gift from Mikael Blaise and

were able to purify the protein as a combination of holo and apo protein. Holo-AcpM is about 12.5 kDa, and when phosphopantetheine is removed in the conversion to apo-AcpM the protein loses about 0.5 kDa. We observed that when AcpM and Rv2795c were combined there was a time-dependent decrease in the amount of holo-AcpM, and a time-dependent increase in the amount of apo-AcpM as observed by gel shift and confirmed by MS of the gel bands (**Figure 9**). In the same time frame no spontaneous conversion of holo to apo-AcpM was observed (not shown). AcpM can dimerize, and the dimer is faintly present in the gel at about 25 kDa, as confirmed by western blot (anti-His antibodies) and gel excision/MS.

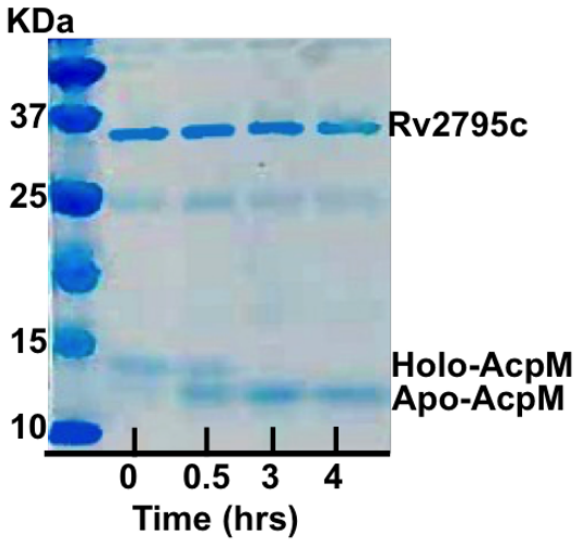

Figure 9: Conversion of holo-AcpM (~14 KDa) to apo-AcpM (~12KDa). Shown as a shift in MW over time (hrs) after addition of Rv2795c.

Upon MS analysis of the small molecules generated by the enzymatic reaction, we observed the appearance of ppt in the reaction mixtures, while AcpM or Rv2795c alone did not release ppt over time (**Figure 10**). The addition of 10 μM 8918 had no impact on this reaction. We also observed that over time the ppt seemed to degrade,

and tests into what degradation products form are currently underway.

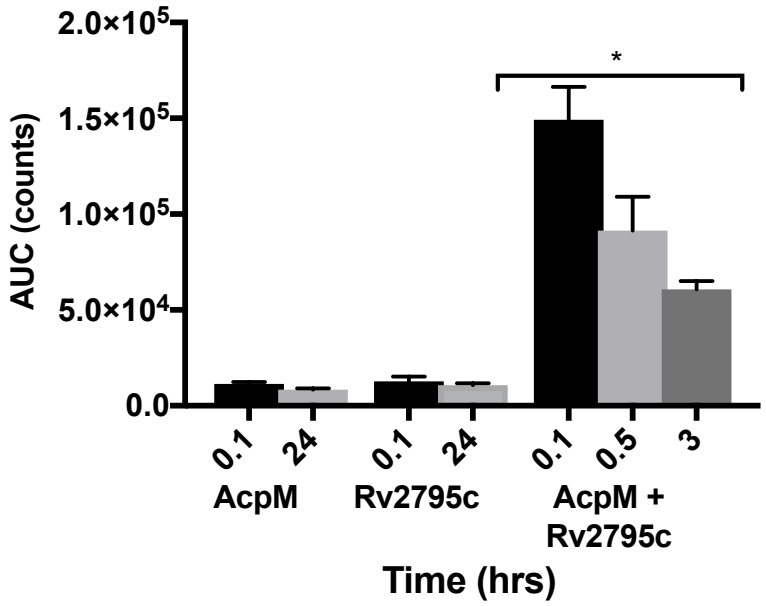

Figure 10: **Phosphopantetheine identified in the small molecule fraction of the reactions containing holo-AcpM alone, Rv2795c alone, or holo-AcpM and Rv2795c together over time (hours)**. The asterisk indicates statistical significance between the reactions and Rv2795c at T 0.1, which was the control sample with the highest amounts of ppt detected. Student's T test and $p < 0.002$ for all reactions.

Discussion

The activity of Rv2795c appears to be integral to the susceptibility of Mtb to 8918. It is possible that a better inhibitor of PptT would not additionally require the activity of Rv2795c to be lethal, but the combination of PptT's crucial cellular role and the presence of active Rv2795c *in vivo* results in Mtb being extra susceptible to PptT inhibition, and incapable of surviving even modest reductions in PptT activity. To our

knowledge, this mechanism of resistance has not been observed previously.

Since we have shown that Rv2795c can act as a phosphopantetheinyl hydrolase, we propose naming it PptH. While the function is homologous to AcpH, we think the structural differences and relationship with PptT justify the different name. We have little understanding of what purpose PptH serves *in vivo*. PptT or AcpS have been shown to be essential for cell growth, in Mtb or other species. Why then, would Mtb also express an enzyme that essentially makes it hypersusceptible to any reduction in the activity of PptT? Their presence in the same operon indicates that their expression may be linked in some way, but we have no knowledge of how they may be linked or regulated, or if they are definitely in an operon and expressed together. *pptH* was identified in a broad scale search of regulatory factor binding sites using ChIP-Seq, and appeared to be associated with the transcription factor Rv0767c, though the p-value was >0.3 indicating that the relationship was not statistically relevant[15]. In a search of proteomics data sets publicly available, Rv2795c was not identified. It may be that the native protein levels of PptH are very low, and (or, alternatively) it is degraded in lysates. Our inability to detect PptH in a western blot may indicate that the native levels are very low.

To attempt to identify if PptH may be conditionally essential, we conducted a search of several data sets including Tn-Seq and microarray. One technique which was of interest to us was TraSH, transposon site hybridization, which was described in a paper specifically looking for genes in Mtb that limited growth in minimal media when mutated[16]. Rv2795c was not identified as a conditionally essential gene for growth in minimal media in the Sassetti study, although they stipulated that "genes for which the intensity fro the rich medium pool did not exceed two-times the background were omitted[16]." If PptH is nearly as active as AcpH, levels of native expression may be extremely low, as higher levels may be very toxic to the cell, and detection may be

challenging to detect above background. We know that native protein levels appear too low to detect by western blot.

In another paper, Talaat *et al.* used microarray to investigate the transcription profile of genes expressed on day 7, 14, and 21 in the lungs of SCID (severe combined immuno-deficient) or BALB/c mice as well as media at the same time points[16]. They published an extensive data set of their results, which included both *rv2795c* and *pptT*. The results were published as a ratio of cDNA/gDNA, as better results were obtained when cDNA levels were normalized to the concentration of genetic DNA observed. The summary of their findings are shown below in **Table 3.**

Table 3: summary of ratios of cDNA/gDNA for *rv2795c* and *pptT* identified by Talaat, *et al*[16]. *Shown ± the standard deviation, n=6-8 hybridizations.*

Condition		Day 7	Day 14	Day 21	Day 28
BALB/c	*pptT*	**2.03** ± 0.81	**3.73** ± 3.93	**1.70** ± 1.16	**4.01** ± 0.56
infection	*pptH*	**4.30** ± 1.79	**6.14** ± 5.00	**1.55** ± 0.56	**3.94** ± 0.85
SCID	*pptT*	**1.00** ± 0.41	**2.53** ± 1.18	**3.67** ± 2.42	**8.02** ± 7.89
infection	*pptH*	**0.69** ± 0.21	**3.23** ± 2.06	**4.62** ± 2.55	**4.89** ± 3.04
7H9 broth	*pptT*	**17.55** ± 15.57	**5.16** ± 2.18	**12.73** ± 3.50	**5.29** ± 4.84
	pptH	**6.51** ± 2.99	**4.19** ± 1.17	**4.10** ± 1.26	**3.54** ± 1.77

In this data, generally the SD for the DNA levels is high, which makes determination difficult. This high variance may again be a factor of *pptH* levels within the cell being relatively low, which would result in challenges identifying it over background. With that caveat in mind, a general trend can be seen that *pptH* levels seem to be higher when Mtb is actively replicating, such as in 7H9 broth. One interesting finding is that on day 7, *pptH* from Mtb in SCID infected mice appears relatively low, while the BALB/c Mtb from the same timepoint seems to be higher.

This may indicate that the host immune system/stress may have some role in *pptH* expression. The late stage infection (day 28) in BALB/c similarly appears to have increased *pptH* expression compared to other conditions, though the authors did not identify *pptH* as a gene with significant change in expression only during growth in BALB/c mice, or 7H9 broth. These results may be interesting to follow up more specifically with qRT-PCR in different stress conditions to determine if they can be replicated and under which conditions.

Another paper used a GeneChip system to identify the signal intensity of mRNA in log phase as well as during the transition to stationary phase[18]. They found that *pptH* was not significantly upregulated during the transition to stationary phase, though it appears that both *pptT* and *acpM* were downregulated during the transition, as would be expected.

Finally, from Tn-seq experiments conducted within our lab, Ruslana Bryk observed within her data set that after exposure to acid (pH 5.5) and NO stress (0.5 mM) that both *pptT* and *pptH* are downregulated as compared to unstressed cells. The summary of her findings can be found in **Table 4**.

Table 4: Summary of Log_2 changes in mRNA levels observed by Ruslana Bryk in cells exposed to acid and nitrite stress, vs unstressed cells.

	Log2 fold change vs. d0				**P-value** Corrected for multiple testing			
	d00	**d05**	**d10**	**d20**	**d00**	**d05**	**d10**	**d20**
pptT	0	-0.92	-1.24	-1.37	1.000	0.007	0.001	0.000
pptH	0	-0.15	0.20	0.13	1.000	0.331	0.176	0.353

From this experiment it seems that *pptT* expression is reduced after exposure to

conditions that would likely result in the cells entering a non-replicating state. The corresponding changes to *pptH* levels are less pronounced, and not significantly changed. It is possible that changes may occur at an earlier time point than day 5 of exposure, though it appears that expression of *pptH* is not necessary for the survival in these conditions at these time points, and it appears to be downregulated during stress responses, usually around 2 fold[17]. In another Tn-Seq experiment conducted in our lab by Kohta Saito, Thulasi Warrier, and Jianjie Mi, they observed that *pptH* had a 1.67 Log_2 reduction in liquid vs agar plates, with an adjusted p value of 0.18. This is a lower p value than was observed in many other data sets investigated, and may indicate that *pptH* is important in solid colonies or biofilm survival. The fold changes in these data sets are not large, but it is possible that if PptH is exceptionally active, that a 2 fold reduction in expression could have significant effects within the cell. Additionally, low expression levels may make detection of *pptH* mRNA challenging or less accurate. We are interested in pursuing the protein expression levels of *pptH* in more detail, and hope that the new library of *pptH* mutants and complements may facilitate this process.

From the above experiments and publications, it seems that *pptH* is generally not essential, and that in many conditions the gene expression levels do not seem to change significantly in a way that would indicate conditional essentiality, though it also seems it is poorly characterized. It seems strange then, that *Mycobacteria* would carry it as a conserved gene, especially as its function appears to be toxic if unchecked. We observed that the population rate of mutation appears to be about 1 in 10^6, and if the gene were truly non-essential it seems as though it would not be conserved among *Mycobacteria* species. It is also interesting that *pptH* is highly conserved in *M. leprae*. This is notable because *M. leprae* has undergone extensive genomic reduction, and only has around 1600 genes[19,20]; as a result the genome now

contains very few nonessential genes, and the organism requires a host for replication. *pptH* is predicted to be nonessential in all *Mycobacteria* species, and in our study with Mtb we confirmed that *pptH* was not required for growth *in vitro*, but it is possible that *pptH* is essential or beneficial to the bacteria in some conditions, perhaps during infection from host stresses, or at very short time points after stress exposure. It seems that the enzyme would not be present nor so highly conserved among mycobacteria if it did not have some benefit, especially in *M. leprae,* given the disadvantages of antagonizing PptT seem to outweigh the benefits of PptH activity.

If PptH is essential in some conditions, the hypothetical utility for the cell may be related to CoA metabolism. It has been shown that CoA may be used as a post translational modification for proteins during stress responses[20]. PptH may exist as a mechanism for the cells to regenerate CoA during stress exposure, and may be important for the cells to survive certain stress responses, including the transition from replicating to non-replicating states during stress or unfavorable conditions. Mtb is a very successful pathogen partially because of its ability to become quiescent and dormant rapidly, and for long periods of time, and it is possible that PptH is involved with some aspects of the regulations of this state. It seems logical that PptT's crucial role in cell growth and membrane production might need to be tempered during stress to preserve resources and energy if cell growth is not a priority. If this is the case, and if a PptH inhibitor could be produced along with a more potent PptT inhibitor than 8918, the two drugs could be administered simultaneously and may inhibit both replicating and non-replicating populations of Mtb. This would require the development of a PptT inhibitor that is not dependent on the antagonizing effect of PptH, as 8918 is. Studies to identify any conditions in which PptH is essential are currently underway, as in our *in vitro* studies PptH is nonessential, but the high degree of conservation among mycobacterial species suggests that it may have some

conditions in which it is essential. Understanding more about the biology of PptH may reveal weaknesses in the ability of Mtb to survive harsh conditions within the host. Additionally, we may discover that *pptH* mutations cannot confer resistance to 8918 during *in vivo* infection if the gene is conditionally essential during infection, which would make a PptT inhibitor more effective.

Knowing more about PptH could also facilitate the discovery of an activator. A PptH activator could potentially be mycobactericidal alone, but would likely be synergistic with a PptT inhibitor. It could effectively lower the required dose of a drug and would almost certainly be extremely narrow spectrum, given the lack of structural homology to other enzymes. The rate of resistance would be relatively high for an antimicrobial, but INH and EMB for instance have rates of resistance around 10^{-5}. A high rate of resistance is less of a challenge to overcome in a multidrug therapy, as the combined rates of resistance become low enough for resistance to be very unlikely. A PptH modulating drug could also be effective against *M. leprae*. While infection caused by *M. leprae* is not as large a threat to global health as TB, new drugs would certainly be welcome, as no new drugs for *M. leprae* have been introduced in at least 30 years[22].

It seems clear that PptH must be carefully regulated in Mtb, as many of our experiments seemed to indicate that overexpression of PptH is toxic, and the reaction it catalyzes logically could be devastating for the cell if unchecked. We therefore are interested in studying how PptH expression is regulated, and how the regulation between PptH and PptT may be related. We also are interested in discovering if *pptH* has any conditions in which it is essential, as an explanation for what benefit Mtb may gain from having the gene.

Materials and Methods

Generation of *rv2795c* KO

Plasmids containing the hyg cassette and recombination regions including SD3 or NTI (SDN) for *pptT* were ordered from GenScript in pUC57. Plasmids contain the hyg cassette followed by the SD3 translation initiation site (KO1) or 24 nucleotides of the end of *rv2795c* for KO2. *pptT* was included in the plasmid as the recombination sequence so that recombination would be less likely to disrupt the expression of *pptT*. Protocol was adapted from the Dirk Schnappinger lab protocol via Caroline Trujillo. The pUC57 plasmids were resuspended in 10 mM Tris pH 8.0 to 100 ng/µL, and tested for concentration using nanodrop. Next the plasmid was digested using PmeI restriction enzyme following the NEB protocol for the PmeI restriction enzyme, and using 1 µg of the pUC57 plasmid. The reaction was incubated 1 hour at 37 °C, at which point another µL of PmeI was added, and incubated another 2 hours at 37 °C. 5 µL of the reaction mix was run on a 1% agarose gel to confirm digestion (~2.3 Kb fragment) and then gel purified using a Qiagen PCR purification kit and eluted with 30 µL elution buffer.

For recombination to occur we used a strain of H37Rv containing the RecET-MA plasmid, (kanamycin resistant) given to us by the Schnappinger lab. The stock was thawed and grown in 7H9 with 0.2% tyloxapol, 10% Middlebrook OADC, and 25 µM Kanamycin (kan). The cells were grown to OD_{580} 1 and then diluted 1:25 and regrown to OD_{580} 1. Once the cultures were ready isovaleronitrile was added to 1 µM and the cells were incubated for 8 hours at 37 °C. Then glycine was added to 0.2 M and incubated overnight at 37 °C.

50 mL of cells were then used to prepare competent cells by pelleting at 4000 RPM for 10 minutes at room temperature. They were then respuspended in half the starting volume of 10% glycerol and repelleted at 4000 RPM for 15 minutes. This procedure was repeated twice more until the cells were resuspended in 2.5 mL of 10%

glycerol. 400 µL of competent cells were used per transformation.

1 µg of the digested fragment was added to each electroporation cuvette containing cells. The cuvettes were gently mixed and incubated for 10 minutes at room temperature. The cuvettes were then electroporated at 2.5 kV, 1000 Ω, 25 µF. Immediately after electroporation 600 µL of prewarmed 7H9 complete was added to the cuvettes and the cuvettes were mixed gently. The transformation cuvettes were incubated for 24 hours at 37 °C, then plated onto 7H10 plates containing OADC and 50 µg hygromycin (Hyg).

When colonies were observed, 9 candidates from each of KO1 and KO2 were grown in 24 well plates, with the wells containing 7H9 and 50 µg Hyg. When cultures were about OD_{580} 1 they were outgrown again in 20 mL 7H9 and 50 µg Hyg for DNA purification and PCR confirmation. They were also streaked onto 7H10 plates containing 10% sucrose to cure the Rec-ET-MA plasmid. When colonies were grown on the plates they were picked and grown in 7H9 containing 50 µg Hyg, and were at this point considered ready for experimental use after confirmation of the correct HygR insertion.

Generation of Complements:

Complement vectors were generated using the gateway system[19,20], and the promoter donor plasmids used were generously given to us by the Schnappinger lab. Complement vectors once completed with the proper promoter and Rv2795c WT or MT were transformed into competent KO1 or KO2 strains, which were made competent and transformed using the same protocol described above for knockout cells. The transformed cells were plated on 7H11 plates with 25 µM Kan, all complementation vectors carried Kan resistance. Candidate colonies were then picked and regrown in 7H9 with 25 µM Kan to confirm resistance, and MIC against 8918 and

several antibiotics were tested.

Purification of AcpM

Protein was expressed in *E. coli* BL21 C41 cells. Cells were grown at 37°C until OD_{580} reached 0.6-0.7, at which point they were induced with 1 mM IPTG and grown overnight at 15°C. Cells were spun down at 3993x*g* for 10 minutes and the pellet was resuspended in lysis buffer (50 mM Tris pH 8.0, 0.4 M NaCl, 5 mM 2-mercaptoethanol (B-me), 20 mM imidazole), then lysed with emulsaflex. Lysates were spun down 45 minutes at 300000 G. Supernatants were incubated on nickel beads for 1 hr and then put in a column for gravity washing, and washed with 600 mL lysis buffer, and then with 600 mL wash buffer (50 mM Tris pH 8.0, 1 M NaCl, 5 mM B-me, 20 mM imidazole) followed by elution with 5 mL 50 mM Tris pH 8, 0.2 M NaCl, 5 mM B-me, 250 mM imidazole. Eluted protein was incubated with 0.5 M DTT overnight at 37 °C, dialyzed in 50 mM Tris pH 8 3x and concentrated on 10,000 MW Centricon.

Purification of Rv2795c

Truncated Rv2795c was cloned removing nucleotides coding for amino acids after number 304 at the C terminus. Protein was expressed in *E. coli* Bl21 AI cells grown to OD_{580} 0.6-0.7 and induced with 0.1% arabinose, and cultured overnight at 15°C. Cells were resuspended in lysis buffer (50 mM $NaPO_4$ pH 7.8, 0.5 M NaCl, 1 mM $MgCl_2$, 20 mM imidazole and 15% glycerol) and lysed by emulsiflex. Lysate was spun at 35000 G for 45 minutes and supernatant incubated on nickel beads for 1 hr. Cells were washed with 1 L lysis buffer, then 30 mL of lysis buffer containing 40 mM imidazole and 5 mM ATP, then 500 mL lysis buffer, 30 mL lysis with 40 mM imidazole and 5 mM ATP, then 500 mL lysis buffer. Protein was eluted with 10 mL 50 mM $NaPO_4$ pH

7.8, 0.5 M NaCl, 1 mM $MgCl_2$, 250 mM imidazole and 15% glycerol, then dialyzed against 50 mM $NaPO_4$ pH 7.8, 0.25 M NaCl, 1 mM $MgCl_2$, 15% glycerol.

AcpM and Rv2795c Reaction

Rv2795c (5 μM) and AcpM (10 μM) were combined with 75 mM Tris pH 8, and 15 mM $MgCl_2$. Reaction was spun with 10000 MWCO centrifuge filter to stop reaction for MS analysis or boiled in SDS-PAGE loading dye at 80°C for 10 minutes before protein gel analysis. Reaction mix was analyzed by SDS-PAGE on a 15% acrylamide stacking gel.

***rv2795c* overexpression plasmid constructs/primers**

Forward: CAAGCAGCTGTCGTTAGGGTGGTAAGTCGTG (PvuII)

Reverse: CTTGAAGCTTCACCGACGCCAGCGTGCCTA (HindIII)

Primers for confirming correct placement of HygR cassette

Forward: caagcagctgtagcagttgggctaggttggc

Reverse (hyg back): agcggacctctattcacagggtac

Forward (hyg out): gaggaactggcgcagttcctctgg

Reverse: cttgaagcttcaccgacgccaccagcgtgccta

Primers for generating donor plasmids for complements:

rv2795c-SD3-atTB2	GGGGACAGCTTTCTTGTACAAAGTGGAGGCGGTATCTCCGTGACCTGGAAAGGATCGGGGCAGGAGACCG
rv2795c-SDN-	GGGGACAGCTTTCTTGTACAAAGTGGTAGGG

atTB2	TGGTAAGTCGTGACCTGGAAAGGATC
	GGGGACAACTTTGTATAATAAAGTTGTCATC
rv2795c-atTB3	GAGACTGCCGTTGCCGCAATCGTTCCCG

Recombinant truncated (301-324) *rv2795c* for pet28:

For: caagcatatggtgacctggaaaggatcggggc (NdeI restriction)

Rev: gcaactcgagtcacgtgatcacgaagtac (XhoI restriction)

REFERENCES

1. Pfam: Family: Metallophos (PF00149). Available at: http://pfam.xfam.org/family/PF00149. (Accessed: 9th December 2017)

2. Thomas, J., Rigden, D. J. & Cronan, J. E. Acyl carrier protein phosphodiesterase (AcpH) of Escherichia coli is a non-canonical member of the HD phosphatase/phosphodiesterase family. *Biochemistry* **46,** 129–136 (2007).

3. Jackowski, S. & Rock, C. Metabolism of 4 ' -Phosphopantetheine in Escherichia coli. *J. Bacteriol.* **158,** 115–120 (1984).

4. Owen, J. G., Copp, J. N. & Ackerley, D. F. Rapid and flexible biochemical assays for evaluating 4′-phosphopantetheinyl transferase activity. *Biochem. J.* **436,** (2011).

5. Malys, N. Shine-Dalgarno sequence of bacteriophage T4: GAGG prevails in early genes. *Mol. Biol. Rep.* **39,** 33–39 (2012).

6. Cortes, T. *et al.* Genome-wide Mapping of Transcriptional Start Sites Defines an Extensive Leaderless Transcriptome in Mycobacterium tuberculosis. *Cell Rep.* **5,** 1121–1131 (2013).

7. Quigley, J. *et al.* The Cell Wall Lipid PDIM Contributes to Phagosomal Escape and Host Cell Exit of Mycobacterium tuberculosis. *MBio* **8,** e00148-17 (2017).

8. Soding, J. Protein homology detection by HMM-HMM comparison. *Bioinformatics* **21,** 951–960 (2005).

9. Jefferys, B. R., Kelley, L. A. & Sternberg, M. J. E. Protein Folding Requires Crowd Control in a Simulated Cell. *J. Mol. Biol.* **397,** 1329–1338 (2010).

10. Williams, N. H. Magnesium Ion Catalyzed ATP Hydrolysis. (2000).

doi:10.1021/JA0013374

11. Cowan, J. A. Structural and catalytic chemistry of magnesium-dependent enzymes. *BioMetals* **15,** 225–235 (2002).

12. Magnesium Hydrolysis | Hydrogen Link. Available at: http://www.hydrogenlink.com/magnesiumhydrolysis. (Accessed: 9th December 2017)

13. C6070-03, C. nos. BL21-AI One Shot® Chemically Competent E. coli. *Methods Enzymol.* **154,** 2006 (2006).

14. Zimhony, O. *et al.* AcpM, the Meromycolate Extension Acyl Carrier Protein of *Mycobacterium tuberculosis* , Is Activated by the 4′-Phosphopantetheinyl Transferase PptT, a Potential Target of the Multistep Mycolic Acid Biosynthesis. *Biochemistry* **54,** 2360–2371 (2015).

16. Sassetti, C. M., Boyd, D. H., and Rubin, E. J. Comprehensive identificatino of conditionally essential genes in mycobacteria. *PNAS.* **98**(22), 12712-12717 (2001).

17. Talaat, A. M., Lyons, R., Howard, S. T., Johnston, S. A. The temporal expression profile of *Mycobacterium tuberculosis* infection in mice. *PNAS.* **101**(13), 4602-4607 (2003).

18. Fu, L. M., Fu-Liu, C. S. The gene expression data of *Mycobacterium tuberculosis* based on Affymetrix gene chips provide insight into regulatory and hypothetical genes. *BMC Microbiol.* **7**(37) (2007).

19. Eiglmeier, K. *et al.* The decaying genome of *Mycobacterium leprae*. *Lepr. Rev.* **72,** (2001).

20. Gómez-Valero, L., Rocha, E. P. C., Latorre, A. & Silva, F. J. Reconstructing the ancestor of Mycobacterium leprae: the dynamics of gene loss and genome reduction. *Genome Res.* **17,** 1178–85 (2007).

21. Tsuchiya, Y. *et al.* Protein CoAlation: a redox-regulated protein modification by coenzyme A in mammalian cells. *Biochem. J.* **474,** 2489–2508 (2017).

22. Hant, P. & Kotra, L. P. Mycobacterium Leprae Infections. in *xPharm: The Comprehensive Pharmacology Reference* 1–7 (Elsevier, 2007). doi:10.1016/B978-008055232-3.60890-6

23. Gateway ® Technology A universal technology to clone DNA sequences for functional analysis and expression in multiple systems.

24. Gateway cloning technology The easy-to-use choice for cloning in multiple expression systems.

Chapter 6

PptT and PptH activity together explain the sensitivity of Mtb to 8918, and represent a new mechanism of resistance by which partial inhibition of the target (PptT) is lethal but loss of function of an antagonistic enzyme (PptH) can confer high level of resistance to a drug-like compound

Conclusion

We found that a small, antimycobacterial compound−8918−could bind to the active site of the essential enzyme PptT. PptT uses CoA as a cofactor, and 8918 appears to bind in the portion of the active site that is normally occupied by the ppt portion of the CoA molecule. Because the ppt portion of CoA is the moiety that is transferred to activate other enzymes, 8918's ability to destabilize this region likely is the mechanism by which catalysis speed is reduced. The generation of the crystal structure showed that 8918 and CoA can bind concurrently, and also indicated that there is a small region of the ppt binding pocket of PptT that is not being occupied by the acyl chain of 8918. These finding may help us use rational drug design to develop better inhibitors of PptT: perhaps larger molecules that can also displace CoA with stronger affinity for the pocket. 8918 is also rapidly metabolized *in vivo*, and the crystal structure with binding information may help us predict modifications which may reduce metabolism, or develop a new family of molecules entirely.

We also confirmed that inhibition of PptT was sufficient to cause cell death at relatively low concentrations, and that mutation of the W170 residue could confer high-level resistance to 8918, likely due to its proximity to the ppt binding pocket on PptT. We were surprised to find that the W170 PptT mutant was still inhibited by 8918, to a degree that does not seem to fully explain the resistance the mutation can

confer *in vivo*. It would be interesting to find out what happens if W170 in PptT is mutated at the same time that *pptH* is knocked out. Maybe metabolomics or lipidomics analysis of the double mutants could provide insights into how the cells function with no PptH but also reduced PptT activity. A conditional knock down strain with ATC regulated PptT and *pptH* knocked out may be a more controlled way to investigate this relationship, but could have a similar phenotype to the W170/Δ*pptH* strain. We also saw that 8918 could suppress Mtb growth in models of Mtb infection in mice, despite the fact that 8918 is rapidly metabolized in mice and blood concentrations decrease rapidly. A modified compound with a lower degree of metabolism might be extremely potent in an *in vivo* model of infection.

Sublethal concentrations of 8918 caused significant decreases in metabolites and lipids associated with enzymes that are activated by PptT. We can infer that at lethal concentrations the reduction of lipids would be much greater and could result in the death of the cell. We also observed that because PptT is involved in the activation of a wide variety of enzymes, that inhibition resulted in significant decreases in a very wide spectrum of products, many expected−sulfolipids, cardiolipins, mycolic acids, and PDIMs−and one unexpected−menaquinone. The finding of menaquinone was interesting as Mtb is especially dependent on menaquinone for electron shuttling[1-3]. PDIMs are important for virulence but are non-essential *in vitro* and reduction of PDIM synthesis could not explain the lethality of 8918. Similarly, cardiolipins and sulfolipids may have important roles *in vivo*, but are not essential for *in vitro* growth, and could not explain the lethality. Mycolic acids, including AcpM, are essential for growth, but menaquinone is a crucial bottleneck for metabolism and lethality of 8918 exposure could plausibly be caused by a depleation of menaquinone. We are interested in further investigating the relationship between menaquinone and mycobactin biosynthesis, as our hypothesis for the depletion of menaquinone hinges on

isochorismate shunting for mycobactin synthesis. We were unable to confirm the identity of mycobactin in our studies, but 8918 may help us understand more about the biochemistry of these two products.

pptT expression is likely downregulated during non-replication[5], and the enzyme is crucial for the production of a number of lipids during replication. We were unable to conclusively identify if mycobactin was reduced in our lipidomic analysis, largely due to the unavailability of standards to compare peaks with. PptT activates MtbB and MtbE, which are involved in mycobactin synthesis[4], so we would expect that 8918 could result in decreased mycobactin synthesis. We are interested in pursuing this hypothesis further and doing a more detailed analysis of mycobactin levels after 8918 exposure, because mycobactin is an important aspect of *in vivo* Mtb viability, especially when the bacteria are sequestered in iron-poor granulomas. PptT may not be utilized during non-replication, but if 8918 can reduce the production of mycobactins then it may be able to reduce the viability of cells even during non-replication. The apparent ability of 8918 to enter the cells or at least stick to the membrane, as indicated by carryover during experiments, may benefit this hypothesis. Concentrations of 8918 could potentially be high around the bacteria for extended periods of time if structure metabolism could be minimized. Activity of a PptT inhibitor might also be more potent if we can understand more about PptH to exploit the relationship between the two enzymes during treatment.

Our confirmation of *rv2795c* as a phosphopantetheinyl hydrolase was significant for a number of reasons. We first were able to classify an enzyme of unknown function, which is a small step in better understanding the biology of Mtb. Additionally, our identification of the activity of PptH represented a huge step in the study of similar acyl carrier protein hydrolase enzymes, as these enzymes have never been demonstrated *in vivo*. We can use PptH and 8918 as tools to understand more

about this puzzling biological process, which at first glance appears to be deleterious to the cells. The presence of functionally homologous enzymes in different species and the conservation of PptH among *Mycobacteria* indicate that this reaction may be important for processes that we do not yet understand. Finally, PptH is involved in a novel mechanism of resistance. Its involvement as an antagonist to the target of a small molecule, and the finding that loss of function of PptH can confer high-level 8918 resistance to Mtb represents a new mechanism of antimicrobial resistance.

The evidence taken together, makes a strong argument for the utility of PptT as a drug target. Mtb appears to be vulnerable to PptT inhibition during *in vivo* infection, even when PptT is only partially inhibited and the compound is being rapidly metabolized. Additionally, a more potent inhibitor may not be dependent on the activity of PptH, and the frequency of resistance would then be about 10x lower, in the same range as RIF. Because PptT is not yet a drug target, an inhibitor would be effective on MDR and XDR TB. We also infer that a PptT inhibitor would be highly specific to *Mycobacteria*, which is a greatly desired trait for Mtb drugs, in part due to the extended time for treatment. It is also possible due to the high structural homology between PptT in *Mycobacteria* that a PptT inhibitor could be used for treatment of Leprosy as well as for TB.

This project also exemplified the utility of studying the activity of small molecules on bacteria, as during the course of our investigation we identified many different new questions and avenues of research related to the biology that 8918 uncovered. We have also identified a novel mechanism of resistance, in which a loss of function in an antagonistic enzyme results in high-level resistance to an inhibitor. This mechanism of resistance opened the door to a relatively unexplored area of biochemistry, as Rv2795c was previously an enzyme of unknown function, and the functional role of a phosphopantetheinyl hydrolase is not understood. Our toolbox of

the PptH knockout and the accompanying complement may be extremely useful in probing the relationship between PptT and PptH, as well as the function of PptH during Mtb survival in various conditions.

Future Directions

Many questions were generated in the course of this project about the role of PptH and its relationship to PptT, and what role PptH has during normal cell metabolism, especially during infection. We hypothesized that because PptH can deplete active precursors of important cell membrane lipids, we may be able to observe differences in membrane permeability between the knockouts and WT. We have examined the permeability of the membrane in WT, Δ*pptH*, and Δ*pptH:pptH* in an ethidium bromide uptake assay, and observed that both the knockout and the complement are more permeable than WT Mtb (**Figure 1)**.

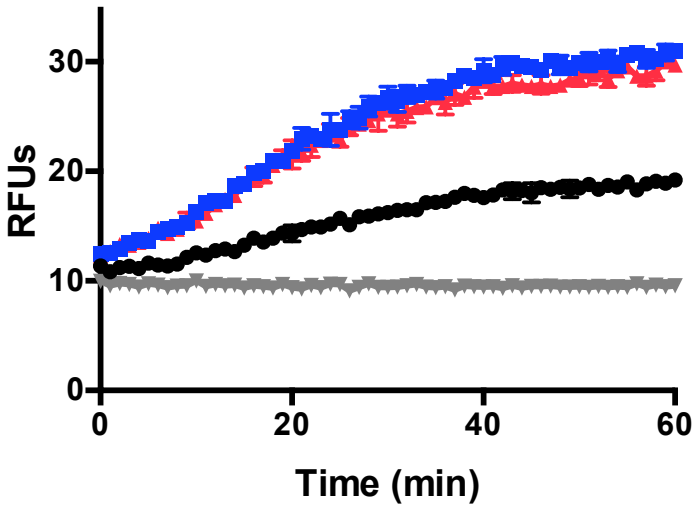

Figure 1: Permeability assay of WT, KO, and complemented KO strains.
Ethidium bromide uptake of WT (black) Δ*pptH* (blue) and Δ*pptH:pptH* (red). Baseline fluorescence is shown in grey.

This indicates that PptH may be involved in membrane permeability, perhaps in regulating membrane lipid turnover in some way. The complement may be slightly less permeable than the full knockout, but it seems apparent that the reintroduction of the WT PptH enzyme is not sufficient to restore normal membrane function. Our initial determination of normal PptH activity was based on the MIC_{90} of 8918. As a result our complement may represent a WT-like phenotype in response to 8918, but the actual levels of PptT and PptH may not be representative of true WT. We hypothesize that for 8918 to have activity, PptT and PptH must be in some sort of balance; the complement may restore this relative balance but the actual activity may be higher which could impact the permeability of the membrane. It is also possible that if the Δ*pptH* strain has a hyperpermeable membrane, more 8918 can get in, but PptT is slightly overexpressed due to the SD3 translation initiation site, and the complement is also slightly overexpressing PptH with the end result having a similar MIC to the WT strain, despite the higher relative abundance of 8918 within the cell.

This experiment would be interesting to repeat and include the H246N PptH mutants, as well as the KO2 strain that was less resistant to 8918 than the KO1, and one of the complemented strains that was hypersensitive to 8918. We may be able to infer more about the balance of PptH and PptT by using these strains, which we think have varying balances of PptH and PptT. We may find that strains hypersensitive to 8918−which we rationalized as functional overexpression of PptH−are less permeable than WT, which may implicate PptH in cell membrane turnover. Additionally, testing the H246N mutant that we have shown to be LOF and functionally identical to the knockout in regards to 8918 activity, might confirm whether the permeability that we observe is related to the loss of *pptH*, or if it might be related to a functional overexpression of *pptT* because of the SD3 translation initiation site controlling the expression of *pptT*. Solidifying the relationship between Δ*pptH* and membrane

permeability may expose a biological explanation for the enzyme, and rationalize a reason why it is expressed.

The MIC of WT, *pptH*$_{H246N}$, *pptT*$_{W170S}$, Δ*pptH* and Δ*pptH:pptH* against 8918 have been discussed. We observed that the MIC_{90} for 8918 on WT was around 3.2 μM, with the complement around 2.7 μM. By contrast, the 2 mutants were extremely resistant, though some inhibition (reaching MIC_{50} at the highest dose tested) could be observed, and the KO was fully resistant. We also observed throughout the course of the project that lidamidine's apparent inactivity on whole Mtb was not very well confirmed by *in vitro* assays, as the WT PptT enzyme was inhibited by lidamidine to a degree that did not correlate with the *in vivo* activity observed. Interestingly, when lidamidine was tested at high concentrations we saw WT was only sensitive at very high doses (as described), only reaching an MIC_{50} at 125 μM (**Figure 2A**), but that the knockout and *pptT* mutant were fully resistant even at high doses, while the *pptH* mutant was slightly less resistant at the highest dose tested (**Figure 2B-D**). Finally, we observed that the complement appeared to be hypersensitive to lidamidine; though it did not pass an MIC_{50}, it reached MIC_{50} at 10 μM as opposed to 125 μM in WT (**Figure 2E**).

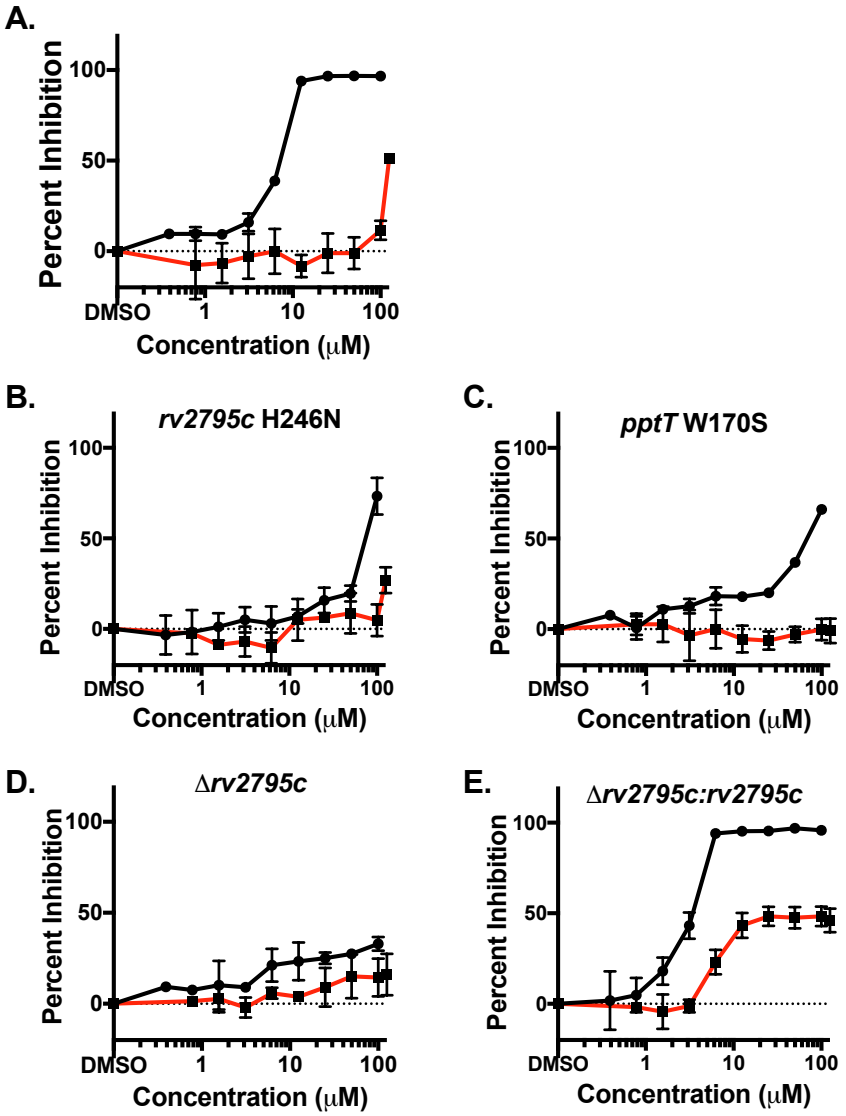

Figure 2: **MIC of 8918 (black) and lidamidine (red) in** (**A**) WT strain (**B**) *pptH*$_{H246N}$, (**C**) *pptT*$_{W170S}$ (**D**) Δ*pptH* and (**E**) Δ*pptH:pptH*.

This result may be an aspect of the hyperpermeability of the membrane in the complement combined with the large degree of accumulation of lidamidine within or around the cells. We are very interested in understanding more about how PptH interacts with membrane lipids and how it can impact membrane fluidity and

permeability, especially during exposure to stress. The impermeability of the Mtb membrane during non-replication has been associated with its ability to survive harsh conditions[6]. We hypothesize that PptH may be involved in mediating the impermeability of the membrane, or perhaps the recycling of membrane components during dormancy. In this way PptH may be conditionally essential only during times in which Mtb needed to cycle from replicating to non-replicating states. It would be interesting to compare the accumulation of lidamidine and 8918 within MT and WT cells as we did previously for metabolomics. We may see that that there is a drastic change in the accumulation in the Δ*pptH:pptH* strain, as the EtBr experiment indicated that the membrane is very permeable but that PptH is still active. It is very interesting that the Δ*pptH:pptH* strain is hypersusceptible to lidamidine and the differences in membrane permeability and accumulation may be informative. We may be able to target experiments investigating any conditional essentiality by learning more about the impact *pptH* modification has on the membrane.

In probing further into the activity of the *pptH* knockout during *in vivo* infection, we wanted to know if the Δ*pptH* strain remained resistant to 8918 treatment during infection, and if Δ*pptH* had a growth defect during mouse infection. We observed that during infection of primary murine bone marrow derived macrophages at a multiplicity of infection (MOI) of 0.1, Δ*pptH* was resistant to 8918 inhibition, while the WT and complement strains were not at 2 different concentrations of 8918 (**Figure 3A-B).** Xiuju Jiang conducted an aerosol mouse infection using WT Mtb, as well as the Δ*pptH* and Δ*pptH:pptH* strain. The summary of her findings can be found in **Figure 3C.**

Figure 3: Graphs of Δ*pptH,* WT, and complement in macrophage and mouse infection. (A) shows the CFU/mL of WT H37Rv (black line) compared to 8918 treated (black dashed line), Δ*pptH* (blue line) vs 8918 treated (blue dashed line) and Δ*pptH:pptH* (red line) vs 89818 treated (red dashed line) recovered after a multiplicity of infection of 0.1, and 10 μM 8918. **(B)** shows the CFU/mL of WT H37Rv (black line) compared to 8918 treated (black dashed line), Δ*pptH* (blue line) vs 8918 treated (blue dashed line) and Δ*pptH:pptH* (red line) vs 89818 treated (red dashed line) recovered after a multiplicity of infection of 0.1, and 1 μM 8918. **(C)** shows the Cfu/lung recovered from a mouse infection of B6 mice with WT H37Rv (blue line), Δ*pptH* (orange), and Δ*pptH* :*pptH* (grey) over the course of 180 days. *Mouse infection conducted by Xiuju Jiang.*

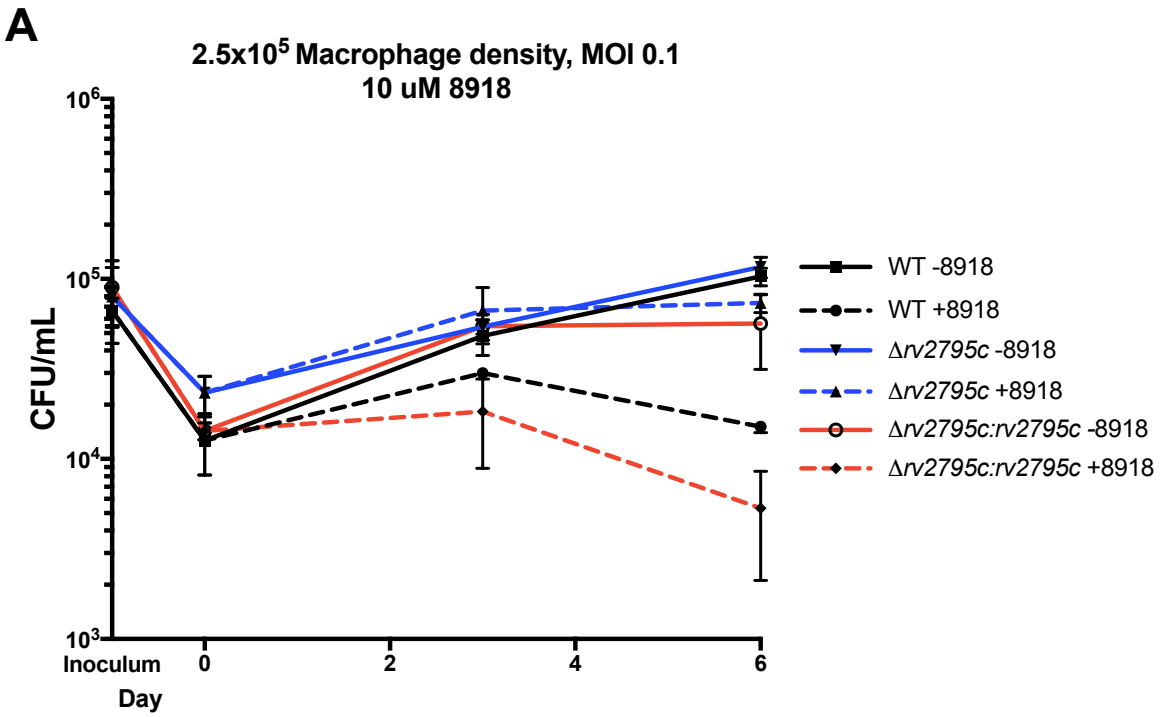
A
2.5x10^5 Macrophage density, MOI 0.1
10 uM 8918
CFU/mL
10^6
10^5
10^4
10^3
Inoculum
0
2
4
6
Day
WT -8918
WT +8918
Δrv2795c -8918
Δrv2795c +8918
Δrv2795c:rv2795c -8918
Δrv2795c:rv2795c +8918

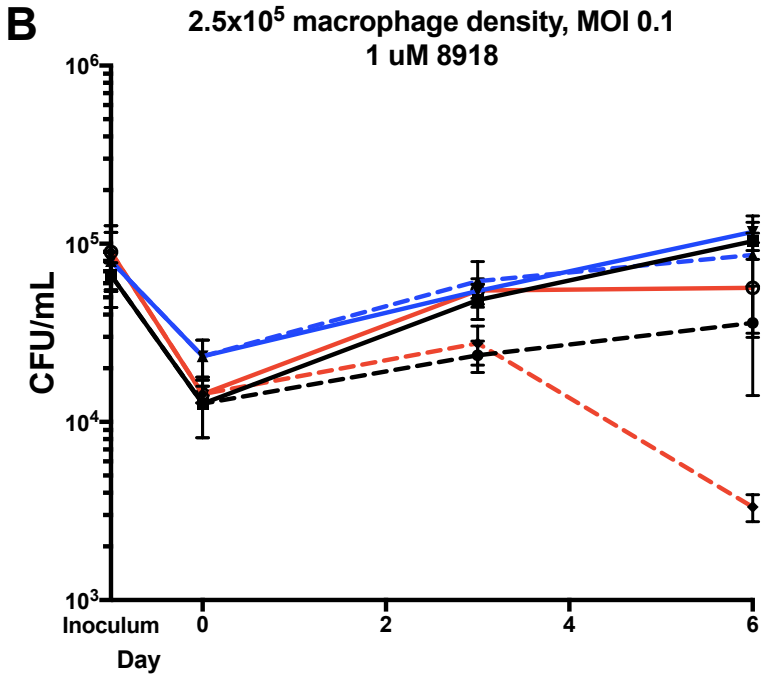
B
2.5x10^5 macrophage density, MOI 0.1
1 uM 8918
CFU/mL
10^6
10^5
10^4
10^3
Inoculum
0
2
4
6
Day

Figure 3 continued
C.

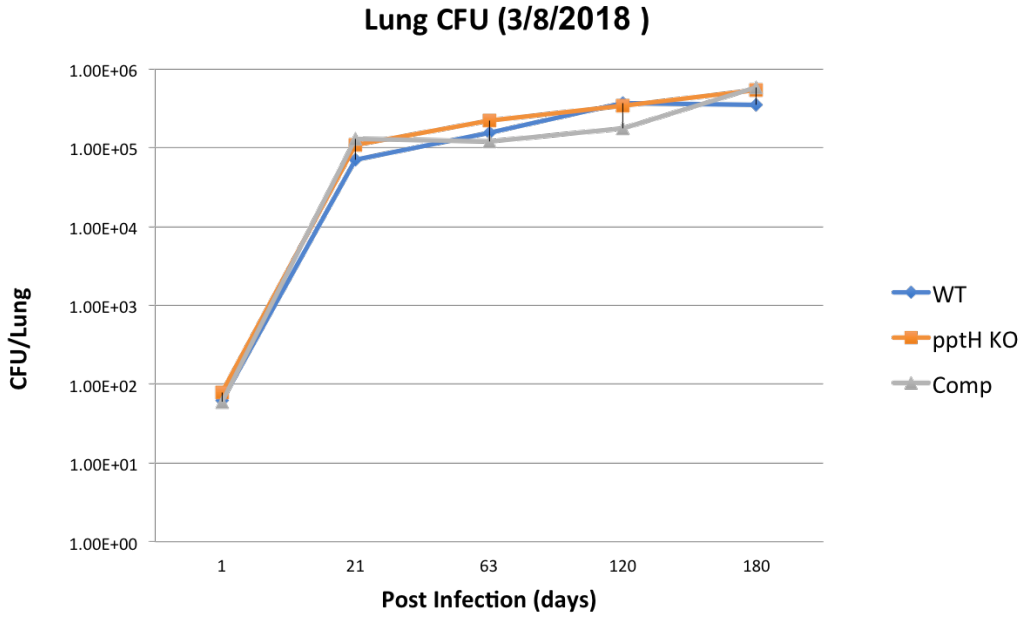

The macrophage experiment shown in **Figure 3A** and **B** supported our *in vitro* findings that the Δ*pptH* strain was resistant to 8918, and showed that it was *in vivo* resistant as well. The mouse experiment indicated that the Δ*pptH* strain did not have a growth defect during mouse infection. This finding conflicts with some of our hypotheses about potential conditional essentiality of *pptH*, though in this experiment the uptake and bacterial burden of Mtb for all 3 strains was very low. We know from our whole genome resequencing that the Δ*pptH* and Δ*pptH:pptH* strains are PDIM deficient, which generally leads to lower CFU burden during infection, as Mtb with PDIM deficiencies is less virulent. It is possible that reduced virulence may mask differences between the WT and *pptH* KO, though it may also be that in this infection model *pptH* is not essential. PDIM mutations arise rapidly during *in vitro* culturing of Mtb, and the number of passages on solid and liquid media necessary to generate a KO and complement make it challenging if not impossible to maintain PDIM during the process. If *pptH* is not conditionally essential during infection, it still is an enigma

as to why Mtb would express it all. We still hypothesize that *pptH* performs some useful role within Mtb that provides a rationale for its conservation, and it appears that our complement--which we hypothesized may have a slight overexpression of *pptH*—may be hypersensitive to 8918 during macrophage infection, which may also help us learn more about the activity of *pptH*.

The presence of *pptT* and *pptH* in the same operon is also interesting to us. We are interested in knowing more about how the two enzymes are regulated and in what conditions expression may be modulated to benefit the cell. It seems clear that PptH can be toxic for Mtb if it is overexpressed, and that the balance of PptT and PptH can have interesting impacts on membrane permeability and susceptibility to lidamidine. We are planning qRT-PCR to learn more about how the two genes may be related, and under what conditions *pptH* might be expressed, and if it might sometimes be expressed over *pptT*. It would also be interesting to examine the *pptH* knock out strains that carried silent mutations in *pptT*. It has been shown that silent mutations can change the rate or degree of gene expression[7,8]. If the silent mutations we observed in the knockouts do modify the expression of *pptT*, it could be further evidence that the regulation and balance of *pptT* and *pptH* is very important to maintain.

As one more question, we are interested in understanding more about other possible purposes for PptH. We have seen some evidence that it may have a role in the composition of the membrane. But we would also like to know more about what it does. For instance, what enzymes can it dephosphopantetheinylate? We have shown that it is active on AcpM but we don't know how active it would be on other enzymes that are phosphopantetheinylated. Is it active on any protein that has ppt? Is it specific to the proteins activated by PptT? Proteomic investigation of the *pptH* knockout may be informative. Similarly, there is some evidence that CoA can be synthesized from extracellular phosphopantetheine[76,97]. Maybe PptH has some role in this process,

especially if CoA sometimes needs to be used as a post-translational modification[89]. It might be informative to add radiolabeled phosphopantetheine in the WT and KO and try to determine if there are differences in the metabolism of the extracellular ppt.

Our discovery of the activity of PptH answered one question, but raised many more. Knowing what reaction an enzyme catalyzes is only a small piece of the puzzle, and how the enzyme fits into the complex web of cell biochemistry is a more complicated question. PptH and its relationship with PptT has opened up an extensive list of questions that hopefully will reveal more about Mtb and phosphopantetheinylation as a cellular process.

Materials and Methods

Ethidium Bromide Uptake Assay:

Mtb H37Rv was grown in 7H9 supplemented with 10% Middlebrook OADC and 0.2% tyloxapol until they reached an OD_{580} between 0.6 and 0.8. The cells were washed once in PBS containing 0.2% tyloxapol and adjusted to OD_{580} of 0.8. Glucose was added to a final concentration of 0.4%. Ethidium Bromide (EtBr) was prepared to 4 μg/mL in PBS with 0.2% tyloxapol and 100 μL were added to each reaction well. 100 μL of Mtb were added to each well and mixed (final OD_{580} 0.4). The plates were quickly transferred to the prewarmed (37 °C) plate reader, and the plates were read every minute for 60 minutes at an excitation of 530 nM and an emission of 590 nM.

Macrophage infection:

Bone marrow macrophages were isolated from B6 mouse femurs and differentiated in 20% LCM and DMEM complete. They were seeded to a density of $2.5x10^5$ per well in 48 well plates, and infection was done at an MOI of 0.1 for 4 hours of exposure. After 4 hours the cells were washed with PBS twice, day 0 macrophages were lysed and plated, and 10% LCM and DMEM complete added back to the remaining. 8918 was

given 24 hours later (day 1), and replaced on day 3, in new 10% LCM and DMEM complete.

REFERENCES

1. Kurosu, M. & Crick, D. C. MenA is a promising drug target for developing novel lead molecules to combat Mycobacterium tuberculosis. *Med. Chem.* **5,** 197–207 (2009).

2. Debnath, J. *et al*. Discovery of selective menaquinone biosynthesis inhibitors against Mycobacterium tuberculosis. *J. Med. Chem.* **55,** 3739–55 (2012).

3. Dhiman, R. K. *et al*. Menaquinone synthesis is critical for maintaining mycobacterial viability during exponential growth and recovery from non-replicating persistence. *Mol. Microbiol.* **72,** 85–97 (2009).

4. Leblanc, C. *et al*. 4′-Phosphopantetheinyl Transferase PptT, a New Drug Target Required for Mycobacterium tuberculosis Growth and Persistence In Vivo. *PLoS Pathog.* **8,** e1003097 (2012).

5. Mawuenyega, K. G. *et al*. Mycobacterium tuberculosis Functional Network Analysis by Global Subcellular Protein Profiling. *Mol. Biol. Cell* **16,** 396–404 (2004).

6. Gengenbacher, M. & Kaufmann, S. H. E. Mycobacterium tuberculosis: success through dormancy. *FEMS Microbiol. Rev.* **36,** 514–32 (2012).

7. Shabalina, S. A., Spiridonov, N. A. & Kashina, A. Sounds of silence: synonymous nucleotides as a key to biological regulation and complexity. *Nucleic Acids Res.* **41,** 2073–94 (2013).

8. Bali, V. & Bebok, Z. Decoding mechanisms by which silent codon changes influence protein biogenesis and function. *Int. J. Biochem. Cell Biol.* **64,** 58–74 (2015).

9. Jackowski, S. & Rock, C. Metabolism of 4 ’ -Phosphopantetheine in

Escherichia coli. *J. Bacteriol.* **158,** 115–120 (1984).

10. Srinivasan, B. *et al.* Extracellular 4′-phosphopantetheine is a source for intracellular coenzyme A synthesis. *Nat. Chem. Biol.* **11,** 784–792 (2015).